Alma Mater Studiorum – Università di Bologna

DOTTORATO DI RICERCA IN

SCIENZE BIOCHIMICHE E BIOTECNOLOGICHE

Ciclo XVIII

Settore Concorsuale di afferenza: 06/A3

Settore Scientifico disciplinare: MED/07

PARVOVIRUS B19: virus-cell interactions, pathogenetic mechanisms and development of compounds with antiviral activity

Presentata da: Dott.ssa Gloria Bua

Coordinatore Dottorato

Prof. Santi Mario Spampinato

Relatore

Prof. Giorgio Gallinella

Esame finale anno 2016

TABLE OF CONTENTS

INTRODUCTION

1. PARVOVIRUS B19

1.1. INTRODUCTION

Parvovirus B19 (B19V) was first identified in 1975, during tests for hepatitis B virus surface antigen. (1) The name originates from the coding of a serum sample, number 19 in panel B that gave anomalous results. Electron microscopy showed the presence of particles of 23nm-diameter resembling animal parvoviruses. In the early eighties, it was linked to transient aplastic crisis in patients with sickle cell disease and erythema infectiosum in children (2, 3). It was officially recognized as a member of the *Parvoviridae* family in 1985 (4). It is the only member of the *Parvoviridae* family to be a human pathogen with a widespread trasmission and association to an ample range of clinical manifestations.

1.2. TAXONOMY

The *Parvoviridae* family is divided in two subfamilies, *Parvovirinae* and *Densovirinae*, based on the ability to infect vertebrate or invertebrate, respectively. *Parvovirinae* are subdivided into 8 genera, according to their transcription maps, the nature of terminal repeats and the ability to replicate either autonomously or with helper virus, like *Dependovirus* genus. B19V infects only humans, does not require a virus helper to replicate and replicates preferentially in erythroid progenitors cells. Thus, B19V is classified as a member of the *Erythroparvovirus* genus and the correct species name is now *Primate erythroparvovirus 1* (5).

1.3. MORFOLOGY

Initial biochemical characterization confirmed that B19V virion has properties typical of parvoviruses, with a composition of two structural properties, VP1 and VP2. VP1 protein accounts for about 5% of the virion mass, while 95% of viral capsid is composed of VP2 protein, which lacks the first 226 amino acids present at the N-terminal of VP1 (VP1 unique, VP1u) (6).

Structural data have been obtained mainly by means of cryoelectron microscopy and crystallographic X-ray diffraction studies with VP2 protein empty capsids, at the beginning, and more recently also with native virions containing or not DNA.

The non-enveloped viral particles are 20-25 nm in diameter and exhibit icosahedral symmetry. The small viral capsid is composed of 60 capsomers. The VP common region constitutes the core structure formed by eight-stranded β-barrel connected by large loops projecting on the outer surface. Similar to other parvoviruses, a cylindrical structure is present at the 5-fold axis, forming a gated channel connecting interior and outer surface of the virion. On the other hand, surface of B19V is significantly different from those of other parvoviruses by lacking prominent spikes on the 3-fold axis involved in host recognition and antigenicity (7-10).
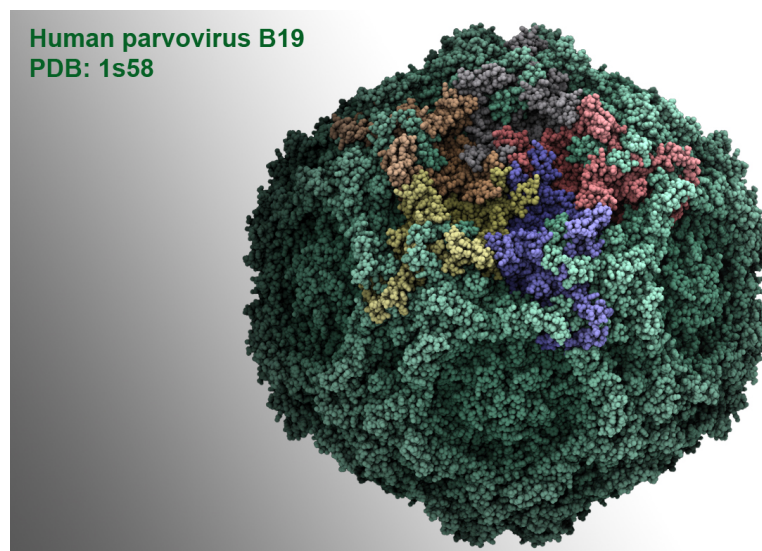
Figure 1: Structure of Parvovirus B19 (10).

Comparison of wild-type B19V virions with recombinant particles consisting of only VP2 protein showed structural differences near the 5-fold axis. The VP2 N-terminal peptide is positioned between neighbouring VP subunits of wild-type B19V virions and is exposed to the surface adjacent to the 5-fold β-cylinder. The position of VP1u region could not be identified in the icosahedrally averaged maps of B19V capsid, possibly because the VP1u is disordered or because of the low copy number of molecules per capsid.

Two possibilities are proposed. VP1u could always appear on the surface of the capsid and its epitopes could be recognized by the immune system, or it is also possible that the protein is located internal to the capsid, proximal to the cylinder at the 5-fold axis, being exposed when virions are damaged or during interaction with target cells (11).

1.4. GENOME

After B19V discovery and its association to erythrocyte aplasia and erythema infectiosum, its genome was characterized. A linear single-stranded DNA molecule of either positive or negative polarity was found to be encapsidated in the viral capsid. It was capable of priming synthesis of its complementary strain in vitro. These properties enabled the classification within the *Parvoviridae* family (12). Viral genome is 5596 nucleotides in length with a unique internal region of 4830 nucleotides, flanked by two inverted terminal repeats of 383 nucleotides each (ITRs) that form an imperfect palindrome (Figure 1) (13).

Figure 2: Schematic diagram of B19V genome. Identical ITRs are present at each end of the genome and form terminal loop structures (45).

As a result of the occurrence of sequence asymmetries within the palindrome, each terminal region can be present in either one of two alternative sequences, creating termini in two inverted complementary sequence orientations, usually referred to as flip/flop. The result of the relative possible combinations is the existence of four different genome isomers (14). The presence of self-complementary sequences in the terminal regions allows the formation of terminal loop and stem structures (15).

Two large open reading frames are present (Figure 3): the left half of the genome encodes for the non-structural protein NS, while the right one codes for the capsid proteins VP1 and VP2. Other minor open reading frames are present, coding for smaller non-structural proteins (11 kDa, 9 kDa, 7.5 kDa).
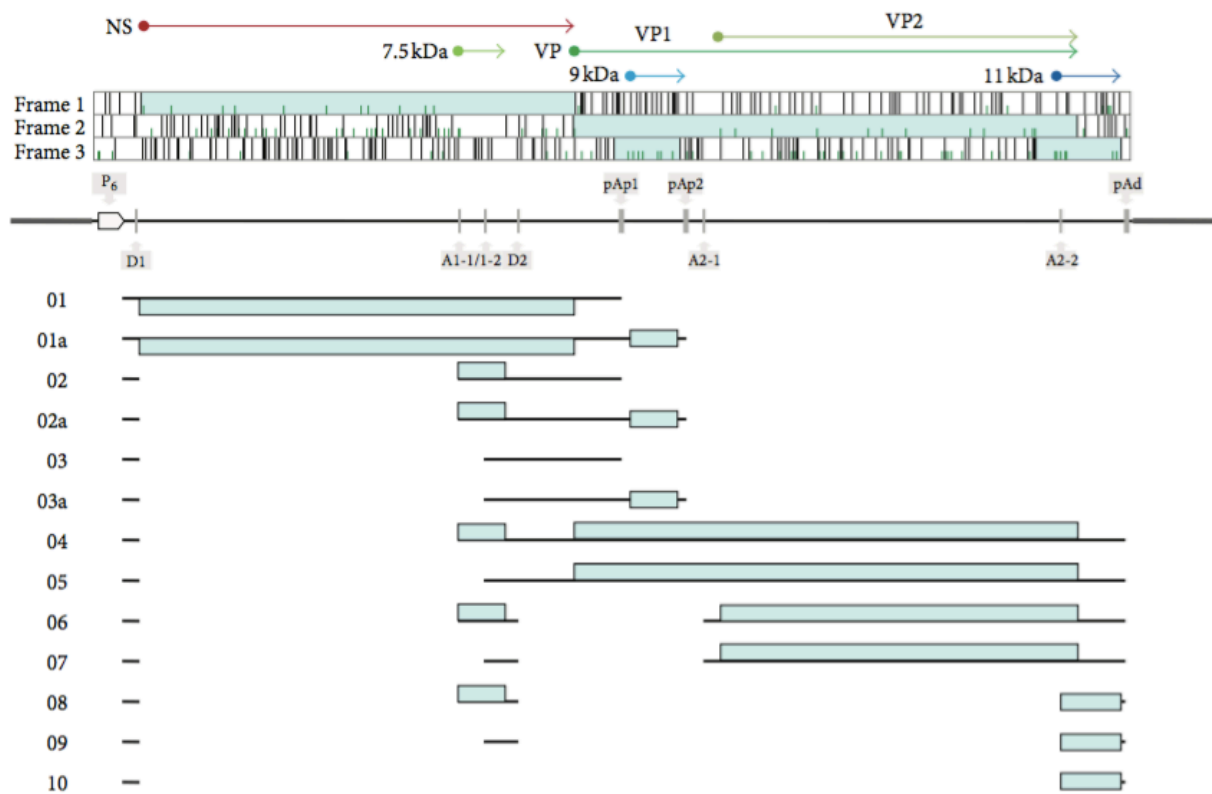
Figure 3: B19V genome organization and map of the whole set of viral transcripts. Top: Open reading frames identified in the positive strand of the genome. Center: distribution of regulatory signals; P6, promoter; D1, D2, splice donor sites; A1-1/2, A2-2/2, splice acceptor sites; pAp1, pAp2, pAd, cleavage-polyadenylation sites. Bottom: viral mRNA species; black lines indicate the exon composition and light boxes indicate the ORFs contained within mRNAs.

2. EVOLUTION

The species B19V is now formally subdivided into three genotypes (16): the genotype 1, which includes prototype strain B19V, the variant genotype 2, including the Lali and the A6 strains (17, 18), and the variant genotype 3, containing the V9 strain (19). At the nucleotide level, the genetic distance between clusters is 5-10%; while the genetic distance within clusters is generally lower for genotype 1, normally less than 2%, and higher for genotype 2 and 3, in the range of 3-10% (14).

The constant insertion of new sequences into the database, leads further subdivisions into subtypes. Therefore, genotype 1 can be subdivided into two subgroups, referred as genotype 1a and 1b (20), and genotype 3 contains two subgenotypes, 3a and 3b (21).

No correlation between specific clinical symptoms and B19V sequence has been observed. All three genotypes showed similar functional characteristics, in term of infectivity of permissive cell lines, mRNA production and expression and transcription efficiencies of the p6 promoter (22).

The global distribution of each genotype is not uniform and depends on geographic area, population and sample type (23-25). Overall, genotype 1 is the major circulating genotype with a worldwide distribution (26); the genotype 2 is rare but found in different geographic areas (27, 28); the genotype 3 is the prevalent variant circulating in western Africa (21).

A massive study has been conducted in Finland, by collecting 523 solid tissue samples (skin, synovium, tonsil and liver), and 1640 sera from patients with various clinical symptoms. Regarding the tissue specificity, genotype 1 DNA was found in all tissue types, with detection rates varying from 16% in tonsils to 35% in synovia. Genotype 2 has a universal distribution too, albeit at a lower frequency, while genotype 3 was absent from all of the tissues studied. Grouping samples according to the birth date of donors, genotype 1 was found almost uniformly in all individuals (except small children), while genotype 2 was strictly confined to the elders. Thus, data suggested that the new variant 2 of B19V circulated earlier in respect to the prototype 1. Results indicated that genotypes 1 and 2 co-circulated in Northern Europe until 1950s at a similar frequency, with genoprevalence rates of 22% and 28%, respectively. Then, genotype 1 became prevalent and genotype 2

disappeared in 1960s-1970s (present in 3% among those born in 1960s and in a single individual born in 1970s), and remained absent thereafter (only genotype 1 was found at low frequency in children born during the 1990s). Moreover, B19V DNA was detected in 17% of sera collected during 1983-1997, all corresponding to genotype 1.

This study confirmed that erythrovirus DNA persistence in human tissue is lifelong and could represent an important source of information, called *Bioportfolio*. The maintenance of the *Bioportfolio* could involve a dynamic interplay between viral replication and the immune surveillance of the host and it provides, at epidemiological and phylogenetic level, a database for analysis of the occurrence and circulation of viruses and their variants (29).

The pattern of evolution of B19V is still under investigation. By inferring the phylogenetic history and evolutionary dynamics of temporally sampled, a high rate of evolutionary change, at approximately 10^4 nucleotide substitutions/site/year, was observed. This rate is within the range seen in RNA viruses and is so similar to those estimated for other parvoviruses, suggesting that high mutation rates may be characteristic of all autonomous parvoviruses (30).

This high rate of mutation was confirmed in a study comparing the rates of sequence change in exogenous virus populations with those in persistently infected individuals, analysing large genotype 1 VP1/VP2 sequence data sets of plasma- and tissue- derived variants of B19V virus with known sample dates. By using linear regression and likelihood-based methods, plasma-derived B19V showed a substitution rate of 4×10^4 and a synonymous substitution rate of 18×10^4 per site per year. The last common ancestor for genotype 1 was predicted to exist around 1956 to 1959, fitting well with previous analyses described above. In contrast, the evolution of B19V amplified from tissue samples was consistent with slow or absent sequence change during persistence. However, paired samples from acute infection and after a period of persistence were not available to directly investigate the sequence change, and this study had to rely on estimates of times of infection, supposing primary infections at the age of 9 and no subsequent sequence change during persistence (31).

Recently, the B19V genomic prevalence was determined in DNA extracts of long bones of 106 anonymous World War II Finnish casualties. B19V DNA was found in 45% of long bone

samples and was exclusively of genotype 2 and 3, thus confirming the hypothesis that prototype 1 virus emerged after World War II. The detection of genotype 3 was in discrepancy with previous studies that revealed an absence of this variant in the North Europe with predominance in Africa. Thus, analysis of mitochondrial DNA of the respective positive two soldiers suggested that they are not of Finnish origin. The rate of B19V sequence change was calculated, using the assumption of primary infection at the age of 9 and no sequence change after infection, as in the previous cited work. The change rate estimated was approximately 2×10^4 substitutions/site/year for the combined NS/VP region, which is was lower than previous analyses based on the whole VP1, a genome region showing substantially greater variability than the conserved NS and VP regions targeted in this study. The time to most recent common ancestor of all three genotypes was estimated as 1833, 1868 for genotypes 2 and 1917 for genotype 3 (32).

The underlying high mutation frequency found for B19V may lead to rapid adaptive changes, more commonly ascribed to RNA virus populations, and to the formation of viral quasi-species. Determining what epidemiological or biological factors led to such a complete and geographically extensive population replacement over a short period is central to understanding the nature of parvovirus evolution. Moreover, understanding viral evolutionary dynamics may be crucial for better monitoring and predicting the epidemiological trajectory of clinically relevant viruses.

3. VIRAL LIFE CYCLE

The life cycle of B19V includes binding of the virus to host cell receptors, internalization and translocation of the genome to the host nucleus, DNA replication, RNA transcription, protein production and finally assembly and release of mature virions.
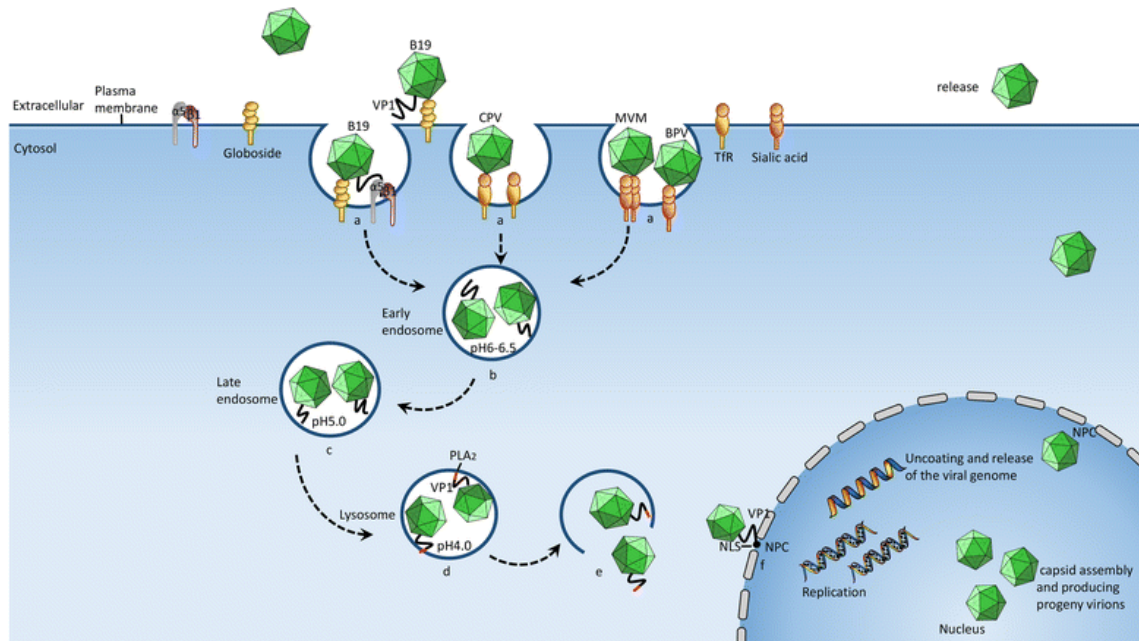
Figure 4: Principal steps of B19V life cycle.

3.1. VIRUS BINDING/UPTAKE

Globoside (erythrocyte P antigen) was identified as the primary receptor for B19V. B19V was initially shown to agglutinate human red cells (33). Thus, by using hemmaglutination, B19V was found to bind the glycolipid globoside. Purified globoside blocked the binding of B19V to erythroid cells and late erythroid colony-forming units (CFU-E) were protected, in a colony formation assay, from the cytopatic effect of B19V in presence of purified globoside, as well as by using monoclonal antibody against globoside (34). Moreover, persons with the p phenotype whose erythrocytes do not express globoside are naturally resistant to B19V infection (35).

Coreceptors like α5β1 integrins and Ku80 were proposed, although their role in virus entry needs further investigation.

The phenotype shift of erythroleukemia cell line K562 from non-adherent to adherent cells that is α5β1 integrin-mediated, renders the cells susceptible to B19V infection. α5β1 integrin coreceptor function in induced K562 cells could be enhanced either by stabilizing the high affinity conformation of β1 integrins or by inducing β1 integrin clustering, suggesting that β1 integrin-mediated signaling might be important for B19V internalization. In addition, virus internalization into purified human erythroid progenitor cells (EPCs) can be completely inhibited by antibodies blocking β1 integrin function (36).
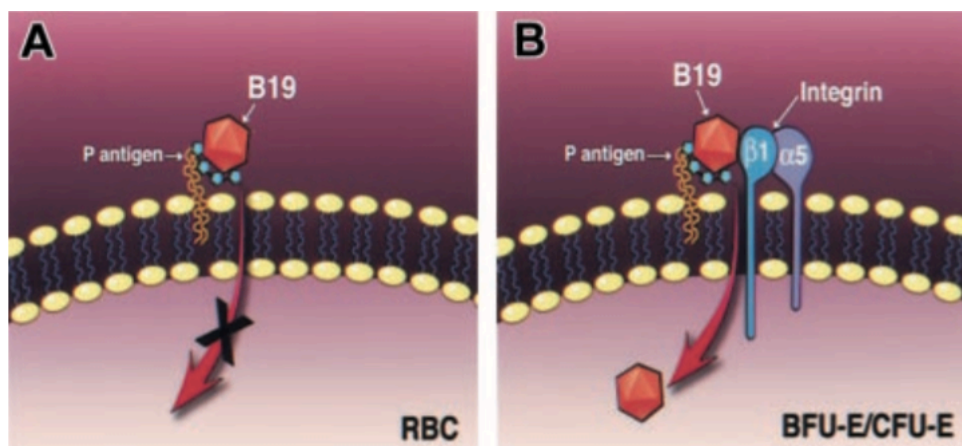
Figure 5: Proposed model of B19V entry into erythroid cells. Mature human red blood cells allow virus binding but not internalization (A), whereas virus uptake occurs in erythroid progenitor cells expressing both globoside and α5β1 integrin (B).

The expression of a constitutively active mutant of the small GTPase Rap1 render K562 cells permissive to B19V infection and this effect is mediated through functional recruitment of β1 integrin coreceptors, as demonstrated by the complete block of transduction with β1 integrin antibodies. The active actin polymerization played a critical role in β1 integrin coreceptor recruitment because the effect is abolished also by inhibition of de novo actin polymerization with cytochalasin D. Furthermore, pharmacological induction of Rap1 GTP significantly increased B19V-mediated gene transfer into human erythroid progenitor cells in vitro, suggesting that these cells possess the cytoskeleton organization capacity for the efficient recruitment of β1 integrins (37).

Although originally described as a nuclear protein, Ku80 was found on the cell surface of different cell types. A study aimed to investigate its role in B19V interaction showed a marked increase in B19V binding in Ku80-transfected HeLa cells that was inhibited by using antibody recognizing the N-terminus of the Ku80, suggesting that B19V interacts with specific sites of Ku80 on the cell surface. Moreover, reduction of Ku80 expression in KU812Ep6 cells by short interfering RNA resulted in the marked inhibition of B19V binding (38). However, the possible role of Ku80 in the B19V life cycle needs to be confirmed.

Cryo-electron microscopy studies of empty B19V capsid complexed with globoside showed that the receptor bound into the depression of 3-fold axis of the virion (39).

However, a successive study, attained much higher resolution, more powerful computational resources and a greater number of particles, failed to confirm the earlier observation, but neither specific complexes nor specific interaction of B19V with reconstituted plasma membrane could be detected. It is thought that globoside alone does not interact directly with B19V, but rather it may function in complex with other molecules (40).

The interaction of B19V with globoside receptor was investigated in more detail.

Results showed that the binding of B19V to the cellular receptor globoside induced conformational changes in the capsid leading to the accessibility of the N-terminal region of VP1 (VP1u) to antibodies. However, the question remains whether VP1u is not accessible because it is buried within the capsid or because it is already external but not accessible to antibodies due to a particular inaccessible conformation.

VP1u exposure did not facilitate the externalization of the viral genome in response to increasing temperatures, but on the contrary, receptor-bound capsids were remarkably more resistant than native or detached capsids. It is proposed that B19V capsids would become more resistant when needed but then become flexible again upon receptor dissociation and endosomal escape to facilitate uncoating. These receptor-induced conformational changes are necessary for subsequent virus internalization: VP2-only capsids, lacking VP1u, were unable to be internalized and virus internalization was

hampered when an antibody recognizing an epitope in the N-terminal part of VP1u was added during binding. However, only a small proportion of cell-bound viruses were internalized, while the majority became detached from the receptor, probably because the interaction of B19V with isolated globoside is highly unstable due to the lack of required stabilizing coreceptors. When added to uninfected cells, the receptor-detached virus showed superior cell binding capacity and infectivity than native virus. The model proposed is a complex internalization mechanism: B19V binds to globoside and this interaction triggers conformational changes that lead the exposure of N-terminal part of VP1u that could now interact with the coreceptors. When this is not possible, the virus detaches from cell surface and the scheme is repeated until the second interaction is possible with subsequent internalization. The mechanism of detachement-reattachment would enhance the probability of productive infection by minimizing the consequences of abortive attachments (41).

Recent studies focused more on the role of VP1u in the early phases of B19V infection, using recombinant full-length or truncated versions of VP1u. The first evidence was that while native virus and virus-like particles of VP proteins (VLPs) were internalized in UT7/Epo cells, no detectable signal was observed in cells incubated with VP2-only particles. Since VP1u is the only region lacking in VP2-only capsids, this result suggested that the presence of VP1u as a component of the capsid is required for internalization. Recombinant VP1u alone is internalized efficiently in UT7/Epo cells, similar to native B19V, while N-terminal truncations totally abolished the internalization. The presence of an antibody directed against the N-terminal part of VP1 inhibited internalization of both N-ter-VP1u construct and native virus, suggesting N-terminal part of VP1u is the region responsible for virus uptake (42).

Further studies using site-directed mutagenesis confirmed that VP1-N-ter region represents the receptor-binding domain required for B19V uptake and identified a cluster of important amino acids playing a critical role. The tertiary structure prediction of the receptor-binding domain and experimental data showed a tertiary assembly of three α-helices and a conserved hydrophobic pocket, which might represent the receptor binding site (43). Overall, this finding may propose a multi-steps mechanism of virus uptake: the binding of

B19V to the globoside receptor may lead to conformational changes that allow the exposure of a critical domain in the VP1u region, which could interact with coreceptors, stabilizing the interaction and favouring the viral uptake.

The early steps of B19V infection were deeply investigated in UT7/Epo cells. B19V and its receptor globoside were found to associate with lipid rafts, predominantly of the noncaveolar type. Pharmacological disruption of the lipid rafts inhibited infection when the drug was added prior to virus attachment but not after virus uptake, indicating that plasma membrane rafts are important for the infectious entry/trafficking of B19V and not for later steps. The virus is internalized by clathrin-dependent endocytosis and spreads rapidly throughout the endocytic pathway, reaching the lysosomal compartment within minutes, where a substantial proportion is degraded. B19V did not permeabilize the endocytic vesicles, indicating a mechanism of endosomal escape without apparent membrane damage. Bafilomycin A1 and NH_4Cl, which raise endosomal pH, blocked the infection by preventing endosomal escape, resulting in a massive accumulation of capsids in the lysosomes. In contrast, in the presence of chloroquine, the transfer of incoming viruses from late endosomes to lysosomes was prevented, the viral DNA was not degraded and the infection was boosted. B19V would require acidification to facilitate the process of endosomal escape, probably with the involvement of the phospholipase activity of VP1. Viral capsids and viral DNA were not detected inside the nucleus because of an inefficient import. However, in chloroquine-treated cells, B19V DNA was efficiently imported into the nucleus and it was not associated with capsids, which remained extranuclear. Moreover, since the number of intact capsids decreased significantly while the viral DNA remained stable in the nucleus, it is plausible that uncoating takes place prior to the DNA import into the nucleus (44).

How B19V escapes from endosomes and the pathway involved in the nuclear import of viral DNA need to be elucidated.

3.2. GENOME REPLICATION

Once the viral genome is exposed within the nucleus, replication of viral genome and transcription of messengers require cellular machinery. Conversion of the ssDNA genome into a dsDNA is the first step and a possible determinant of infection restriction. A hairpin-primed model of DNA replication is proposed (Figure 4). ITRs present at each end of genome contain complementary sequence allowing the formation of double-stranded terminal hairpin structures that function as priming sites for cellular DNA polymerase to synthesize the complementary strand on the parental genome. Transcription of the dsDNA is necessary for production of viral proteins essential for genome replication. NS protein, with endonuclease and helicase activity, binds the replication origin (Ori), nicks the so-called terminal resolution site to form a novel 3'-OH for starting DNA synthesis. ITRs are than repaired and a duplex replication intermediate is formed. The helicase activity of NS protein is required for strand displacement leading reinitiation of the process. The rolling-hairpin dependent replication proceeds with cycle of nicking and release of ssDNA that is finally packaged into the capsid (45, 46).
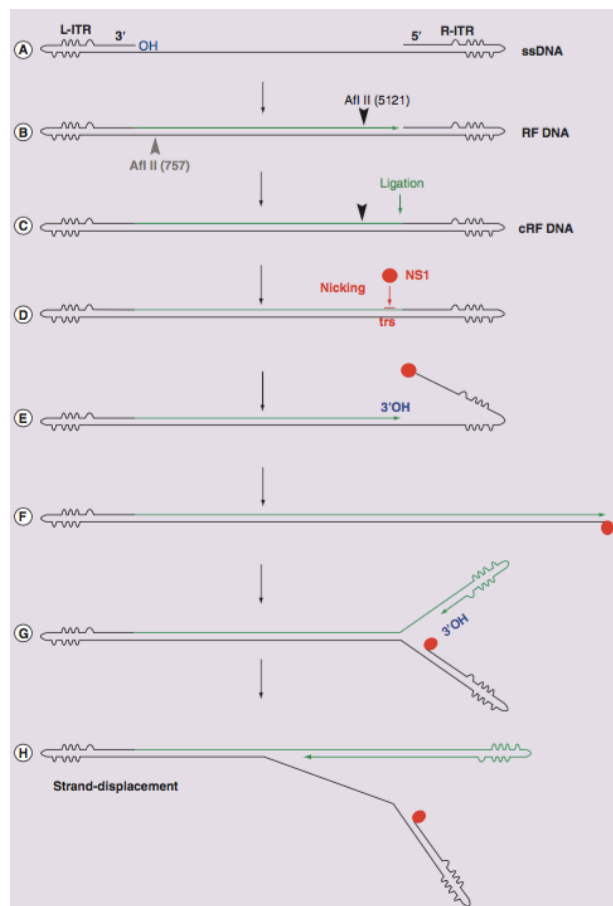
Figure 6: Rolling-hairpin model for B9V replication (46).

Replicative intermediates of B19V have not been thoroughly characterized. ssDNA, monomeric dsDNA and dimeric dsDNA forms were detected in permissive cells (47, 48). By using the 293 cell transfection system, a B19V DNA replication origin has been identified (45). The minimum origin of B19V DNA replication is only 67 nucleotides (nucleotide 5214 to 5280), and covers a NS-terminal resolution site and four repeated NS-binding elements (NSBEs). B19V-NS specifically binds to the NSBE1-NSBE2 region in an in vitro binding assay, while NSBE3 and NSBE4 may provide binding sites for potential cellular factors (49), which should assemble a nucleoprotein complex involving cellular factors to separate the dsDNA and enable NS protein to nick the top strand at the terminal resolution site.

3.3. GENOME EXPRESSION

The double-stranded intermediate is a transcriptional active template. A unique functional promoter, p6, directs transcription from the left to the right of the genome (50, 51). A fragment upstream of the promoter containing two GC-box motifs was identified. Mutations of this GC-box reduce in vitro transcription from the p6 promoter, suggesting the GC-box motif is a controlling sequence for in vitro transcription (52). Strong activity of the p6 promoter was measured even in non-permissive cell lines (53). To determine promoter activity and to characterize regulatory elements, sequences spanning the total p6 promoter and subfragments of them were introduced into a eukaryotic expression vector upstream of the luciferase gene. Several cis-acting elements were identified for the transactivating activity of NS proteins and for recognition of transcription factors (54).

P6 promoter controls the synthesis of at least nine transcripts. The set of mature transcripts originates by a combination of co- and post- transcriptional events due to the presence of two splicing donor sites (D1 and D2), each followed by two alternative splice acceptor sites (A1-1/2 and A2-1/2), and of two transcriptional termination sites in the middle and at the right of the genome (pAp and pAd) (55). All viral mRNAs share a common sequence of 60 nucleotides at their 5'-end, then, one class of mRNA is not spliced and terminates in the middle of the genome, containing the ORF coding for the NS protein, while all other classes undergo single or double splicing, terminating either in the middle or

at the right end of the genome, containing ORF coding for viral capsid proteins or other small proteins (56).

Precise mapping of splicing junctions and cleavage-polyadenylation sites was first obtained by cloning and sequencing of cDNA libraries obtained from infected erythroid cells (57). All the spliced B19V mRNA transcripts contain the 60 nt long 5' leader sequence spliced from the D1 splice site to the central exon, which spans the A1-1/A1-2 to D2 splice site. Further splicing at the D2 donor site is a central step in the control of B19V pre-mRNA processing, depending on the balanced recognition of cis-elements at A1-1/A1-2 or D2 splice sites (58).

A second key factor in the mapping of viral mRNAs is the frequency of cleavage-polyadenylation events at the centre or right end sites present in the genome. Cleavage at pAp1 will generate the most abundant classes of viral mRNAs, cleavage at pAp2 will occur at tenfold lower frequency and generate alternative mRNAs potentially including an additional small ORF for a 9 kDa protein, while read-through will generate mRNAs extending into the capsid coding region and coding for VP1 protein. Competitive splicing from D2 to A2-1 or A2-2 sites will regulate the production of mRNAs coding for VP2 or 11 kDa proteins, respectively. All of these events appear to be coordinated and in relation to the replicative process involving the DNA template (59-61).

A first model of B19V genome expression was obtained in infected UT7/Epo-S1 cells. RNA transcription appeared as an early event following infection, with viral RNA detected about 6 hours after infection (hpi) and with an earlier appearance of non structural protein RNA (6 hpi) compared to capsid protein RNA (24 hpi). Viral replication, in contrast, did not start before 16 hpi, suggesting an 'early and late model' of gene expression (62).

A more precise reevaluation of the expression profile of B19V genome by using quantitative Real Time-PCR array proposed to considering B19V genome as a single replicative and transcriptional unit, characterized by two-state expression profile, either silent and non-replicating or transcriptionally active and replicating. Viral RNA was detected at 6 hpi in permissive cells, its increase preceded that of viral DNA and utilization of the processing signals is relatively constant throughout the viral infection cycle (63, 64). Overall, such data indicate that the genome of B19V can be considered as a single functional unit, whose expression profile can be clearly differentiated depending on the degree of intracellular

restriction. In non-permissive cellular environments, the viral genome can be present but is silent, while in permissive cellular environments, the genome is active and both full transcription and replication of the viral genome occur, resulting in a productive replicative cycle. The generation of a full complement of viral mRNAs appears to occur and be maintained before the onset of template replication, thus contrasting the previous distinction between early and late events (14).

3.4. PROTEOME

The proteome potentially encoded by B19V appears to be limited (56, 65-68). A total of six ORFs are present on the genome. In the left half of the genome, unspliced mRNAs contain a major ORF in frame 1, coding for NS protein. In the right half of the genome, single-spliced mRNAs contain a major ORF in frame 2 encoding for VP1, and double-spliced mRNAs contain a portion of the same ORF encoding for VP2. As both capsid proteins are coded from the same ORF in frame 2, the two structural proteins differ only for the so-called VP1 unique region (VP1u). Two ORFs in frame 3 are present in the middle and right end of the genome and have the potential to code for a 9 kDa and 11 kDa proteins, respectively. A small additional ORF, positioned in frame 2 ahead of the ORF for VP proteins, has the potential to code for 7.5 kDa protein. However, the RNA complement is only indicative of the potential viral proteome. A deep analysis for characterization of the whole viral proteome, definition of post translational modifications of viral proteins, investigation of the dynamics and interactions of viral proteins produced in infected cells, and the role of the minor proteins, is still lacking.

3.4.1 NS protein

The NS protein (74 kDa) is composed of 671 aa. It is produced early in infected cells and it possesses a DNA-binding domain, endonuclease, helicase and transactivating activities. It is essential for viral replication promoting terminal resolution and strand unwinding on DNA replicative intermediates, necessary for priming of strand displacement synthesis (45). NS protein transactivates its own promoter promoting viral replication and transcription (69),

but it is able to transactivate other promoters in heterologous system, such as IL-6 and TNF-α promoters in NS-transduced K562 and U937 cells, respectively (70,71).

All their activities may explain its cytoxicicity (72) that was abolished when the nucleoside triphosphate-binding motif was mutated (73). NS protein expression in erythroid lineage cells induces DNA fragmentation and apoptosis, activating a caspase-3 dependent pathway. Caspase 3, 6, and 8 inhibitors repressed B19V- and NS- induced apoptosis. Since Fas-FasL interaction seemed not involved, the cells were sensitized to TNF-α-induced apoptosis (74). Sensitivity to TNF-α was not due to upregulation of TNF-receptor or TNF-α expression, thus NS protein might modulate TNF-receptor signaling by direct interaction with certain components of the signaling pathway downstream of TNF-receptor (75).

3.4.2. VP proteins

Two capsid proteins form the capsid shell, VP1 of 781 aa (86 kDa) and VP2 of 554 aa (61 kDa). The two proteins are identical except for a sequence of 227 aa present at the N-terminus of the VP1 protein, which constitutes the VP1u region with phospholipase activity (76). Both proteins accumulated through the course of infection and are transported to the nucleus where virion assembly may occur. The relative abundance of the two proteins depends in part on the relative abundance of their mRNAs and in part on different efficiencies of translation. A non consensus basic motif in the C-terminal region of VP1/VP2 mediates transport of capsid proteins to the nucleus, where capsid assembly and genome packaging may occur (77).

VP proteins can be express in mammalian and insected cells. The baculovirus expression system is the most diffuse method for heterologous expression of VP proteins. While VP2 protein alone can self-assemble without viral DNA to form virus-like particles (VLP) that are similar to native virions, VP1 protein alone does not (78-81).

VP2 protein was shown to interact directly with B19V receptor, an event that favours the exposure of VP1u region. The main neutralizing epitopes of B19V are in the VP1u region and the phospholipase A2 (PLA2) activity is required for viral infectivity. Mutations of critical amino acids strongly reduce both PLA2 activity and, proportionally, viral infectivity, but cell surface attachment, entry, and endocytosis are not affected. PLA2 activity could be

critical for efficient transfer of the viral genome from late endosomes/lysosomes to the nucleus to initiate replication (76, 82).

3.4.3. Small proteins

The B19V genome encodes for at least three small proteins. Two of these are in frame 3, the 9 kDa and 11 kDa proteins, and one in frame 2, the 7.5 kDa protein. The 11 kDa protein is the best characterized. It translated from the small, double spliced mRNA cleaved at the pAd site. It is a proline-rich protein presenting SH3 binding sites and with cytoplasmatic localization. It is essential in maintaining infectivity, probably involved in post-transcriptional events necessary to have a correct balance of capsid proteins and in altering the cellular environment to promote viral replication and maturation. Interaction with some cellular factors, such as receptors-binding protein 2, has been demonstrated (83). 11kDa protein induced apoptosis in infected primary erythroid progenitor cells, by caspase-10 pathway (84). 7.5 kDa protein expression was discovered by in vitro mutagenesis and was also observed in COS-7 cells transfected with a plasmid containing the B19V genome as well as in human peripheral mononucleocytes infected with B19V, by immunoprecipitation of cell lysates with polyclonal antibodies raised against a synthetic peptide corresponding to a portion of the predicted protein sequence. (68). It was not associated to any function right now.

The expression of the predicted 9 kDa protein has not been actually traced in infected cell, thus the exact function of its corresponding small mRNAs is not elucidated.

3.5. LATE EVENTS

The last phases of B19V life cycle are poorly characterized. After translation in the cytoplasm, viral proteins are transported back to the nucleus where the assembly of the virions into large inclusion bodies occurs. New progenies escape from infected cells presumably after cell lysis, as supported by the pronounced cytopathic effect seen in the bone marrow cells.

4. TROPISM

4.1. CELLULAR RECEPTORS

B19V infection is restricted by the narrow tropism of the virus. In vivo, the main target cells are erythroid progenitor cells from bone marrow (85). B19V was first propagated in suspension cultures of human erythroid bone marrow, stimulated with erythropoietin, from patients with B19V infection (47, 48). Virus inoculation in vitro reduced the number of erythroid cells and alters the morphology, as demonstrated by the presence of characteristic giant erythrocells.

B19V purified from viremic sera inhibited bone marrow-derived erythroid cells in a colony formation assay and the virus was detectable in infected EPCs. The susceptibility of hematopoietic stem cells to B19V was assessed by the inhibition of colony formation and the target cells were identified in the limited lineage from BFU-E to erythroblasts (86).

Erythroid progenitors cells susceptible to B19V can be obtained also from peripheral blood, foetal liver and umbilical cord blood (87-89). Anyway, due to its strictly tropism, only few cell lines support B19V infection, including erythroid leukemic cell lines, KU812Ep6 and JK-11, and human megakaryocytic cell lines, UT7/Epo and UT7/Epo-S1 (90, 91). UT7/Epo-S1 is the most sensitive and widely used cell line for in vitro studies, although it shows limited ability to support viral infection and low viral yield.

The lacking of adaptation to growth in vitro cell cultures have impaired a thorough understanding of viral life cycle and limiting the source of virus to sera of viremic patients. Recently, new advances in developing erythroid culture systems starting from peripheral blood hematopoietic stem cells provided a more suitable model system to study B19V replicative cycle in primary target cells (91, 92).

The cellular factors influencing B19V permissiveness are not yet identified and are a major filed of interest to understand the pathogenic potential of B19V.

Many factors contribute to the strictly tropism of B19V. The first determinant of cellular sensitivity is the expression of globoside. However, globoside is expressed on several cell type, not only of the erythroid lineage, such as megagaryocytes and in some endothelial cells, and these cells are not permissive to B19V infection. Thus, the presence of globoside

by itself is not sufficient to explain the narrow tropism and the role of coreceptors in virus entry need further investigation (94).

As described, the VP1u domain plays a critical role in the viral uptake by direct interaction with cellular surface. Recently, this property of VP1u region was exploited to develop a cell specific targeting system. B19V-VP1u was conjugated to NeutrAvidin as a loading platform for biotinylated cargo. Using a biotinylated fluorescent dye as a reporter molecule, the VP1u–NeutrAvidin appeared as a unique marker for intermediate erythroid differentiation stages, around the proerythroblastic/early basophilic stage, and specifically detected early erythroid precursors or erythroleukemic cells in heterogeneous cell populations from different tissues. Thus, this system could represent a reliable marker for targeting B19V susceptible cells and the possibility of a yet unknown cellular receptor exclusively expressed during the intermediate erythroid differentiation could be intriguing (95).

Since B19V DNA can also be detected in additional cell types, such as endothelial cells of the myocardium, alternative mechanism of infection are supposed. B19V bound primary endothelial cells at a similar level as that of UT7/Epo-S1 cells, but internalization of the virus was strongly reduced. This deficiency in internalization was significantly enhanced by preincubation of the virus with anti B19V-antibodies. Antibody-dependent enhancement (ADE) was mediated by the direct interaction of B19V-antibodies complex with the complement factor C1q and its receptor CD93 on the cell surface. This alternative mechanism of virus uptake could play a role in the pathogenicity of cardiac B19V infection (96).

4.2. ERYTHROPOIETIN DEPENDENCE

Another key factor shared by all the megakaryocyte-erythroid lineage cells productively infected by B19V is the need of erythropoietin (Epo) for growth (47, 90). Epo is not only necessary for cell growth but also to activate the signal cascade downstream of Epo receptor (EpoR) that achieves a productive viral replication. EPCs culture in fact did not support B19V replication in the absence of Epo, although virus entered the cells. The EpoR/Janus kinase 2 (Jak2) pathway played a direct role in supporting replication of the B19V genome, involving the signal transducer and activator of transcription 5A (STAT5A),

mitogen-activated protein kinase (ERK/MAPK) kinase (MEK) and phosphatidylinositol-3 kinase (PI3K) (97).

4.3. HYPOXIA

Hypoxia also promotes viral replication. EPCs cultured in hypoxic condition showed a significantly increase of B19V expression and replication compared to EPCs cultured under normoxia. The low oxygen tension levels measured in bone marrow and during foetal development could contribute to B19V replication in sensitive cells in vivo (98). Hypoxia promoted replication of B19V genome within the nucleus, regulating Epo/EpoR receptor signaling trough a STAT5A and MEK/ERK signaling, rather than the canonical PHD/HIFa pathway. The simultaneous up-regulation of STAT5A signaling and down-regulation of MEK/ERK signaling boosted the level of B19V infection in EPCs under normoxia to that in cells under hypoxia. The MEK/ERK pathway is therefore a negative regulator of B19V infection in EPCs. The B19V small 11 kDa protein has been shown to interact with Grb2, a crucial adaptor for the activation of MEK/ERK signaling, which is activated by phosphorylation of EpoR. These findings may lead to suppose that 11 kDa protein interacts with Grb2 to inhibit MEK/ERK signaling, thereby facilitating B19V DNA replication during infection (99).

4.4. MACROMOLECULAR SYNTHESIS

Conversion of the incoming parental ssDNA into a dsDNA is the first step in the macromolecular synthesis and a possible Achilles' heel for a productive replicative cycle. Non-permissive cells may be not able to support the synthesis of the complementary strand, although they can be susceptible to viral entry. For example, HepG2 hepatocellular carcinoma cells cannot support B19 virus replication, although viral DNA was detected within cells, but neither genome replication nor transcription and protein expression were measured (100).

Cell permissiveness could depend also on the ability to express the full set of viral mRNA, either at transcriptional and translation level. In permissive cells, mRNAs splicing of mRNAs at the second intron lead to generation of sufficient amounts of VP2 transcript, permitting

virus assembly. A blockage in the production of full-length transcripts at the internal polyadenilation site is associated with the limited permissiveness to B19V infection because of the relative absence of VP proteins (101). Replication of the viral genome on the contrary promotes read-through of pAp and the polyadenilation of transcripts at the distal site pAd, leading to generation of full-length transcripts that encode for essential proteins (61). Moreover, the expression profile shifted preferentially on the left half of the genome lead to a mainly production of NS and 7.5 kDa proteins, and a consequent abortive infection and cell death due to its cytotoxic and apoptosis-inducing properties.

4.5. CELL CYCLE ARREST

B19V induces cell cycle arrest and apoptosis (102). In infected UT7/Epo-S1 cells, more than 60% of the cells showed the 4N karyotype at 48 hpi, indicating an accumulation of the G2/M-phase cell population. The cell cycle progression is critically regulated by sequential activation of cyclin-dependent kinases (cdks). Cyclins A and B are involved in regulation of the S and G2/M phases of the cell cycle. Expression of cyclin A becomes detectable near the G1/S transition and peaks in the S phase, and interacts with both cdk2 and cdc2 to ensure completion of DNA replication before entering into mitosis. Cyclin B is synthesized through the S and G2 phases and associates with cdc2 to become an inactive complex, called the pre-mitosis-promoting factor (MPF). Translocation of active MPF containing cyclin B1 from the cytoplasm into the nucleus is indispensable for cell cycle entry into the M phase. In B19V-infected UT7/Epo-S1 cells, cyclin B1 accumulated in the cytoplasm but not in the nucleus at 24 hpi without an up-regulation of its mRNA. These observations suggest that MPF is activated in the cytoplasm of B19V-infected cells, but cannot translocate to the nucleus, thus resulting in suppression of cell cycle transition from G2 phase into M phase (103).

In the presence of a mitotic inhibitor, B19V infection induced not only G2 arrest but also G1 arrest. UV-irradiated B19V, inactivating the expression of NS, still harboured the ability to induce G2 arrest but not G1 arrest. Furthermore, treatment with caffeine, a G2 checkpoint inhibitor, abrogated the B19V-induced G2 arrest despite expression of NS. These results suggested that the B19V-induced G2 arrest is not mediated by NS expression (104).

Furthermore, NS expression significantly increased p21/WAF1 expression, a cyclin-dependent kinase inhibitor that induces G1 arrest. Thus, G1 arrest mediated by NS may be a prerequisite for the apoptotic damage of erythroid progenitor cells upon B19V infection (105).

Primary EPCs, B19V infected or NS transduced, displayed G2 arrest mediated by NS-dependent enhancement of nuclear import of E2F4/E2F5 as well as repression of E2F4/E2F5 target genes and deregulation of a variety of transcription factors important for cell cycle control and differentiation. NS-dependent E2F4 and E2F5 nuclear translocation is likely an early event and initiate G2 arrest, allowing B19V to deregulate host cell cycle in order to create a favourable environment for its replication. Infected EPCs showed also time-dependent increase of E2F7, E2F8, p53, and p21 as well as the activation of p53, known to be induced in response to DNA damage. Thus, the proposed model is that interaction of NS with E2F4 or E2F5 induces exclusive redistribution of these repressive E2Fs to nucleus, leading to stable G2 arrest and eventually impairing erythroid differentiation by downregulation of E2F target genes. Subsequently, activation of G2-related transcription factors and/or DNA repair proteins enhances viral transcription and DNA replication. As B19V infection progresses, viral replication activates p53 signal transduction and upregulates E2F7 and E2F8 in the context of the DNA damage response, blocking cell cycle progression. In this way, virus production would be maximized while simultaneously abrogating the cell differentiation machinery (106).

A more careful examination of B19V infected EPCs using 5-bromo-2'-deoxyuri- dine (BrdU) pulse-labeling and DAPI staining, which precisely establishes the cell cycle pattern based on both cellular DNA replication and nuclear DNA content, was performed. Although both NS protein transduction and infection immediately arrested cells at a status of 4N DNA content, B19V-infected 4N cells still incorporated BrdU, indicating active DNA synthesis. Moreover, several S phase regulators were abundantly expressed and colocalized within the B19V replication centers. Taken together, the results confirmed that B19V infection triggers late S phase arrest, which presumably provides cellular S phase factors for viral DNA replication. It is possible that B19V-DNA replication induced DNA damage response

that cause cell arrest at S phase, while NS alone arrests cells at a status G2/M and that the compromising of these two arrest blocks the infected cells at late S phase (107).

4.6. DNA DAMAGE RESPONSE

Several studies have shown that parvovirus infection induces a DNA damage response (DDR) that plays an important role in viral DNA replication. DDR is triggered by damage DNA structures, such as ssDNA breaks, dsDNA breaks and stalled replication forks. In particular, B19V infection induced a broad range of DDRs by triggering phosphorylation of all the upstream kinases of each of three repair pathways: ATM (ataxia-telangiectasi mutated), ATR (ATM and Rad3 related), and DNA-PKcs (DNA-dependent protein kinase catalytic subunit). Inhibition of kinase phosphorylation, through treatment with either kinase-specific inhibitors or kinase-specific shRNAs, revealed that only signaling via the ATR-Chk1 pathway is critical to B19V replication, while DNA-PK signaling contributed to a lesser extent and ATM signaling was not influent. The replication of B19V DNA following the rolling-hairpin model involves steps that could activate a DDR, such as formation of replication origin complex, nicking at the terminal resolution site or unwinding. It is possible that ATR recognizes the nicked site within the terminal sequence of the genome and that the ssDNA binding protein RPA32 is recruited to the displaced ssDNA, which mimics a stalled replication fork. However, knockdown of ATM, ATR and DNA-PKcs did not affect B19V infection-induced G2/M arrest, suggesting that B19V infection causes G2/M arrest through a DDR-independent cell cycle checkpoint (108).

Preventing replication of the B19V dsDNA genome by mutating the endonuclease domain or helicase-A motif within NS protein, which prohibits the DDR, did not reduce the percentage of cells arrested at G2/M. Therefore, B19V utilizes the mechanism of a DDR only to promote viral DNA replication, and the NS-induced G2/M arrest is dispensable for viral DNA replication (109).

5. PATHOGENESIS

5.1. EXPERIMENTAL INFECTION

The kinetics of B19V infection has been studied in two set of experiments involving adult healthy volunteers (110). Subjects inoculated with 10^8 virus particles showed viremia after 6 days reaching a peak of 10^{11} virus particles/ml after 8-9 days. Viral DNA was found in throat swabs during viremia but not in urine or faeces. Viremia disappeared with the activation of immune response. On days 6-8, the first phase of illness occurred with viral infection-related symptoms such as headache, myalgia, chills and pyrex, typically correlated to cytokine release, even if production of α-interferon was not detected. This first episode of illness coincided with viremia and the detection of circulating IgM (Figure 7). The bone marrow examination showed an almost complete loss of erythroid precursors at day 10, and the number of BFU-E and CFU-E in peripheral blood was decreased. A second phase of clinical illness could be recognized on days 15-17, when IgM levels were highest and IgG production started, with symptoms typical of B19V infection, such as maculopapular rash, arthralgia and in some cases arthritis. The illness was short-lived, with the rash fading after 2/3 days, while the joint symptoms persisted. In this period, viremia was absent.
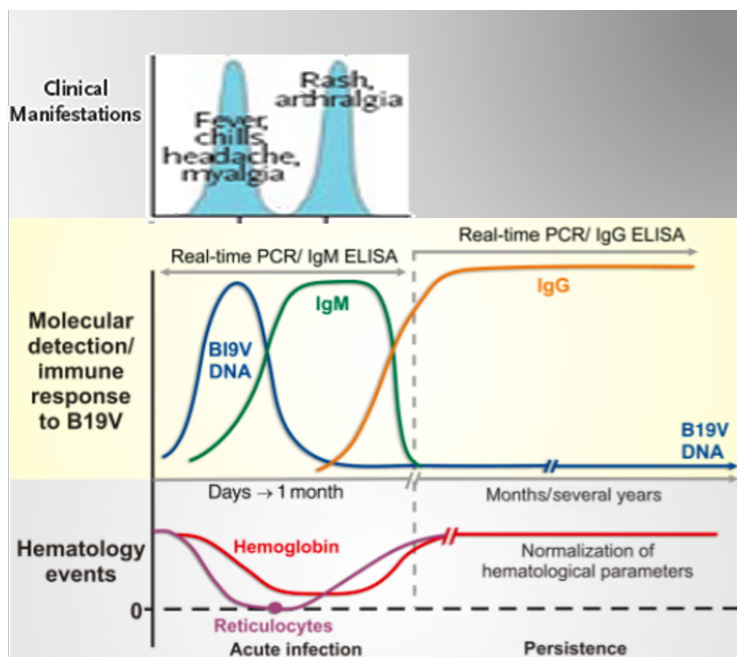
Figure 7: Clinical course following B19V infection (126).

5.2. CLINICAL MANIFESTATIONS

B19V is spread by respiratory route. The mechanisms of virus transmission from the oropharyngeal mucosa to the target cells are unknown: a first cycle of virus replication could occur in tonsils and the lymphoid vessels could be involved in spreading infection, or the virus can gain access to vessels by transcytosis through respiratory epithelia.

When the virus reaches the bone marrow, it can infect erythroid progenitors cells. The cytopathic effect on infected cells is manifested as giant pronormoblasts with large eosinophilic nuclear inclusion bodies and cytoplasmatic vacuolization (Figure 8). The consequently block of erythropoiesis derives from the capability of the virus to induce cell-cycle arrest, to inhibit the formation of bone marrow derived erythroid colonies at the BFU-E and CFU-E stages, and eventually to cause apoptosis of infected cells. However, the block in erythropoiesis is temporary because the more undifferentiated precursors are resistant to B19V and infection can be resolved with a neutralizing immune response. The productive infection in the bone marrow allows virus release in the blood, starting a secondary viremia, that can reach high levels (10^{12} virus/ml), and leading the systemic distribution of the virus (14).
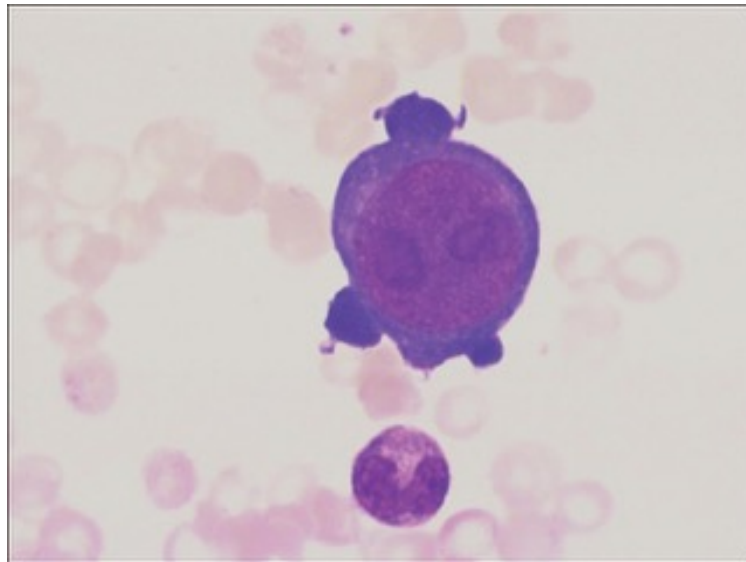
Figure 8: Giant pronormoblast with typical 'dog-ear' projections (126).

In normal subjects, production of neutralizing antibodies contributes to the rapid clearance of infection, usually within 3-4 months (111, 112). The decrease of haemoglobin levels is

only transient and the destruction of reticulocytes has minimal clinical effect, as erythrocytes have long life spans. Approximately 25% of infected individuals will be completely asymptomatic during their infection, while 50% will have only non-specific flu-like symptoms of malaise, muscle pain, and fever. The two classical late clinical manifestations in immunocompetent hosts are erythema infectiosum, typical of children, and arthropathies, typical of adults.

5.2.1. ERYTHEMA INFECTIOSUM

The first association of B19V with erythema infectiosum is dated 1983, when the discovery of specific B19V-IgM in the serum of involved patients confirmed the etiology of the disease (113). Erythema infectiosum, also known as fifth disease, appears approximately 18 days after infection and is characterized by slapped cheek rash and relative circumoral pallor. A second stage eruption, with erythematous maculopapular exanthema on the trunk and limbs, often appears 1 to 4 days later. Prodromal symptoms often may include fever, coryza, headache, and nausea. The rash is characterized by pink maculae that usually undergo a central fading. It may be transient or recurrent and variations of intensity can depend on environmental factors, such as light exposure and heat.

Figure 9: Erythema infectiosum with rash and slapped cheeks.

5.2.2. ARTHROPATIES

Arthralgia and arthritis are the most common manifestations in adults. The first evidences of the link between arthropaties and B19V are dated back to 1985 (114). In children, arthritis can accompany erythema infectiosum at low frequencies (10% or less), while the incidence in adults is approximately 60% in females and 30% in males. Typical symptoms are acute peripheral polyarthritis, usually symmetric, affecting mainly the small joints of hands, feet and keens (115, 116). Joint symptoms usually resolve in three weeks, although in some cases, arthropathy may become chronic and about one half of patients whose sympotms become chronic meet the criteria of American Rheumatoid Association for a diagnosis of rheumatoid arthritis (117).

The involvement of B19V in the development of rheumatic diseases is subject of continuous investigations. Since the occurrence of arthralgia coincides with the detection of circulating IgM and IgG direct against the viral capsid proteins, it is possible that immune complexes deposited in the synovial fluid are involved in the pathogenesis of B19V-related arthropaties.

A variety of autoimmune disease, rather than arthopaties, has been associated to B19V, such as systemic lupus erytematosus, Kawasaki disease, vasculitis and others. Some clinical features of both acute and chronic B19 infection are very similar to those of autoimmune diseases, leading the researchers to investigate the role of autoimmunity in the pathogenesis of B19V (118). The production of autoantibodies against proteinase 3 and myeloperoxidase and the detection of antinuclear antibodies have been reported in the course of B19V infection.

The production of antiphospholipid antibodies in patients with rheumatic disease was associated with persistent B19V infection. This link is supported not only by the presence of autoantibodies but also by the similarity in the clinical symptoms present in B19V-infected patients and in subjects with the antiphospholipid syndrome. A possible mechanism involved in the production of this kind of antibodies may be the phospholipase A2 activity of VP1u region. The enzymatic activity of VP1u can induce the production of leukotrienes and prostaglandins, which contribute to the inflammatory process, and of unusual cleavage products from cellular phospholipid factors that may activate the antiphospholipid

antibodies response. This is a possible explanation for the formation of autoantibodies together with the classic molecular mimicry mechanism. It has been shown in fact that VP1-specific IgG react specifically with human keratin, collagen type II, single-stranded DNA and cardiolipin (119).

The NS protein may be involved too in the autoimmune phenomena. It has a transactivating domain that can work on the viral p6 promoter as well as on cellular promoters, like those controlling the expression of TNF-α and IL-6. The costant stimulus derived from these proinflammatory cytokines during persistent B19 infection may result in the induction of autoimmune reactions (120).

B19V DNA may be found in inflamed joints and in synovial membranes (122). However, its presence is not a sufficient marker since it was found also in control samples without chronic arthritis. The mechanism by which the virus can persist in the synovial membrane is unknown: synovial membrane cells are not permissive to B19V, although globoside is expressed on the human synovium (123). However, it was demonstrated that normal human synovial fibroblast treated in vitro with B19V positive serum show an invasive phenotype that means an increased ability to degrade reconstituted cartilage matrix (124).

In subjects with alterations in the erythropoiesis process or defects in the immune system, infection becomes manifest as pure red-cell aplasia and anemia.

5.2.3. TRANSIENT APLASTIC CRISIS

In patients with haematological disorders with improved red cell turnover, including increased red blood cells destruction (sickle cell disease, hereditary spherocytosis, chronic autoimmune anemia) or decreased red blood cells production (iron deficiency anemia, thalassemia), B19V infection can lead to the classical aplastic crisis (125). The arrest of the production of erythrocytes and the reduced lifespan of red cells lead to a marked drop in haemoglobin. Usually, aplastic crisis presents with anaemia, weakness, dyspnoea, and confusion, rarely with congestive heart failure and in the most severe cases bone marrow necrosis. In some cases, concurrent thrombocytopenia, neutropenia or pancytopenia is

found. The aplastic crisis is typically self-limited as the activation of a specific immune response clears the infection and red cell production returns to baseline. (126)

5.2.4. PURE RED CELL APLASIA

In immunocompromised patients, where the immune system fails to clear B19V infection, anaemia can become chronic and persistent or recurrent viremia can be detected. This can lead to hypoplasia or aplasia of the erythroid cells and precursors, reduction of peripheral reticulocytes and a severe acute or chronic anaemia, which can be life-threatening. This condition includes situations of congenital or acquired immunodeficiencies, such as HIV-infection, of malignancies, such as acute lymphatic leukaemia, acute or chronic myeloid leukaemia, of bone marrow or solid organ transplantation, and of chemotherapy treatment. In immunocompromised patients B19V infection generally does not manifest with the classic rash or joint symptoms, may be due to the inadequate immune response, but clinical hallmarks are fatigue and pallor (127-131).

5.2.5. MATERNAL INFECTION

In case of maternal infection, B19V can cross the placental barrier and infect the fetus, leading to asymptomatic infection or adverse outcomes, such as fetal anemia, hydrops fetalis or fetal death (132). The risk of fetal infection and tissue damage is greater in the second trimester. This can be linked to the expression of globoside on the placental trophoblast that is higher in the first and second trimester but decrease with gestional age (133, 134). The change in the expression level of globoside can therefore reflect the frequency of intrauterine infection. Moreover, the site of erythrocyte production during early development is the fetal liver and, because of the boosted demand from the growing fetus, there is an increase in red blood cell mass and a reduction of red cell life span. These factors make the fetus particularly vulnerable at deficiencies in the erythropoiesis process. Trophoblasts are not permissive to the virus but they may promote its transcytosis to the fetal circulation (135). When the virus is in fetal circulation, it can infect erythroid progenitor cells. The consequent block of fetal erythropoiesis and red cell precursors destruction may lead to severe anemia, fetal death and non-immune hydrops fetalis.

Hydrops fetalis is caused by functional failure of the liver and is characterized by anemia (hemoglobin levels of 2 g/dL or lower), hypoalbuminemia, peripheral oedema and congestive heart failure that can be lethal (136). Cardiac failure can also be associated to fetal myocarditis as a consequence of direct infection of fetal cardiomyocytes (137, 138).

The outcome of fetal infection is influenced by several factors. First, the immune status of the mother is crucial since the presence of specific IgG is protective for the fetus. A second aspect is the gestational age: as described above, the rate of intrauterine transmission is higher in the first two trimesters. The consequences for the fetus also depend on its development stage. The risk of fetal loss is higher when infections occurring in the earlier stages, when the rate of hematopoiesis increases and the fetus is more vulnerable to low hematocrit due to high tissue oxygen demand. Furthermore, hydrops is most common in the central part of pregnancy, while the incidence of B19V-related fetal loss is lower in the third trimester (139). Finally, congenital infections have been occasionally associated to neonatal anemia or abnormalities, but the number of case reports is too low to support a link between B19V infection during pregnancy and fetal malformations (140).

The spectrum of clinical manifestations associated to B19V infection is in constant expansion.

5.2.6. CARDIOMYOPATHIES

In the recent years, a major concern aspect is the cardiac tropism of B19V.

The presence of B19V has been revealed in endomyocardial tissue and in the nuclei of fetal myocytes (141). Its association with myocarditis was proposed in both children and adults (142-144). Infection of myocardial endothelial cells activates inflammatory responses in the cardiac tissue that, together with endothelial dysfunction, induces cardiac cell injury. At a second level, the specific cellular immune response is able to recognize and destruct infected cells. Moreover, the immunological cross-reaction to epitopes shared between viral antigens and myocardial cellular antigens may promote an autoimmune response that enhances the inflammatory process. (145)

A recent in vitro study suggests that the phospholipase activity of B19V-VP1 can cause inflammatory cardiomyopathy and endothelial cell dysfunction through downregulation of Na+/K+ ATPase. This induce a wide range of cellular effects, such as loss of ionic equilibrium, hyperpolarization or depolarization of cell membrane, effects on the expression of different genes, that promote cell death, shrinkage or swelling (146). The molecular mechanisms responsible for the reactivation of latent B19V infection, the influence of immune response in chronic myocarditis, and immune-independent viral pathogenesis in non-inflamed hearts need more investigations to be clarified.

However, considering the rare occurrence of myocarditis in respect of the widespread circulation of B19V, it is possible that the virus is only mildly cardiotropic or that other unknown factors are needed in order to manifest clinical disease.

5.2.7. OTHER ASSOCIATIONS

The presence of B19V was detected in cases of encephalopathy, meningitis and neurologic amyotrophy, but they are very few cases and the mechanism for the neurological symptoms is unknown. Elevated levels of liver transaminases are common during B19V infection and the virus was associated to fulminant hepatitis. Other associations have been reported with necrotinzing vasculitis, Kawasaki's disease and a variety of complications, but all these associations need more investigation to be supported (126).

6. EPIDEMIOLOGY

B19V infection occurs wordwide. Data accumulated in the years report values differing widely in dependence of the sensitivity of the methodologies used, the epidemiological context, the tissue type and the geographic area.

The seroprevalence increases with age from 2% to 10% in children under 5 years old, to 40-60% in adults and up to 85% in the elderly population. During outbreaks, the rates increase at 70% in children aged 5 to 15 years and 20% in subjects older than 15 years.

The peak incidence of infection shows seasonal variation, occurring mainly in late winter and early summer with epidemic peaks every 3 to 4 years. (14)

Transmission of B19V occurs mainly via the respiratory route. Although B19V infection is not primarily associated with respiratory symptoms, viral DNA is detected in respiratory secretions during viremia.

The virus can be transmitted transplacentally to the fetus. Approximately 30%-40% of pregnant women lack measurable B19V-specific IgG and are therefore susceptible to B19V infection. However, the incidence of primary infection during pregnancy has been estimated at 1% to 5%, and subsequent transplacental transmission is 25%-50%, but the risk of fetal loss is estimated to be quite low, lower than 10% (14, 147, 148).

The presence of B19V in blood during the viremic phase of infection poses a risk of iatrogenic transmission of the virus via blood and blood components, in particular packed red cells from blood collected during the short pre-seroconversion viremic phase. B19V viremia frequency in blood products ranged between 1.3% and 0.006% according to the sensitivity of molecular assays used and seasonal epidemiologic circumstances (149, 150).

7. IMMUNITY RESPONSE

7.1. INNATE IMMUNITY

The role of innate immunity during B19V infection has not been investigated in detail but most studies have focused on the adaptive immune response.

Like other viruses, B19V-PAMPs may be recognized by cellular PRRs, the viral components acting as PAMPs are still unknown. B19V has been associated with various Toll-like receptors (TLRs), such as TLR-4, -5, -7 and -9 (151). A work investigated the role of CpG-ODN 2006 in the inhibition of erythroid progenitor cells showed that this TLR-9 ligand affects hematopoiesis by a selective inhibition of growth and development of human erythroid progenitor cells. It probably acts as a siDNA for the erythropoietin receptor (EpoR), resulting in down-regulation of EpoR expression, inhibition of EpoR mRNA expression and decrease of Epo binding (154). A possible same mechanism can be shared by B19V, whose genome has a ssDNA consensus sequence that could be potentially involved in the inhibition of erythroid progenitor cells.

A recent study investigated the effect of B19V on the expression of defensins and TLRs. The authors reported a significantly increased expression of defensins and TLR-9 on COS-7 epithelial cells after transfection with a vector expressing NS protein, but to a less extent after transfection with a vector expressing VP2 protein. Moreover, they also suggested that the cytotoxicity of viral NS protein might play a crucial role in eliciting TLRs and defensins expression since no significant variations were observed in COS-7 cells transfected with a vector expressing the mutant form of NS protein without the cytotoxicity. These findings provide a clue in understanding the role of innate immunity in B19V infection (151).

7.2. SPECIFIC IMMUNITY

7.2.1 Humoral response

Specific IgM and IgG antibodies are produced in naturally and experimentally infected individuals and are supposed to be able to progressively clear the infection. IgM are produced first, 10-12 days post infection, and usually persist for 3-6 months. IgG are detectable two weeks after infection and are assumed to be long-lasting and protective

against secondary infections. IgA can also be detected and probably plays a role in protection against infection by the natural nasopharyngeal route.

Several neutralizing epitopes have been mapped in the VP1u region and are mainly linear, while epitopes located in the common region of capsid proteins are mainly conformational. However, linear epitopes in the VP1u region and in VP1-VP2 junction regions seem to elicit a more efficient immune response than epitopes of VP2 region (152-157). It was shown that, although VP2 region contains neutralizing domains, empty capsids composed only of this protein are similarly antigenic but fail to induce high titer neutralizing antisera, compared to empty capsids composed of VP1-VP2 that elicit a stronger neutralizing antibodies response. This evidence could be in contrast with the presence of neutralizing epitopes in the VP2 region and, anymore, convalescent phase sera from patients exposed to B19V show activity confined to the common region of VP2. The data suggest that VP1 is important to enhance the antigenicity of neutralizing regions, promoting the mature capsid conformation (158-159).

A work aimed to examine the specific immune response against B19V showed that the humoral response in recently B19V infected children is dominated by antibodies directed against conformational epitopes on VP1 and VP2 and against linear epitopes on VP1u region, while linear epitopes present on VP2 are poorly immunogenic. In long-term convalescent patients, antibodies against conformational epitopes of VP1 and VP2 persist, while immunoreactivity against linear epitopes on VP1 is lost. This probably depends on the induction of B-cell memory that is maintained by the persistence of conformational antigens on specialized follicular dendritic cells (160).

Humoral immune response against NS poteins is poor investigated.

Three antigenic regions on the B19V NS protein were identified in healthy subjects when using linear peptides mapping the NS sequence. The frequencies of reactivity against NS proteins were found similar between healthy and persistent infected people, except that the latter group showed a lower reactivity to the C-terminal end of VP1/VP2 (161). However, in previous studies, aimed to investigate a possible different reactivity among patients with acute or past B19V infection, it has been supposed that NS-antibodies are

most often present in patients with chronic infection, especially in B19V-related arthritis. A possible explanation is the prolonged antigenic stimulation in persistence infection. Usually, during replication in erythroid progenitor cells, only few amounts of NS protein are produced, maybe insufficient to stimulate antibodies production; that is why the majority of sera from infected people are negative for NS-specific antibodies. In a persistence infection, on the contrary, non-permissive cells could be infected and NS protein is preferentially expressed. The NS cytotoxicity causes cell death and release of large amounts of protein that may induce a specific immune response. NS antibodies are not likely to be protective, since the virus can persist in the serum despite the presence of NS-specific immunoglobulins (162).

7.2.2. Cellular response

The cellular immune response is harder to study.

T-cell reactivity to B19V infection was first shown by measuring the proliferation responses of PBMC after in vitro stimulation by recombinant B19V proteins. The results indicated that T cells of subjects with preexisting B19V immunity show HLA II-restricted responses against B19V capsid proteins (163).

T cell reactivity after stimulation with the VP1/2 capsid antigen was than confirmed in patients with recent or remote B19V infection and not only in patients with arthropathy, as previous described. Even if the recently infected patients generally had stronger B19V reactivity than the remotely ones, some of the strongest responders are remotely infected patients that show specific responses comparable to the highest values seen among the recently infected patients. Their strong VP1/2-specific reactivity is most readily explained by a good general ability to maintain T cell memory to recall antigens. Moreover, HLA class II-restricted CD4^{+} cells are responsible for T-cell reactivity, as depletion of CD4^{+} T-cells from PBMC abrogate T-cell responses as well as the blocking by HLA class II-specific antibodies (164).

A first approach, using a peptide library designed to cover the entire NS sequence, was used to identify B19V-epitopes for CD8^{+} lymphocyte cells-mediated immunity. Following PBMC stimulation with peptides and by measuring the cytolitic activity of CD8^{+} T-cells

against autologus B-cell lines, a single HLA-B35-restricted epitope was identified. It was strongly immunogenic in B19V-seropositive donors, able to stimulate CD8$^+$ T-lymphocyte cells that showed rapid expansion in vitro, cytolysis and rapid effector function ex vivo. The strong T-cell responses may result from a continuous or intermittent exposure to viral antigen, which may be endogenously presented or easily reexposed due to the high levels of virus in the population (165).

A more extensive assessment of the specificity and kinetics of the acute CD8$^+$ T-cell responses was studied with 210 peptides synthesized to cover the sequence of NS protein, VP1u region and VP2 protein. The peptides were used to test in vitro cytotoxicity and ex vivo stimulation assays and to estimate HLA restrictions. Novel CD8$^+$ T-cell epitopes were identified, nine in the NS protein and one in the VP2 protein, while no responses were observed to the VP1u region. Seropositive healthy patients with symptomatic B19V infection rapidly develop cellular immune responses with multiple specificities. The responses are maintained at high levels for months, sometimes more than two years, maybe as the result of continuous antigenic stimulation. At the opposite, subjects with B19V persistence showed higher reactivity to the structural proteins, whereas responses to the NS protein were of lower magnitude. The immunological discrepancies between healthy and persistently infected individuals may reflect both failed immunity and antigenic exhaustion (166).

The importance of CD8$^+$ T-cells was confirmed by studying the number and phenotype of B19V-specific CD8$^+$ T-cell responses, during and after adult infection, using HLA-peptide multimeric complexes. Results indicated a continued increase in magnitude of CD8$^+$ T-cell responses during acute B19V infection, sustained even at later time points, long after resolution of clinical symptoms and control of viremia. T-cells possessed strong effector function and intact proliferative activity. B19V-specific cytotoxic T-lymphocytes were also detectable in healthy individual with remote infection, tested many years after infection, at low frequencies but with mature phenotype. Thus, data suggest that the acute infection induce persistent activated CD8$^+$ T-cell responses, possibly due to low-level antigen exposure after the resolution of acute viremia. Since the most active CD8$^+$ T-cell responses were seen when clinical symptoms had resolved, these T cell responses are not likely to be

directly volved in the acute phase, but they ultimately may contribute to the long-term control of infection and viral clearance (167).

The involvement of T-helper cells in the immune response to B19V infection was also investigated. As describe previously, first evidence was the strong proliferation of CD4^{+} T-cells, when stimulated with VP1/VP2 capsids, of both recently and remotely infected adults (164). The role of T-helper cells was explored by using recombinant VLPs composed of VP1/VP2 proteins or VP2 protein alone. The ability of VLPs to stimulate PBMC to proliferate and secrete IF-γ and IL-10 was determined in recently and remotely infected individuals. In general, B19V-specific IFN-γ responses were stronger than IL-10 responses in both recent and remote infection. VP1/VP2 capsids and VP2 capsids elicited similar T-helper cell proliferation and IL-10 responses, while the IFN-γ response was higher with VP2 capsids than with VP1/VP2 capsids. Thus, epitopes on VP2 protein are important to elicit T-helper cell responses for activation of B19V-specific B-cells in remotely infected subjects. On contrast, whereas VP1u-specific IFN-γ responses were very strong among the recently infected subjects, the VP1u-specific IFN-γ and IL- 10 responses were absent among the remotely infected subjects. This finding is in contrast with the documented persistence of VP1u-specific IgG during late convalescence (168, 169).

The peptide library approach was used also to investigate the magnitude and breadth of the CD4^{+} T-cell response to the capsid proteins in acutely infected individuals with arthropathy and in remotely infected individuals. Both groups maked broad CD4^{+} responses, but whereas responses following acute infection were detectable ex vivo, responses in remotely infected individuals were detected only after culture. Several VP-peptide pools were identified in CD4^{+} T-cell responses of acutely infected individuals, while a single dominant epitope in the VP common region was evident in remotely infected people. Phenotypic analysis of B19V-specific CD4^{+} cells suggests that they are mainly "central" memory, thus following a different evolution, after acute infection resolution, compared to CD8^{+} T-cells. Indeed, CD8^{+} T-cell responses showed an increase in frequency and the acquisition of a mature phenotype, as well as maintaining activation, over many months after acute disease. Overall, the exact role of B19V-specific CD4^{+} T-cells upon acute

infection is unknown. Hypothetically, B19V-specific CD4^{+} T-cells recognizing persisting B19 or cross-reactive self-antigens could play a role in both viral elimination and the pathogenesis of autoimmune disease, while CD8^{+} T-cell responses would limit viral replication and, in turn, reduce CD4^{+} T-cell activation and control viral persistence (170).

7.2.3. Cytokine Expression

The proinflammatory and T helper Th1/Th2 cytokine responses during acute B19V were characterized. In addition to proinflammatory cytokines IL-1β, TNF-α, IL-6 and IL-8, elevated levels of the Th1 type of cytokines IL-2, IL-12 and IL-15 were evident at time of the initial peak of B19V viral load in a few patients during acute infection. This pattern was sustained during the follow-up period. In contrast, cytokines associated with a Th2 type of immune response, IL-4, IL-5 and IL-10, as well IFN-γ response remained low during the observation time. Thus, the continuous viremia in the acutely infected patients may be associated with an aberrant cytokine profile with a selective IFN-γ deficiency despite Th1 cytokine induction. On the other hand, persistently infected patients did not exhibit an apparent imbalance of their cytokine pattern except for an elevated IFN-γ response, but this cannot explain the persistence status of the virus (171).

7.3. AUTOIMMUNITY

B19V was associated to a variety of autoimmune diseases and the relationship between B19V and autoimmunity is constantly investigated. The production of autoantibodies against proteinase 3 and myeloperoxidase and the detection of antinuclear antibodies have been reported in the course of B19V infection.

The production of antiphospholipid antibodies in patients with rheumatic disease was associated with persistent B19V infection. This link is supported not only by the presence of autoantibodies but also by the similarity in the clinical symptoms present in B19V infected patients and in subjects with the antiphospholipid syndrome. A possible mechanism involved in the production of this kind of antibodies may be the phospholipase A2 activity of VP1u region. The enzymatic activity of VP1u can induce the production of leukotrienes and prostaglandins, which contribute to the inflammatory process, and of unusual cleavage

products from cellular phospholipid factors that may activate the antiphospholipid antibodies response. This is a possible explanation for the formation of autoantibodies together with the classic molecular mimicry mechanism. It has been shown in fact that VP1-specific IgG react specifically with human keratin, collagen type II, single-stranded DNA and cardiolipin (119).

The production of antiviral antibodies with autoantigen binding properties has been previously demonstrated in chronic parvovirus B19 infection. IgG antibodies directed against VP proteins were purified from the sera of patients with persistent parvovirus infection, using a synthetic immunodominant VP peptide. Such anti-viral peptide antibodies reacted specifically with human keratin, collagen type II, single-stranded DNA, and cardiolipin. The main reactivity was against keratin and collagen type II, and there was a correlation between the clinical manifestations and the autoantigen specificity: immunoglobulins from patients with arthritis reacted preferentially with collagen II, whereas immunoglobulins from patients with skin rashes reacted preferentially with keratin. When mices were immunized with the viral peptide, antibodies able to bind the viral peptide and to cross-react with different autoantigens, including keratin, collage II, ssDNA and cardiolipin, were detected in those that developed a strong antiviral response (172, 173).

The NS protein may be involved too in the autoimmune phenomena. It has a transactivating domain that can work on the viral p6 promoter as well as on cellular promoters, like those controlling the expression of TNF-α and IL-6. The costant stimulus derived from these proinflammatory cytokines during persistent B19V infection may result in the induction of autoimmune reactions (118, 120).

NS protein is known to induce apoptosis and host DNA damage as well as form NS-DNA adducts in non-permissive cells. It has been proposed that B19V induction of autoimmunity may occur when T cells specific for NS protein are stimulated during a reoccurrence of B19V infection or reactivation of NS expression. Specific Th cells would then provide second signal to anergized autoantigen specific B-lymphocytes. Apoptotic bodies (ApoBods) were detected in HepG2 cells, a non-permissive system to B19V infection, transduced with recombinant baculovirus to express NS protein. ApoBods usually contain only self-antigens

that typically do not cause inflammatory or immune responses, but impaired clearance of apoptotic cells has been proposed to cause autoimmunity by increasing the quantity of ApoBods and expanding the diversity of self-antigens presented to the immune system. Characterization of the purified ApoBods formed in the trasnduced HepG2 cells revealed that they contained modified host cell DNA as well as nucleosomal self-antigens, such as Smith, ApoH, histone H4 and phosphatidylserine, which are associated with autoimmunity. In addition, when purified ApoBods were added to dTHP-1 cells, a differentiated macrophage cell line, recognition and uptake occurred, suggesting that ApoBods could expose a repertoire of self-antigens to the immune system. Thus, uptake of ApoBods, with B19V NS protein-DNA adducts and nucleosomal and lysosomal antigens within them, by anergic B lymphocytes would allow presentation of NS peptides to NS-specific T helper cells, thereby breaking tolerance. Reaction to self- and non self- antigens by professional antigen presenting cells (APCs) and lymphocytes would elicit tissue damage that in turn accelerates autoimmune disease (173).

The idea that $CD4^+$ T-cells may have direct cytolytic activity is emerging. One cell-killing mechanism involves the granule exocytosis pathway, which employs perforin and granzymes to induce cell death. This enzymatic activity is thought to potentially contribute to autoimmunity by creating novel autoimmune epitopes from self-proteins. The cytolytic potential of B19V-specific T cells was explored by stimulating PBMC from seropositive healthy subjects with recombinant VP2-VLPs. Results indicated a strong correlation between B19V-induced perforin and granzyme secretion. Depletion of $CD4^+$ or $CD8^+$ T-cells from PBMC and the HLA restriction assays showed that the responses were largely confined to $CD4^+$ T-cells. Intracellular cytokine staining confirmed that granzymes and perforin were co-expressed in the same B19V-specific $CD4^+$ T-cells that produced also IFN-γ. Moreover, these $CD4^+$ T-cells were directly cytotoxic in a lactate dehydrogenase release assay. Finally, they showed expression of the natural killer cell surface marker CD56, together with the CD4 marker. $CD4^+$/$CD56^+$ T-cells have proved to be important in autoimmune diseases. $CD4^+$ T-cells secreting granzymes may potentially contribute to control B19V by guarding against reactivation in cases where viral helper function is provide by other pathogens (175).

8. DIAGNOSIS

The lack of adaptation to in vitro cell cultures implies that virus isolation methods cannot be used in diagnostics. The presence of giant pronormoblasts in a bone marrow aspirate could be indicative of B19V infection but is not diagnostic.

Numerous techniques are now available for the diagnosis of B19V infection based on direct methods, searching the presence of viral genome or proteins, or indirect, detecting a specific immune response. Plasma and serum specimens are suitable for both viral DNA and antibodies detection. Bone marrow aspirates or bioptic samples can also be used. During B19V infection in pregnancy, analysis of the amniotic fluid can reveal the presence of viral DNA, while fetal or placental tissues are analysed in case of fetal death (176, 177).

B19V genome can be detected in peripheral blood, bone marrow or tissues by direct hybridization (178-180) or nucleic acid amplification. Although direct hybridization is sensitive enough to detect viral DNA in acute infections, lower viremia will be missed due to its detection limit. Thanks to the constant advances in the development of molecular analytic techniques, real-time quantitative PCR assays are nowadays the standard analytical method for B19V molecular detection. These more sensitive techniques allow the detection of all B19V genotypes, a calibrated quantification of viral target and can be challenged by international proficiency panels using international standard (181-184).

In situ hybridization techniques can be useful, in association with PCR, for the analysis of bioptic sample for the direct identification of infected cells.

Detection of B19V specific antibodies is the most common laboratory test for B19V infection and correct interpretation of results is helpful to define active, recent or past infection.

Viral capsids purified from serum of viremic patients were initially used in immunological tests (185). Afterwards, recombinant expression systems allowed the production of B19V antigens suitable for antibody tests. Currently, most antigens are produced by the baculovirus expression system to obtain capsid proteins as VLPs with antigenic configuration correlated with that of native virus (186).

Acute B19V infection is usually diagnosed by detection of specific IgM antibodies. B19V-specific IgM are generally found within 7-10 days after viral exposure and remain detectable for approximately 2-6 months. Therefore, the presence of IgM, especially at low titers, is not necessary a conclusive proof of recent infection. Acute infection can also be diagnosed retrospectively by checking serum samples collected in the acute and convalescent phase (approximately four to six weeks later) to measure a fourfold or greater increment of B19V-specific IgG titer/avidity. IgG antibodies usually appear and begin to rise approximately two weeks following infection and then persist for life.

Unlike nucleic acids amplification technics, serological tests do not appear to suffer from recognition issues between genotypes 1, 2, and 3 as the level of divergence among the strains at the amino acid level is significantly less than that seen at the nucleotide level. Several B19V-specific IgM or IgG enzyme immunoassays (EIAs) are commercially available. The different kits vary in their antigen composition: some contain recombinant VP2 alone, while others consist of a combination of VP1 and VP2 antigens. Kits containing conformational B19 antigens have improved performance over kits containing only linear B19 antigens, since IgG directed against conformational epitopes are maintained long term (126).

Since B19V infection can follow different courses, depending on the balance between active viral replication and physiological and immune status of the subject, a multiparametric approach is necessary to define a clinically significant diagnosis.

In immunocompetent hosts with the classic rash of erythema infectiosum, the presumptive diagnosis can be made on the clinical manifestations alone and diagnostic tests are generally not essential to clinical care. Confirmation of the viral etiology became important when the result would affect management decisions, as in atypical presentations of the infection or in patients with new-onset arthropathy of unclear cause. In these cases, serologic tests can confirm the diagnosis of acute B19V by revealing B19V-specific IgM.

Detection of viral DNA by PCR is generally not useful for the diagnosis of acute infection in immunocompetent hosts without aplasia since viremia generally falls down when symptoms arise. Furthermore, low levels of B19V DNA may persist in serum or tissues, even in healthy patients; so, viral DNA detection does not necessarily indicate acute infection.

In patients with hematological disorders or defects in the immune system, who present with anemia, the diagnosis of B19V infection may rely on the detection of B19V DNA by PCR. In immunocompetent patients with transient aplastic crisis, serology can also be useful to support the diagnosis, even if the absence of IgM antibodies does not exclude the possibility of B19V infection; on the contrary, it is not useful in immunocompromised patients unable to develop sufficient antibody levels.

9. THERAPEUTIC OPTIONS

Usually, B19V infection in healthy subject does not require specific therapy. Infection is often asymptomatic and the immune response is able to clear it. Erythema infectiosum is a self-limited and mild illness that not requires treatment. However, an intervention could be relevant in patients with hematological disorders or deficits in the immune system and in infected pregnant women because of the risk of fetal death.

Currently, no specific antiviral drug is available against B19V; treatment, when required, is limited to ameliorate the symptomatology.

In patients with transient aplastic crisis, anemia is treated with transfusion until the immune response clear the infection and red cells production resumes (187), while non-steroid anti-inflammatory drugs can be helpful in case of arthritis and arthralgia.

9.1. INTRAUTERIN BLOOD TRANSFUSION

Intrauterine blood transfusion of packed red cells, into the umbilical vein, is indicated to prevent fetal lost in case of severe anemia. The optimal period for the treatment is between 18 and 35 weeks of gestation because before 18 weeks it is technically difficult due to the small size of the relevant anatomic structures, while after 35 weeks it is considered riskier than postnatal transfusion therapy. Ultrasound and Doppler, used to detect signs of anemia and cardiac failure, are supportive for the optimal fetus management. Several case studies reported an enhancement in the rate of fetal survival. In a large study of the Society of Perinatal Obstetricians, the incidence of fetal death was 6% of cases of B19V-related hydrops treated with transfusion, while 30% of fetus with hydrops that did not receive transfusion died in utero. There is only one study indicating that 30% of 24 hydropic fetus, who were transfused, died and 30% of the survivors had delayed psychomotor development (188, 189).

9.2. IVIG THERAPY

In immunocompromised patients, the lack of an efficient immune response can lead to persistent and chronic infection. Effective therapy of persistent infection consists of passive

immunization by infusion of immunoglobulin (IVIG). IVIG are therapeutic preparations of normal human IgG obtained from large pools of donors and contain a wide spectrum of antimicrobic specificities, including high levels of B19V-neutralizing antibodies, as the majority of the adult population has been exposed to the virus.

In a retrospective study of 10 patients with pure red cell aplasia associated with B19V infection, IVIG therapy appeared to be effective in 9 of the 10 subjects. Normal levels of hemoglobin were completely restored after one year. Treatment failed with low doses suggesting the use of at least 2 g/Kg of IVIG per course. The data are in agreement with the literature that indicates a complete remission of B19V-associated pure red cell aplasia (PRCA) in 93% of cases. However, relapse occurs in 37% of the responders within a mean of 4.3 months. IVIG are not able to completely clear the infection, so additional courses of IVIG treatment are required. Interstingly, in patients with severe immunodeficiencies, especially with HIV infection, the prognosis is worse than in other situations. Usually, clearance of infection occurs when a specific antiviral immune response becomes effective. If the immunodeficiency improves, chronic infection may resolve, as examples, with the starting of antiretroviral therapy in patients with HIV infection or after discontinuation of immunosuppressive therapy in post-transplant. Concerning the tolerance of the treatment, 10% of patients showed adverse side effects (190).

In conclusion, IVIG therapy seems to be effective for the treatment of PRCA associated to B19V infection in immunocompromised patients. However, therapy with IVIG preparations is still empirical since no clinical trials have been carried out to define an optimal therapeutic scheme for their administrations. Therefore, additional studies are needed to define an optimal dose as well as risk factors of PCRA relapse (191-193).

9.3. VACCINE

The development of a vaccine for B19V could be questionable. Infection is often asymptomatic or causes a self-limited, wild illness or could be chronic, so a vaccine might be of doubtful utility. However, a vaccine might be a benefit for some categories of patients, such as subjects with hematological disorders, to prevent aplastic crisis, and B19V seronegative women of childbearing age, to prevent pregnancy complications. B19V capsid

proteins can be expressed in eukaryotic systems, were they self-assemble in VLPs that are antigenically similar to native virions. Two previous study reported a double-blind, phase 1 trial to evaluate a recombinant human B19V vaccine composed of VP1 and VP2 expressed in insect cells by a recombinant baculovirus system.

In the first study, the vaccine was composed of 25% of VP1 and of 75% of VP2. It was given to 24 B19V-seronegative adults in a series of three doses over six months. The vaccine was found to be safe, well tolerated and highly immunogenic. All received subjects seroconverted after at least two doses and all volunteers developed neutralizing antibodies with a peak titer after three immunizations and the high titer is conserved for at least one year. However, a phase I/II trial of a National Institute of Allergy and Infectious Diseases (NIAID) initiated to assess the safety and immunogenicity of the recombinant vaccine was suspended due to vaccine-associated adverse events (194).

In the second study, the vaccine was composed of 22.6% of VP1 and 77.4% of VP2. 89 healthy seronegative adults were enrolled to evaluate two distinct doses and with or without the MF59 adjuvant. The trial was halted after immunization of 43 subjects because of unusual skin manifestations (erythematous, indurated lesion, systemic rash) in two vaccine- and one placebo- recipients. No clear cause was established, although it is possible due to insect cell contaminants or to the phospholypase A2 activity (PLA_2) of the VP1u that can modulate the release of arachidonic acid and precursors of potent inflammatory mediators (195).

A recent study was aimed to investigate a new B19V vaccine candidate designed to avoid potential causes of reactogenicity. The previous vaccine was based on the co-infection of insect cells with two recombinant baculoviruses, one expressed VP1 and one VP2. This approach might lead to different ratios of the two proteins because not every insect cells can be infected by the same ratio of the two viruses. In this recent work, VLPs were expressed in S.cerevisiae using a single bicistronic plasmid expressimg VP1 and VP2 in a fixed ratio. The high homogeneity of VLPs led to an efficient purification. Moreover, the PLA_2 activity was suppressed by a point mutation to eliminate a possible cause of reactogenicity. The vaccine, administered with the adjuvant MF59, was immunogenic in mice (196).

9.4. SCREENING OF BLOOD PRODUCTS

Good practices for reducing B19V transmission remain the best measure to prevent infection. Screening of blood products is the aspect of major concern. The absence of symptoms during the high-titer viremic phase, the possible occurrence of low-titer chronic infection, as well as the slow clearance of virus from bloodstream, underlie the care for the risk of B19V transmission through contaminated blood or blood products. Moreover, the small size of B19V virion and the lack of a lipid envelope make B19V extremely resistant to physical inactivation.

The range of incidence of B19V antibodies or DNA in blood derivatives is very large according to the reports carried out in the last twenty years, although results can be the very different depending on the epidemiological settings, the sensitivity of the methods used and the seasonal variations in B19V trasmission. Several reports of B19V trasmission by pooled plasma components are present, but transmission due to single-donor components is rare (197).

Observations in healthy volunteers suggest that a high threshold level of viral DNA of 10^7 International Units per ml is required in order to transmit B19V infection after administration of blood. Furthermore, the presence of neutralizing activity in the donor pools may interfere with infectivity and the existence of previous immunity in recipients will be protective. Therefore, considering the high seroprevalence rate in the population and the low frequencies of high-titer viremic blood units, the risk of acquiring infection by exposure to single blood or blood components unit is low. Systematic donor screening is therefore unjustified, although B19V-free donation could be indicated in patients with hematological disorders, immunodeficiencies and pregnant women. Greater attention is focus on blood products that are manufactured from large pool of donation, with a consequent increased probability of contamination by high-titer viremic units. Postmarketing studies of plasma manufactured by VITEX, revealed the presence of B19V antibodies or B19V DNA. Plasma with high titer of B19V DNA was given to 19 recipients, of whom 18 seroconverted after 3 months, with also viral replication in 14 cases. So, the antibodies present in the pooled plasma were not protective. On the contrary, 58 patients who received plasma with low B1V DNA titer remain seronegative and no viral

DNA was detected. This evidence led the Food and Drug Administration to set the limit of 10^4 genome copies/ml of B19V DNA for the manufacturing pools of plasma. Similarly, the European Farmacopoeia imposed a threshold level of 10^4 IU/ml in immunoglobulins and pooled plasma. Of note, B19V transmission by pooled plasma products was almost always demonstrated by recipient seroconversion without clinical manifestations, while B19V-related disease associated to transmission by contaminated plasma is less frequent (198-201).

In conclusion, sensitive molecular assays for screening and the viral decontamination during the manufacturing plasma process increased the safety of blood products, minimizing the risk of transmission.

AIM OF THE STUDY

10. AIM OF THE STUDY

Parvovirus B19 (B19V) is the main human pathogenic virus of the Parvoviridae family. It can cause clinical complications in particular situations, such as persistent anemia in immunosuppressed patients, transient aplastic crisis in subjects with haematological disorders, and hydrops fetalis and congenital anemia during maternal infection. Viral replication and productive infection are restricted by the narrow tropism of the virus. In nature, B19V replicates preferentially in human erythroid progenitors cells of bone marrow, although restricted infection of other tissue has been reported. The restricted tropism results from combinations of several factors. First, virus attachment is mediated by globoside receptors expressed on cell surface and by coreceptors. However, the presence of receptors and corecptors is not sufficient to achieve a productive infection, but intracellular events are likely to affect the outcome of B19V infection. The strictly tropism has impaired a deep understanding of virus dynamics and life cycle. Only few cell lines in fact can support B19V replication, although to a limited extent. Recently, new advances in generation and differentiation of human progenitors cells (EPCs) in vitro allow the study of viral characteristics in a highly permissive environment mimicking the in vivo infection in bone marrow. EPCs can be obtained from peripheral blood by culture in medium containing erythropoietic growth and differentiation factors. This culture system not only provides an effective permissive cell population but consents also the study of the changes in cellular expression patterns that occur during erythroid differentiation regulating viral replication.

A first aim of the present study was the characterization of B19V dynamics, in terms of distribution of productively infected cells, macromolecular synthesis and production of infectious virus, in dependence on the differentiation stage of EPCs obtained from peripheral blood. A window of permissiveness to a productive infection of B19V was found and was constituted by a heterogeneous population of differentiating cells, around the pronormoblast phase, consenting an efficient viral replication, a mature mRNAs synthesis and production of infectious virus. All these characteristics describe a model system suitable for studying virus-cells interaction, understanding viral pathogenesis and researching compounds with potential antiviral activity.

PBMC-derived EPCs constitute a reference system representing, in vitro, the primary target cells of natural infection in vivo and a permissive cellular system suited to assess the inhibitory effect of potential antiviral drugs on B19V replication. Nowadays, no specific antiviral drugs active against B19V are present and current treatments are effective only to ameliorate symptoms. Although B19V infection is usually asymptomatic or causes a mild, self-limited illness, a specific antiviral treatment would be useful in the acute phase of aplastic crisis, in immunocompromised patients not able to mount immune responses for infection clearance, and in maternal infections with the risk of fetal loss. Current treatments include blood transfusion, to overcome acute or chronic anemia, and intravenous immunoglobulins (IVIG) administration for neutralizing infection in immunocompromised patients. IVIG therapy however has some limitations, considering that virus clearance become effective when a mature immune response develops, and treatment cycles are empirical since no clinical trials are available to define an optimal therapeutic scheme.

Strategies for discovery and development of antiviral compounds include rational drug design, which is focused on identifying molecules that specifically target known viral components, and testing of compounds with known biological activity. The second approach was thus used in the present work in order to investigate the potential inhibitory activity of Cidofovir on B19V. Cidofovir is a monophosphate nucleotide analogue that has shown activity against all not retrotranscribing dsDNA viruses. A second aim of this work was then the investigation of inhibitory activity of Cidofovir on B19V replication in the model system constituted by differentiating EPCs isolated from peripheral blood.

MATERIAL AND METHODS

11. B19V REPLICATION AND EXPRESSION IN ERYTHROID PROGENITORS CELLS

11.1. Cells

Erythroid progenitor cells (EPCs) were generated in vitro from peripheral blood mononuclear cells (PBMC) obtained from the leukocyte-enriched buffy coats of anonymous blood donors. PBMC were isolated using centrifugation in Ficoll-Paque Plus (GE Healthcare Bio-Sciences AB) and cultured in IMDM medium containing erythropoietic growth and differentiation factors. In particular, IMDM was supplemented with:

- serum substitute BIT 9500 (StemCell Technologies), diluted 1:5 for a final concentration of 10 mg/ml bovine serum albumin, 10 mg/ml recombinant human (rhu) insulin, and 200 mg/ml iron-saturated human transferrin,
- 900 ng/ml ferrous sulphate (Sigma),
- 90 ng/ml ferric nitrate (Sigma),
- 1 mM hydrocortisone (Sigma),
- 3 IU/ml rhu erythropoietin (NeoRecormon, Roche),
- 5 ng/ml rhu IL-3 (Life Technologies),
- 20 ng/ml rhu stem cell factor (Life Technologies).

Cells were maintained at 37°C in 5% CO_2, at an initial density of 2-3x10^6 cells/mL, then splitted at day 4±1 and maintained at a density of 0.5-1.0x10^6 cells/mL for up to 20 days post-isolation.

11.2. Flow Cytometry Analysis

During cell growth and differentiation, in vitro cultured EPCs were characterized using flow cytometry (FACSCalibur, Becton Dickinson). Aliquots of 5x10^5 EPCs were stained with antibodies specific for erythroid differentiation markers (CD36, CD71, CD235a) and known B19V receptors (globoside, α5β1 integrin). CD36 and CD71 expression was evaluated by phycoerythrin (PE)-labeled monoclonal antibodies (BD Biosciences). CD235a, α5β1 integrin and globoside expression was evaluated by monoclonal mouse anti-CD235a (BD Biosciences), monoclonal mouse anti-α5β1 (Immunological Sciences) and polyclonal rabbit

anti-globoside (Matreya), followed by anti-mouse-Alexa 488 (Life Technologies) or anti-rabbit-FITC (DakoCytomation) antibody, respectively. Aliquots of cells were collected and analyzed every three days during in vitro culture, up to 18 days. Antibody binding was performed incubating samples at 4°C for 30 minutes (min) and washing twice in PBS to remove unbound antibody. Cells were finally resuspended in 500 μl of PBS and analyzed.

For each experimental series and each marker analyzed, negative controls were used to define the percentage of positive cells. In case of direct staining, a corresponding sample were treated equally but without adding the conjugated antibody, while in case of direct staining only the secondary antibody was added in the control sample. The control histogram was subtracted from the sample histogram and the percentage of positive cells was calculated as number of events in the resulting subtracted histogram in comparison to the total events of sample histrogram. Data were analyzed using the Cell Quest Pro Software (Becton Dickinson).

11.3. Virus and Infection

A B19V viremic serum sample, identified in our laboratory in the course of routine diagnostic analysis and available for research purposes according to Italian privacy law, was used as source of virus for the infection experiments. The viremic serum contained 10^{12} B19V genome copies (geq)/mL, and resulted negative by routine diagnostic assays to other viruses.

Viremic sample, appropriately diluted in PBS, was added to a define number of cells, at the density of 10^7 cells/mL, in order to obtain a multiplicity of infection (moi) of 10^3 geq/cell. Following adsorption for 2 hours (h) at 37°C, the inoculum virus was washed twice in PBS and the cells were incubated at 37°C in complete medium at an initial density of 5×10^5 cells/ml, for a time course of infection of 48 h.

11.4. Infectivity assay

Equivalent aliquots of supernatants separated from the respective fraction of infected cells at each time point and day series were processed for nucleic acid purification and analysis of viral DNA.

100 μl of supernatants collected at 12 hpi and 48 hpi from cells infected at the different days of culture, were then used to infect 1x10^6 cells of a new in vitro culture at day 9±1. Following absorption for 2 hpi at 37°C, cells were washed, then, an aliquot of cells were stored and an equivalent aliquot were resuspended in complete medium for 48 h. Samples collected at 2 hpi and 48 hpi for each infection were processed for nucleic acids purification and analysis of viral DNA amount by qPCR assay.

11.5. Flow-FISH Assay

To detect viral nucleic acids by flow-FISH assay, 1x10^6 cells were collected at the appropriate time points post-infection. Cells were fixed in 300 μl of PBS-paraformaldehyde 0.5% at 4°C overnight and permeabilized in 200 μl of PBS containing 0.2% saponin at room temperature (RT) for 45 min. Finally, cells were resuspended in 50 μl of a hybridization solution containing 2× SSC, 70% formamide, 250 g/ml DNA calf thymus and 10% Dextran sulfate. A digoxigenin-labeled DNA probe mixture specific for B19V nucleic acids was generated by the random priming method on a cloned full-length genomic DNA template, according to the manufacturer's instructions (Dig-High Prime, Roche). The probe mixture was denatured at 95°C for 5 min, then added at 2 μg/mL to the cell suspension, previously heated at 70°C for 5 min. Hybridization reaction was performed at 70°C for 5 min and 37°C overnight. Following hybridization, cells were washed with 1× Stringent Wash (Zytovision) at RT for 15 min, then at 55 °C for 5 min and again at RT for 5 min. For the detection of the hybrids, the cell suspension was incubated for 1 h with a FITC-conjugate antidigoxigenin antibody (Roche) diluted 1:20 in 100 μl of PBS-BSA 1%. Finally, cells were washed twice in PBS and resuspended in 500 μl of PBS for cytometer analysis. A parallel aliquot of mock-infected cells was treated equally as control sample. Samples were gated on the FSC (forward light scatter) versus SSC (side light scatter) plot to exclude cellular debris and 50000 events per sample were collected. The percentage of positive cells was calculated on the number of events showing fluorescence intensity greater then a fixed gate set in order to have at least 99.5% of mock-infected cells below threshold.

11.6. Nucleic acids purification

Equal amounts of cell cultures, corresponding to 2×10^5 cells, were collected at the appropriate time points following infection (hours post-infection, hpi), resuspended in 200 µL of Buffer ATL and processed by using the EZ1 viral nucleic acid kit on a EZ1 platform (Qiagen), following the manufacturer's instructions, in order to obtain a total nucleic acid fraction, containing both viral DNA and RNA, in a final elution volume of 120 µL. Volumes of 10 µL were then used in the subsequent qPCR and qRT-PCR assays for the quantitative evaluation of target viral nucleic acids. For quantitative analysis of viral DNA, aliquots of the eluted nucleic acids were directly amplified in a qPCR assay, while for viral RNA analysis, corresponding aliquots were first treated with Turbo DNA-free reagent (Ambion) and then amplified in a qRT-PCR assay.

11.7. Quantitative real-time PCR and RT-PCR

Standard targets for the quantification of viral nucleic acids were obtained from plasmid pHR0 that contains an insert corresponding to the complete internal region of B19V genome (nt. 346-.5245) (). From pHR0 plasmid, in vitro amplified DNA or in vitro transcribed RNA corresponding to the viral insert were obtained, purified, quantified and used as genome equivalents (geq) standards. Serial dilutions of the standard products, from 10^1 to 10^8 geq/reaction, were amplified to obtain calibration curves by plotting Cp values as a function of log of target copy number.

DNA amplification was performed by using QuantiTect PCR SybrGreen PCR Kit (Qiagen). The primer pair R2210-R2355, located in the central exon of B19V genome, was used for amplification at a final concentration of 0.5 µM in a total volume of 20 µl. Thermal profile consisted in 15 min at 95°C, then 40 cycles of 15 sec at 95°C, 30 sec at 55°C, and 15 sec at 72°C and 15 sec at 78°C both coupled with signal acquisition. A final melting curve was performed, with thermal profile ramping from 50°C to 95°C at a 12°C/min rate, coupled with continuous signal acquisition.

RNA amplification was performed by using QuantiTect SybrGreen RT-PCR Kit (Qiagen). The primer pair R2210-R2355, being located in the central exon, could amplify both DNA and the whole set of viral transcripts. Thus, it was used for quantification also of the total RNA, at a final concentration of 0.5 µM in a final volume of 20 µl. For each sample, two parallel

reactions were performed, either including (RT+) or omitting (RT-) the reverse transcriptase in the reaction mix, to discriminate the residual viral DNA present after DNase treatment. DNA contamination was considered negligible during viral RNA quantification if there is a difference of al least 3 cycles between RT+ and RT- amplified sample. Thermal profile consisted in the same amplification reaction of qPCR with the addition of an initial step of retrotranscription at 30 min at 55°C.

To obtain a systematic functional analysis of B19V genome expression a PCR array was designed in order to specifically discriminate all the diverse classes of viral mRNA. Oligonucleotide primers were selected and combined to define genome expression profile on the basis of splice definition and exon/intron composition.

Primers and primer combinations used in the qPCR and qRT-PCR assays are indicated in Table 1 and mapped with respect to B19V genome in Figure 10.

All oligonucleotides were obtained from MWG Biotech.

Primer	Sense	Primer	Antisense	DNA Target
18Sfor	CGGACAGGATTGACAGATTG	18Srev	TGCCAGAGTCTCGTTCGTTA	Genomic 18S rDNA
R2210	CGCCTGGAACACTGAAACCC	R2355	GAAACTGGTCTGCCAAAGGT	Virus DNA
Primer	**Sense**	**Primer**	**Antisense**	**RNA Target**
		R0622	ATAGCTCCATGTTAGTATGT	Intron 1, unspliced
R0534	TGGGCTGCTTTTTCCTGGAC	R2101*	CTGGGTGGAGGGCATCTGTT	Intron 1, splice D1/A1.1
		R2221*	CAGTGTTCCAGGCGCCTGTT	Intron 1, splice D1/A1.2
R1882	GCGGGAACACTACAACAACT	R2033	GTCCCAGCTTTGTGCATTAC	Intron 1, unspliced
R2210	CGCCTGGAACACTGAAACCC	R2355	GAAACTGGTCTGCCAAAGGT	Central exon, total RNA
		R2377	TCAACCCCAACTAACAGTTC	Intron 2, unspliced
R2210	CGCCTGGAACACTGAAACCC	R3238*	CAGGGGCAGCTGCACAGTTC	Intron 2, splice D2/A2.1
		R4897*	GTTTTGCATCTGTAGAGTTC	Intron 2, splice D2/A2.2
R2210	CGCCTGGAACACTGAAACCC	R2377	TCAACCCCAACTAACAGTTC	Intron 2, unspliced, pAp+pAd cleaved
R3180	TGGGTTTCAAGCACAAGTAG	R3342	TGCACCAGTGCTGGCTTCTG	Intron 2, unspliced, pAd cleaved
R4899	ACACCACAGGCATGGATACG	R5014	TGGGCGTTTAGTTACGCATC	Distal exon, pAd cleaved

Table 1: Primers used in the qPCR and qRT-PCR assay.
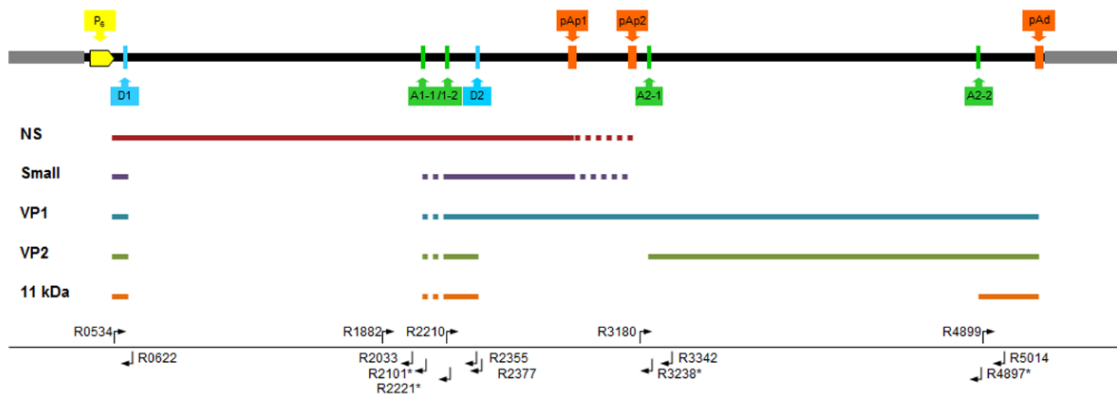
Figure 10: A simplified map of B19V transcripts with the position of primers used in the PCR array.

Real-time PCR and RT-PCR were performed and analysed by using the RotorGene 3000 system and the RotorGene 6.0 software. All reported experiments were carried out in duplicate series. Melting curve analysis was used for the determination of the specificity of the amplification products. Quantitation of viral DNA and of total viral RNA was obtained by the absolute quantitation algorithm, converting quantification cycle (Cq) values to geq number using external DNA or RNA calibration curves. Relative quantitation of the different subsets of viral transcripts was obtained by efficiency-corrected comparative quantitation using LinRegPCR software, and subsequent normalization within each combination set and to the amount of total viral RNA.

The program GraphPad Prism version 5.00 for Windows (GraphPad Software, San Diego California, USA) was used for data analysis.

12. ANTIVIRAL ACTIVITY OF CIDOFOVIR

12.1. Cidofovir

Cidofovir (CDV), [(S)-1-[3-hydroxy-2-(phosphonylmethoxy)propyl]cytosine], was purchased from Sigma at a purity degree >98%. The drug was dissolved in H_2O to a final concentration of 5 mg/mL and stored at 20 °C.

12.2. Cells

UT7/EpoS1 cells were cultured in IMDM (Cambrex), supplemented with 10% FCS (Cambrex) and 2 U/mL rhu erythropoietin (NeoRecormon, Roche), at 37°C and 5% CO_2. Cells were kept in culture at densities of 1-2x10^5 cells/mL, and used for infection experiments when at a density of 3x10^5 cells/mL.

Erythroid progenitor cells (EPCs) were generated and cultured as previous described and used for infection experiments after 9 ± 1 days of culture.

12.3. Antiviral Assay

For infection of both UT7/EpoS1 and EPCs, 5x10^5 cells were incubated in 50 µl volume of PBS, in the presence of 5 µl of the viremic serum, diluted in PBS in order to obtain different moi, from 10^4 geq/cell to 10^1 geq/cell. Following adsorption for 2 h at 37°C, the inoculum virus was washed and the cells were incubated at 37 °C at an initial density of 5x10^5 cells/mL in the respective complete medium, in the absence of drug or in presence of different concentrations of CDV (range 0.1 µM-500 µM).

12.4. Cell Viability and Proliferation Assays

For cellular assays, UT7/EpoS1 and EPCs cells were seeded at the density of 5x10^4 cells/well in a 96-well culture microplate, and volumes of 100 µl of CDV freshly diluted in the respective medium at the different concentrations were added. Cells without drug were seeded too as reference point of maximum activity. Cells were then cultured for 72 h, for UT7/EpoS1 cells, or 24 h, for EPCs.

The effects of CDV on viability of cells were monitored by the alamarBlue assay (Life Technologies). 10 μl of reagent were added to cells and after, the incubation period, absorbance was read on a plate reader spectrophotometer, according to manufacturer's instruction. AlamarBlue cell viability reagent is a redox indicator dye that yields a fluorescent signal in response to metabolic activity functions. When cells are alive, they maintain a reducing environment within the cytosol of the cell. Upon entering cells, resazurin, the active ingredient of alamarBlue reagent, is reduced to resorufin, a compound that is red in color and highly fluorescent. Both absorbance and fluorescence can be measured.

Evaluation of 5-bromo-20-deoxyuridine (BrdU) incorporation (Cell proliferation ELISA BrdU Assay, Roche Diagnostics) into newly synthesised DNA was suitable for monitoring the effects of CVD on cell proliferation. BrdU is a pyrimidine analogue of thymidine, selectively incorporated into cell DNA at the S phase of the cell cycle. The assay consists in multistep of fixation of cells after the incubation with BrdU, labeling of BrdU incorporated with anti-BrdU antibody, detection of the complex BrdU/anti-BrdU antibody by a secondary antibody conjugate with peroxidase, and colour development by adding a colorimetric substrate. Absorbance is read at 450nm and 630nm.

12.5. Quantitative real-time PCR and RT-PCR

Nucleic acids purification and quantitative Real-Time PCR were performed as described. In particular, the primer pair R2210-R2355 was used for amplification of both viral DNA and the whole set of viral transcripts, the primer pair R1882-R2033 for the amplification of the mRNAs coding for NS protein, and the primer pair R4883-R5014 for the amplification of the mRNAs coding for capsid VP1 and VP2 proteins.

12.6. Immunofluorescence Assay

Aliquots of cell culture samples, corresponding to 0.5×10^5 cells, were centrifuged at 4000g for 5 min. Pelleted cells were washed with PBS, spotted onto glass slides and fixed with 1:1 acetone:methanol for 10 min at 20 °C. Slides were then incubated at RT for 1 h with a monoclonal mouse antibody against VP1 and VP2 proteins (MAB8293, Chemicon), diluted

1:200 in PBS/BSA 1%. After washing in PBS, slides were incubated for 1 h with AlexaFluor488 anti-mouse secondary antibodies (Life Technologies), diluted 1:1000 in PBS/BSA 1%. After further washing, slides were stained with Evans blue, washed, mounted and viewed on a fluorescence microscopy with a fluorescein isothiocyanate filter set.

12.7. Statistical Analysis

Experiments were carried out in triplicate series, and for each quantitative determination, triplicate values were obtained. Statistical analysis was carried out by using the programme GraphPad Prism version 5.00 for Windows (GraphPad Software, San Diego California, USA). Linear regression analysis was carried out to correlate input moi values and calculated amounts of viral nucleic acids. One-way ANOVA (analysis of variance) followed by the Dunnett' Multiple comparison test was used to compare data obtained in different experimental conditions. EC50 and EC90 values for the different moi were determined by non-linear regression curve on percentage inhibition of viral activity for each different concentration of CDV.

RESULTS

13. B19V AND ERYTHROID PROGENITORS CELLS

13.1. EPCs dynamics and differentiation

PBMC isolated from peripheral blood of normal donors were grown in culture medium containing erythropoietic growth and differentiation factors. In these conditions, the cell population expanded and maintained viability for 15-20 days. The progressive change of cell population composition was monitored by cytofluorimetric analysis (Figure 11).
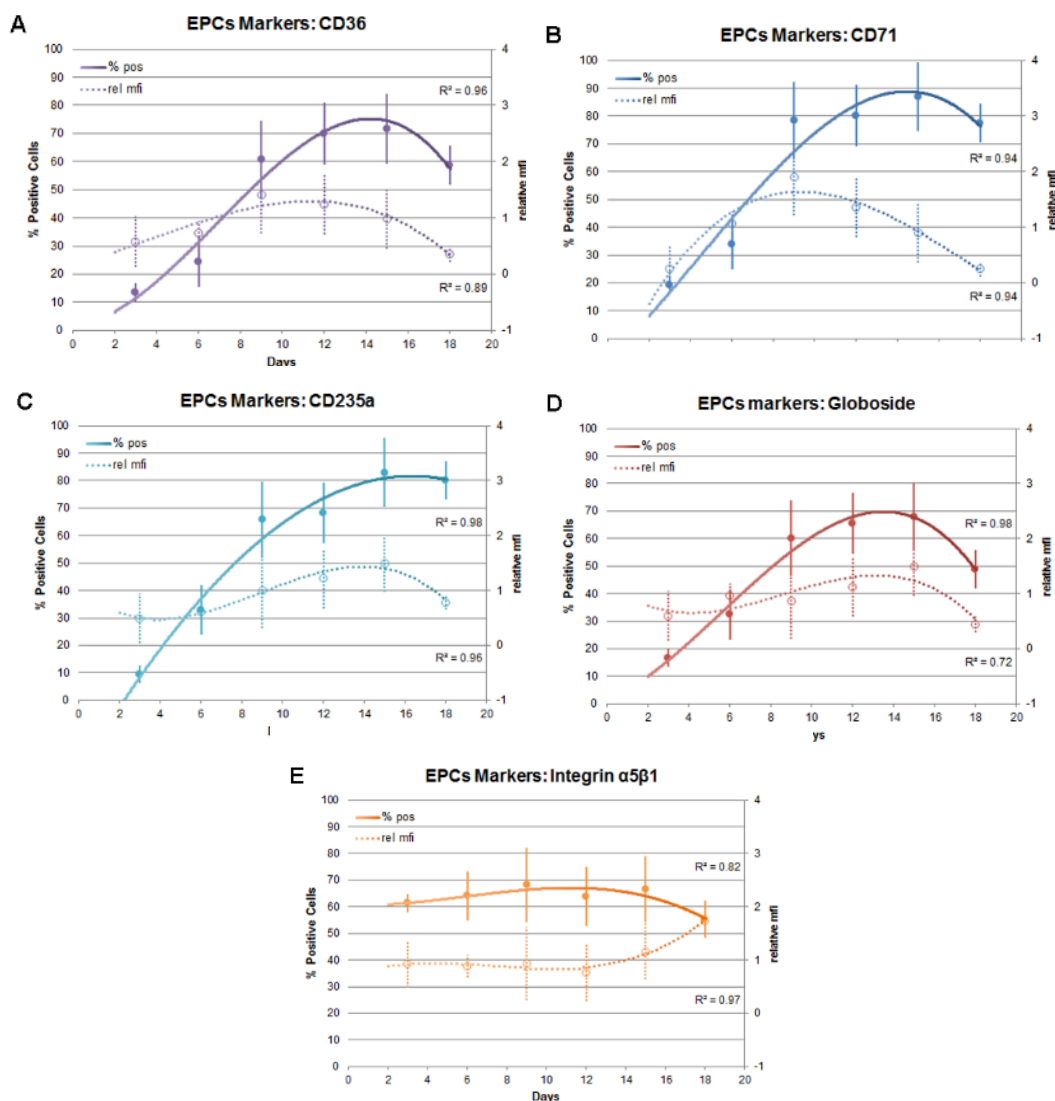

Figure 11: Phenotipic characterization of differentiang EPCS. Each graph reports the percentage of cells positive for each indicated marker and the relative Mean Fluorescence Intensity.

During the time of culture a progressively higher proportion of cells expressed erythroid lineage-specific markers, such as CD36, CD71 and CD235a, reaching highest values between days 9-15, while during the last day of culture (18 day), markers expression decreased. Concerning B19V receptors, the trend of globoside expression followed that of erythroid markers, while the distribution of α5β1 integrin appeared constant. Overall, these results indicated a progressive in vitro differentiation of isolated PBMC through erythroid lineage, obtaining a culture system potentially susceptible to B19V infection.

13.2. Viral replication in EPCs

Efficiency of viral replication was studied in dependence on the degree of erythroid differentiation. Cells were infected with B19V at 3 days intervals of culture, from 3 to 18 days post isolation, for a 48 h course of infection. Equal amounts of cells were collected at 2 hpi, 24 hpi and 48 hpi and the respective amounts of viral DNA were determined by qPCR. Viral DNA measured at 2 hpi represented the virus input, the amount of virus that entered the cells. Increment of viral DNA between 2 hpi and 24-48 hpi is indicative of viral replication. For the different days of culture and each infection course, the Log B19V DNA increase at 24 and 48 hpi versus 2 hpi was calculated as the mean of 2 to 5 independent experiments. At 3 days cells were susceptible, but not permissive to B19V replication, as indicated by the detection of viral DNA at 2 hpi but showing a mean 0.5 Log decrease in the amount of viral DNA associated with cells during the 48 h of infection (Figure 12). From day 6 to day 18 cells were susceptible and became also permissive to viral replication, although to different extents. Viral replication was maximal at days 6-9, with a mean 2.2-2.8 Log increase, while at days 12-18 cells replication occurred at reduced degree, with a mean 1.5-1.6 Log increase. Overall, data confirmed that viral replication depends on the differentiation stage of in vitro cultured erythroid cells.
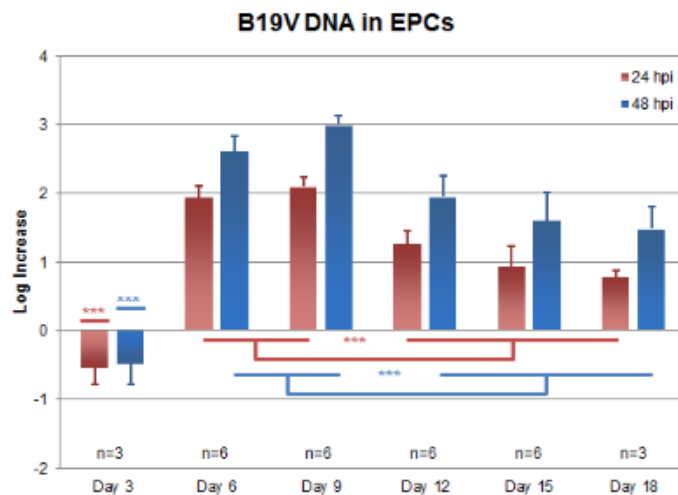
Figure 12: B19V replication in EPCs. The amount of B19V DNA was determined by qPCR, and the Log increase measured between 2 hpi and 24-48 hpi. Columns indicate the mean values obtained from independent experiments, bars indicate the standard error of means.

13.3. Viral distribution in EPCs

Viral replication and distribution of productively infected cells within a differentiating population of EPCs was investigated in a selected representative experiment by parallel qPCR and flow-FISH assay. EPCs at different days of in vitro culture (6-18 days) were infected with B19V, and equal amounts of cells were collected at 2, 24 and 48 hpi. For each sample, qPCR analysis was carried out to determine the amount of viral DNA, and flow-FISH assay was performed to determine the percentage of B19V positive cells (Figure 14, A and B). The overall trend of replication activity correlated with the trend previous described. The observed increase in the amount of viral DNA was maximal (3.4 Log) for cells at days 9, 2.5-2.6 for cells at days 6, 12, 15, and 2.0 Log for cells at day 18. In accordance with these values, the percentage of FISH positive cells was higher (41.4%) at day 9, lower at days 6 (3.8%) and 12 (5.2%), and lowest at days 15 (1.6%) and 18 (1.1%). The dot-plot graphs (Figure 13) showed a diffuse pattern of positive cells, suggesting a continuous distribution in the amount of intracellular viral nucleic acids within the fraction of FISH positive cells.
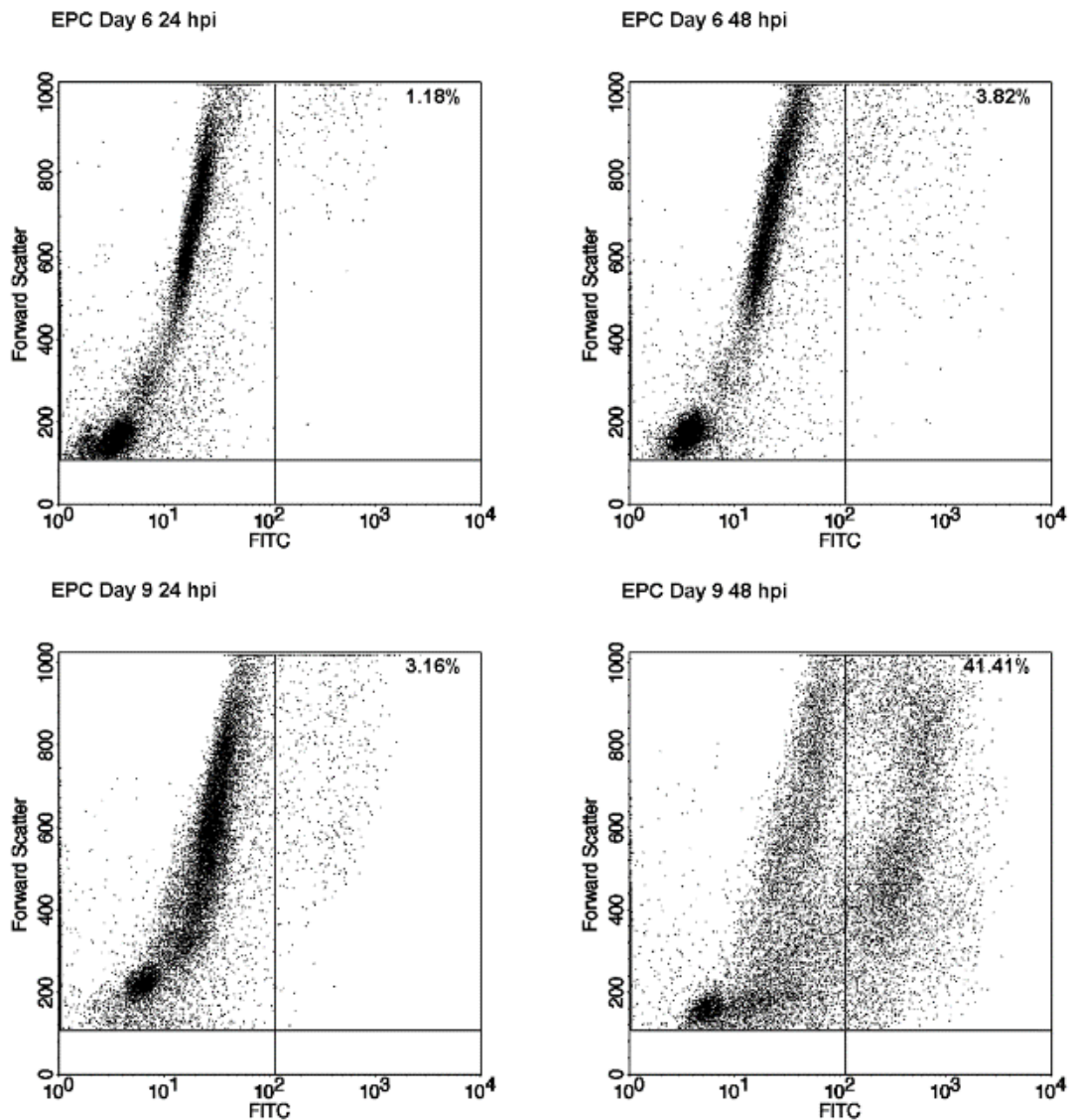
Figure 13: B19V replication and distribution in EPCs. The dot plot graphs of Flow-FISH assay in EPCs infected at day 6 and 9 are reported.

Plotting the percentage of FISH-positive cells versus the Log of viral DNA amount at the respective time points, a linear correlation was evident (Figure 14, C). This correlation indicated that B19V replication was confined to a limited permissive fraction of the potentially susceptible cells within the EPC population, not uniquely identified by any of the cell surface markers analyzed, but rather depending on the presence of other cellular factors linked to the differentiation stages. Therefore, the extent of replication of virus in

differentiating EPCs was mainly the result of the extent of recruitment of permissive cells within a heterogeneous population of potentially susceptible cells.
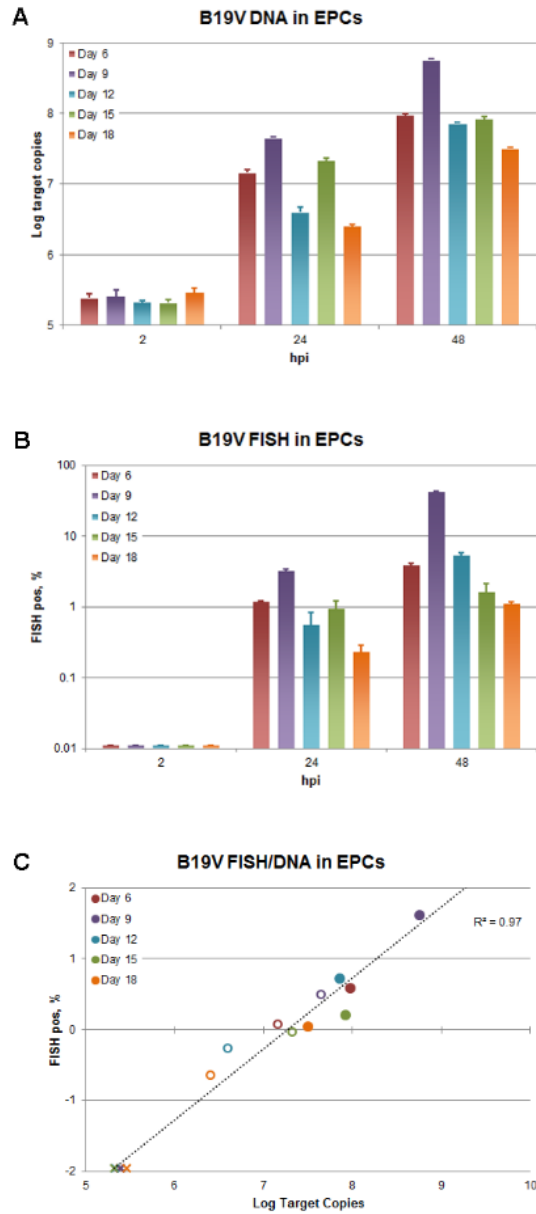
**Figure 14: B19V replication and distribution in EPCs**. (A) Amount of B19V DNA expressed as Log DNA geq/10^4 cells. (B) Fraction of positive cells determined by the flow-FISH assay. (C) Correlation of dat obtained by the two different assays. X: samples at 2 hpi; o: samples at 24 hpi; •: samples at 48 hpi.

13.4. Viral macromolecular synthesis in EPCs

To assess a deep systematic analysis of the dynamics of viral macromolecular synthesis in a selected representative experiment, cells at different days from isolation were infected with B19V, and equal amounts of cells were collected at early (2, 6, 12 hpi) and late (24, 36, 48 hpi) time points post infection. The amount of viral DNA and total RNA were quantified by qPCR and qRT-PCR, respectively. The same primer pair 2210-2355, being located in the central exon of genome, was used to amplify both viral DNA and total RNA. The amount of viral nucleic acids was expresses as Log target copies/10^4 cells.

Viral DNA kinetic in the selective experiment (Figure 15, A) reflected the overall kinetic observed in several experiments (Figure 12). Viral binding/entry seemed independent cell differentiation stage, since comparable amounts of viral DNA were measured at 2 hpi in cells from day 3 to 15 of culture, while lower amounts (-0.6 Log) were observed only for day 18. On the contrary, the ability to replicate was correlated to the erythroid stage of EPCs. Cells infected at day 3 represented a non permissive environment for viral replication since a DNA decrease of 1.0 Log was measured between 2 hpi to 48 hpi, although viral DNA was detectable during the entire time course of infection. On the contrary, a permissive window for viral replication ranged from day 6 to day 15. In particular, in these cells, after an early steady state, viral replication started from 12 hpi. The highest increase in DNA amount occurred between 12 hpi and 24 hpi (+1.6-2.0 Log), and further increase was measured up to 48 hpi (+0.6-1.4 Log from 24 to 48 hpi). Cells infected at day 9 sustained the maximal B19V replication activity with a viral DNA amount increment of +3.1 Log from 2 to 48 hpi. At day 18, lower amounts of B19V DNA were measured at 2 hpi and lower levels of replication were observed with an overall increment of +0.9 Log from 2 to 48 hpi.
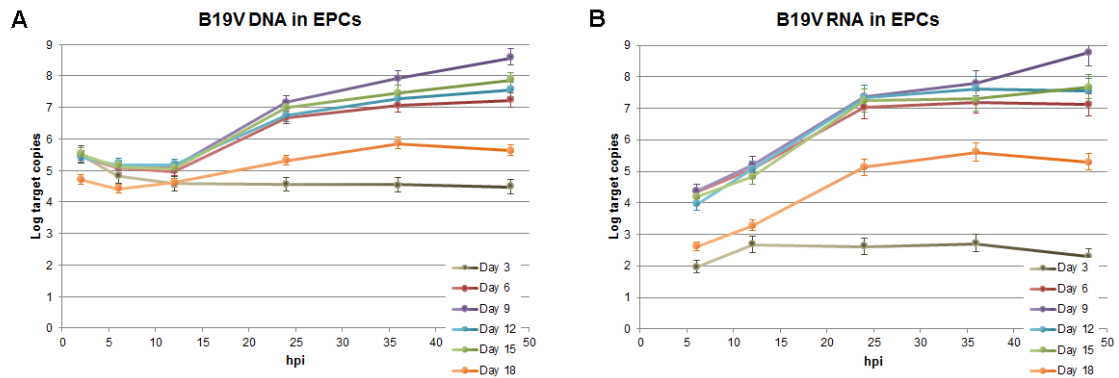
Figure 15: B19V replication and expression in a time course of infection in EPCs. (A) Amount of B19V DNA expresses as Log DNA geq/10^4 cells. (B) Amount of B19V total RNA expresses as Log RNA target copies/10^4 cells.

Parallel analysis of viral RNA (Figure 15, B) demonstrated a strictly association between genome replication and transcription, thus a very low amount of viral RNA was detectable at day 3, while accumulation of viral RNA was observed at days 6-15 and at day 18, although to a lower level, accordingly to the lower amount of viral DNA. In detail, viral RNA was detected starting from 6 hpi for all series, with similar amounts for day 6-15 series and lower amount for day 3 and day 18 (-2.3 Log and -1.6 Log for the day 3 and day 18 series, respectively, compared to the day 6-15 series). Then, after a slight increase between 6 hpi and 12 hpi, no further increment occurred at day 3, while for the other day series viral RNA dynamic followed viral DNA synthesis. In particular, viral transcription boosted from 12 hpi to 24 hpi (+1.8-2.4 Log), in coincidence with the start of viral DNA synthesis. No significative additional increment occurred between 24 to 48 hpi, with the exception of day 9 where viral RNA amount reached the highest levels, with a further increse of 1.4 Log between 24 hpi and 48 hpi for an overall increment of >3.0 Log from 12 to 48 hpi. Results indicated that a productive infectious cycle rely on a biphasic macromolecular synthesis with an early transcription phase on the parental template, followed by late transcription on the replicating templates. The reduced transcriptional activity in days 3 and 18 series could be a result of a block in the second-strand DNA repair synthesis, thus preventing the generation of a transcriptionally active template, and limiting viral genome replication.

The complete set of mature viral mRNAs originates from the combination of splicing and cleavage-polyadenylation events (Figure 10). A detailed analysis of the relative abundance

of the different mRNAs classes was carried out by using a set of selective primers for qRT-PCR analysis (Figure 16).
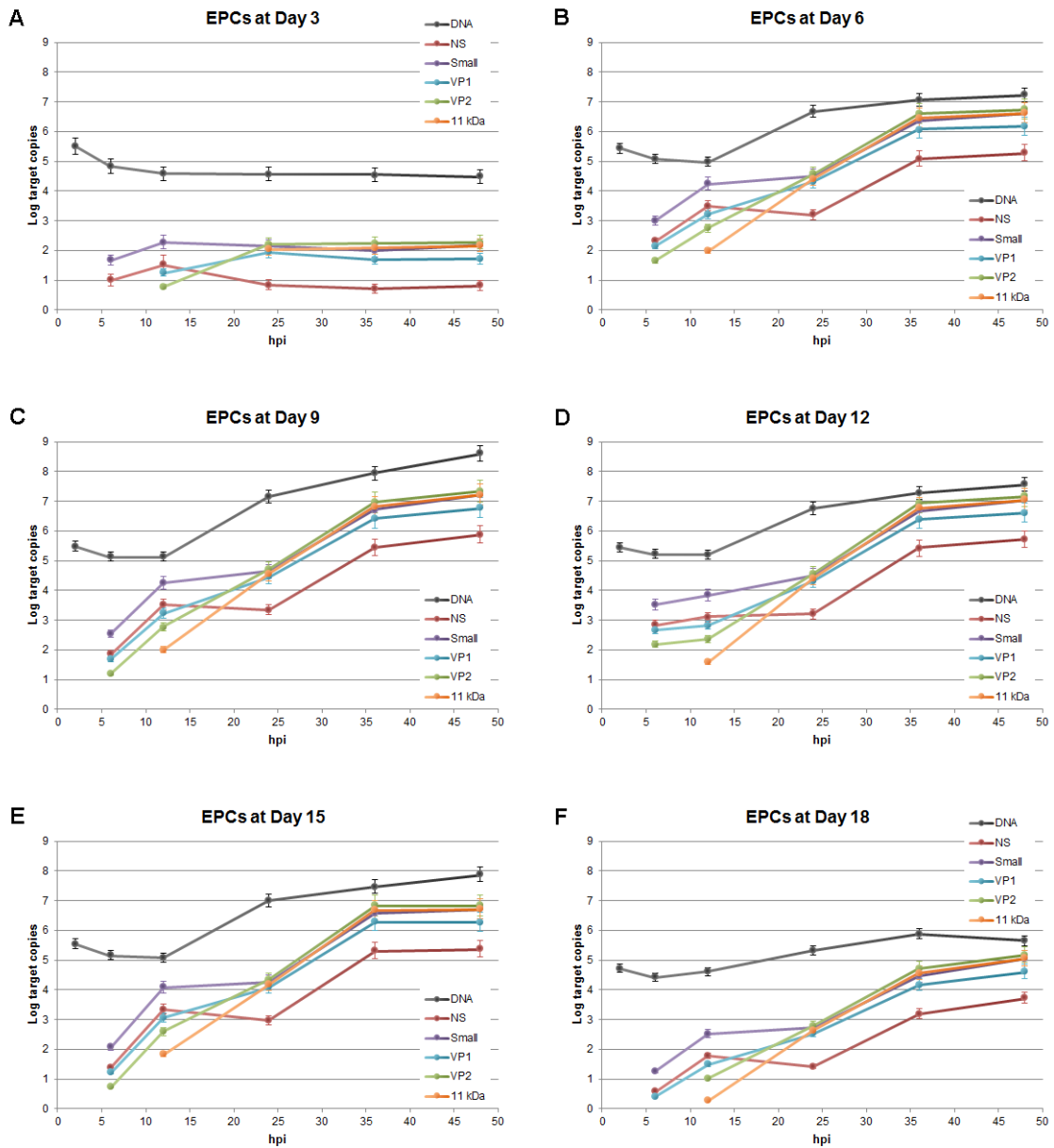
Figure 16: B19V replication and expression in a time course of infection in EPCs. The dynamics of accumulation of viarl DNA and of the major classes of viral mRNAs in infected EPCs is reported.

The primer pair R2210-R2355, being located in the central exon, was used to amplify the whole ensemble of viral transcripts. Usage of the first splice donor (D1) and selection of the first splice acceptor (A1.1/2) was analyzed by combining primer R0534, positioned in the common leader region, with either primer R0622 (specific for unspliced transcripts),

R2101* (specific for the proximal first acceptor site A1.1) or R2221* (specific for the distal first acceptor site A1.2). The primer pair R1882-R2033 was used to define unspliced transcripts, coding for NS protein. Usage of the second splice donor (D2) and selection of the second splice acceptor (A2.1/2) was analyzed by combining primer R2210 (common primer positioned in the central exon) with either primer R2377 (specific for unspliced transcripts), R3238* (specific for the proximal second acceptor site A2.1) or R4897* (specific for the distal second acceptor site A2.2). Usage of the proximal and distal cleavage-polyadenylation signals was analyzed by the primer pairs R2210-R2377 (upstream of pAp1), R2998-R3103 (upstream of pAp2), R3180-R3153 (readthrough of pAp), and R4899-R5014 (upstream of pAd). With the exception of the day 3 sample series, where the level of mRNA transcription was too low to a comparative analysis, the dynamics of accumulation of the different classes of viral mRNA in the days 6-18 sample series was similar and largely independent on the degree of cellular differentiation. Two pattern of expression could be distinguished as a result of a changing frequency of mRNA processing events: an early pattern at 6-12 hpi replaced by a later pattern at 24-48 hpi (Figure 17). In the early phase of infection, cleavage at the pAp site occurred at a frequency of 81-92%, while in later phases of infection cleavage at the pAd site accounted for 66-72% of events. In the processing events of intron 1, 12-19% in early phases, but only 0.2-0.3% in late phases did not undergo splicing, while in the remaining cases splicing occurred 1.4-2.2 times more frequently at acceptor site 1.1 over 1.2, increasingly at later times post-infection. In the processing events of intron 2, 97% in early phases and 34-46% in late phases did not undergo splicing, while in the remaining cases splicing occurred only at acceptor site 2.1 in early phases, and 1.3-1.4 times more frequently at acceptor site 2.1 over 2.2, at late times post-infection. In summary, the relative abundance of viral mRNAs classes through the course of infection clearly distinguished an early and a late pattern of expression profile. In the early phase, prior to the beginning of viral replication, mRNAs were mostly cleaved at the proximal site, leading to a higher relative abundance of small mRNAs and mRNA coding for NS protein, that is essential for viral replication. In the later phase, in coincidence with viral DNA replication, mRNAs were mostly cleaved at the distal site, leading to a higher relative abundance of mRNAs for VP1, VP2 and 11kDa proteins. The overall finding therefore

confirmed the linked coordination of viral DNA replication, viral RNA transcription, and differential usage of mRNAs processing signals to achieve a productive replicative cycle in EPCs.
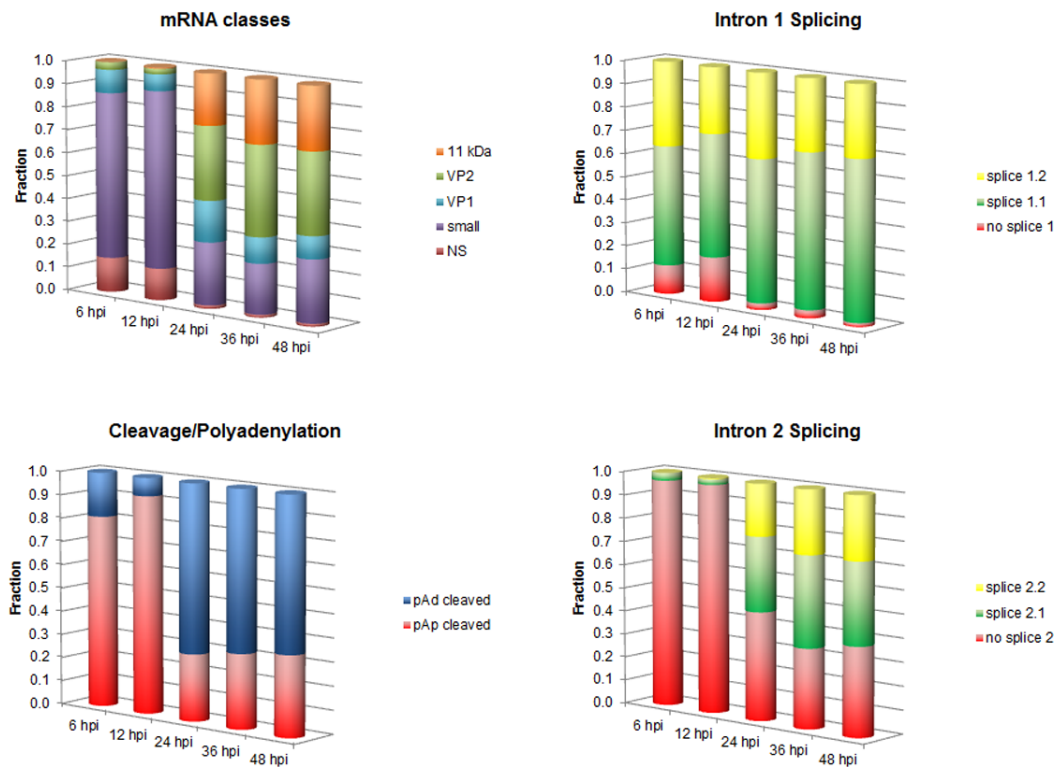

Figure 17: Transcript processing in a time course of infection in EPCs. Composite columns indicate the frequency of processing events at intron 1, intron 2 or pAp/pAd sites, and the resulting overall composition of the major classes of viral mRNAs. Cumulative data are averaged for each time point for the days 6-18 experimental series.

13.5. Virus release and infectivity

In the same experiment, the corresponding supernatant of infected cells was collected at each time points and analyse in qPCR to determine the extracellular release of virus (Figure 18, A). Results indicated that accumulation of viral DNA in the supernatant of infected cells was mainly proportional to viral DNA present within the corresponding cellular fraction (Figure 15, A). In fact, in the non-permissive cells of day 3 series, DNA remained to background values for the whole time course. In the day 6-15 series, viral DNA accumulated starting from 24 hpi and reaching maximum level at 48 hpi (+1.9-2.8 Log increase over

background values). However, this correlation between extracellular and intracellular B19V-DNA was not observed for the day 18 cell series, where viral DNA in the supernatant remained at a constant background level within the 48 hpi, like day 3 cell series, with the difference that a modest increase in intracellular DNA occurred at day 18 but not at day 3.
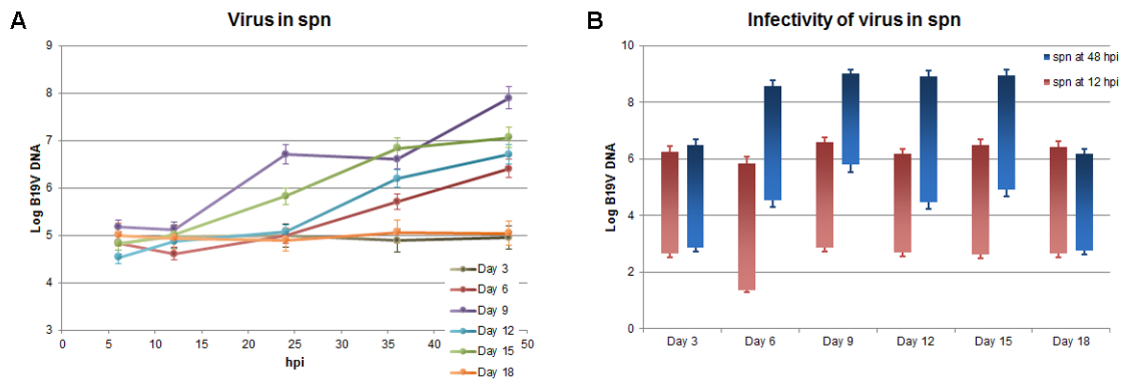

Figure 18: Virus release from EPCs and infectivity. (A) Log of viral DNA target copies measured in 100 µl of supernatant collected from infected EPCs. (B) Infectivity of virus released from EPCs. The amount of viral DNA was calculated at 2 and 48 hpi in supernatants-infected EPCs. DNA amounts are reported as variation bars: lower limits of bars are the amount of viral DNA detected at 2 hpi; upper limits are the amount detected at 48 hpi.

The ability of collected supernatants to start a new infection cycle was investigated to test the infectivity of virus released from EPCs. Equal amount of supernatants obtained at 12 and 48 hpi from each samples series were used to infect new EPCs at day 9 of culture (Figure 18, B). Supernatant collected at 12 hpi was chosen to verify a possible residual activity, because it was collected before viral replication started. Thus, potential infectivity of supernatants from 12 hpi could not be ascribed to new viral progeny released from infected cells. After infection with supernatants, viral replicative activity in the infected cells was determined comparing the amount of viral DNA at 48 hpi with respect to that at 2 hpi. Supernatants obtained at 12 hpi showed a comparable residual infectivity for each of the tested sample series, leading to a mean increase of 3.8 Log from 2 to 48 hpi. Supernatants from 48 hpi of day 3 and day 18 cell series showed similar infectivity (mean increase 3.5 Log) to the supernatants collected at 12 hpi of the same day 3 and day 18 cell series, suggesting that no viral progeny was released from 12 hpi to 48 hpi in these cells. On the

other hand, supernatants obtained at 48 hpi for day 6-15 series yielded infectivity results coherent with the amounts of virus present in supernatants, with a mean increase of 4.4 Log of viral DNA in infected cells. For day 6-15 series, the difference of infectivity obtained with supernatants of 48 hpi with respect to that obtained with supernatants of 12 hpi, indicating that for these day series production and release of new infectious virus occurred. These results confirmed that B19V productive viral cycle is restricted to a limited differentiation of phase of erythroid lineage.

14. B19V AND CIDOFOVIR

14.1. Inhibitory effect of cidofovir in UT7/EpoS1

The antiviral activity of CDV was first evaluated in a reference cell line (UT7/EpoS1), largely used to study B19V pathogenesis. UT7/EpoS1 cells were infected with different concetrations of B19V, from 10^4 to 10^1 geq/cell, and following absorption phase for 2 h at 37°C, cells were incubated in the absence or in presence of different concentration of CDV (range 0.1-500 µM) for a total course of infection of 72 h.

Following the same experimental outline as for EPCs, UT7/EpoS1 cells were infected with B19V and cultured in the absence, as a control, and in the presence of the different concentrations of CDV. Viral replication was determined by quantification of viral DNA amount present in cells collected at 72 hpi (the optimal time course of infection for this cell line) and comparing it with the amount of viral DNA present at 2 hpi in an equivalent aliquot of cells. Calculated amounts of viral DNA (by interpolation with external standard curve) at 2 hpi and at 72 hpi are plotted as a function of the moi, for the different concentrations of CDV studied (Figure 19, left), and are expressed as Log of target copies (geq) normalized to 20000 cells. Linear regression analysis showed that the amount of viral DNA within cells is correlated with the moi used, for the different experimental samples. Virus binding and uptake was proportional to viral concentration inoculated with a constant ΔLog at 2 hpi between the serial dilutions of virus. A constant replicative activity of B19V was also evident within cells, since a regular variation in the amount of viral DNA from 2 hpi to 72 hpi was measured for the different moi tested, as demonstrated by the equivalent slopes for the 2 hpi and 72 hpi sample series in absence of CDV. Eventual shift along the Y-axis indicated a lower replicative activity attributable to inhibitory effects of CDV on B19V DNA replication. CDV 0.1 µM possessed no significative inhibitory activity, while progressively lower increases of viral DNA were detected in the 10 µM -100 µM range, and a complete inhibition of viral DNA replication was reached with 500 µM CDV, because the amount of viral DNA at 72 hpi was lower than viral DNA detected at 2 hpi. The progressively reduced replicative activity in presence of increasing CDV concentrations compared to control sample without drug indicated that CDV showed a dose-dependent inhibitory effect

on B19V replication in infected UT7/EpoS1 cells. The dose-dependent relationship allowed defining EC50 and EC90 values for CDV for all the different moi tested by plotting the percentage inhibition of replication as a function of CDV concentration and analyzing trough a non-linear regression function (Figure 19, right). For the highest moi tested, EC50 value corresponded to 34.35 µM.
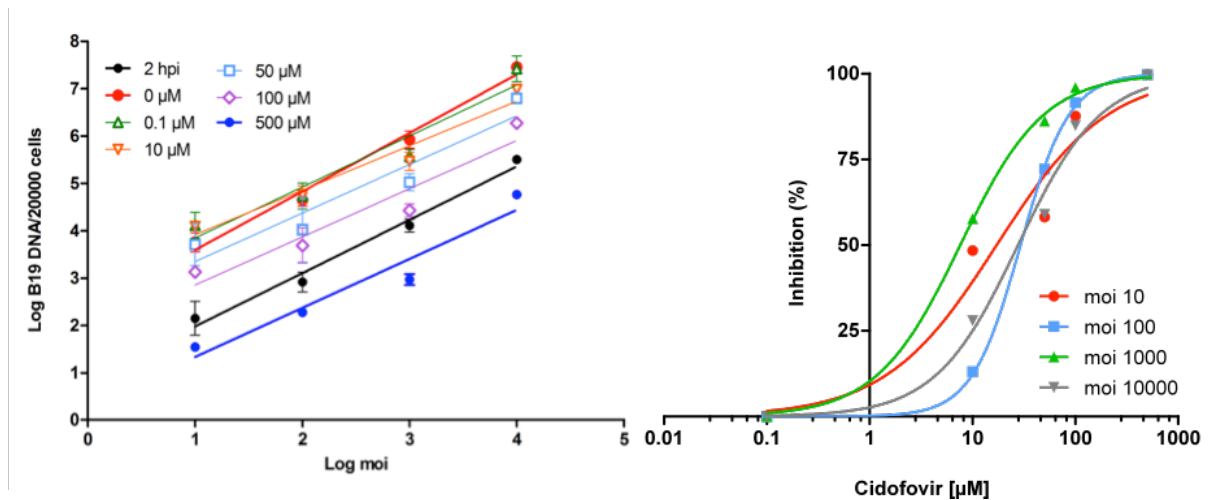
Figure 19: Inhibitory activity of CDV in UT7/EpoS1 cells. (Left) Calculated amounts of B19V DNA in infected cells at 2 and 72 hpi were plotted as a function of moi for the different concentrations of CDV tested. (Right) Normalised response to CDV in UT7/EpoS1 cells. EC50 and EC90 values can be derived from the plot.

Parallel analysis of total viral RNA synthesised in infected UT7/Epo S1 cells was determined at 72 hpi. Significative reduction in viral transcriptional activity was appreciable only for high moi and with the highest CDV concentration tested (Figure 20).
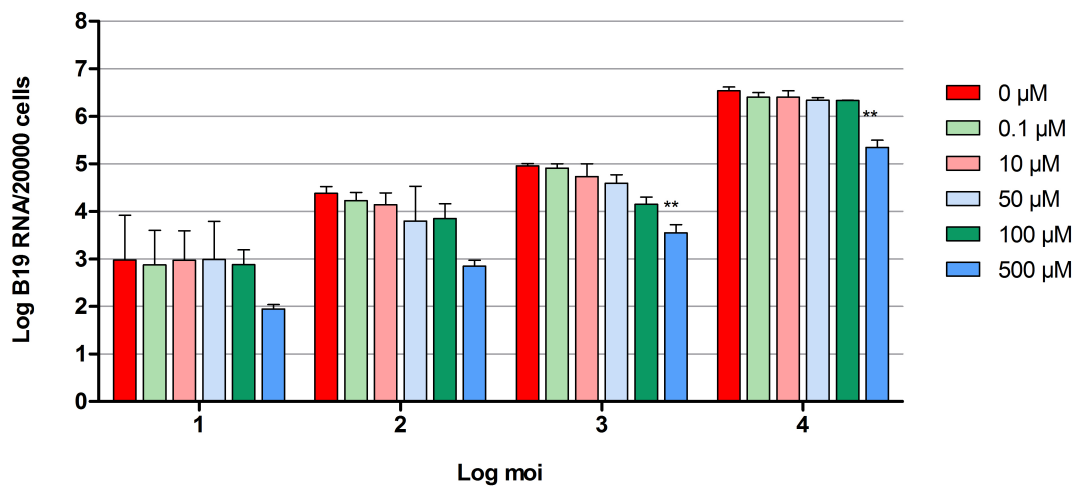
Figure 20: Analysis of variance in the amount of B19V RNA in UT7/EpoS1 cells. Amount of total RNA was measured in infected cells at the different moi and in presence of different CDV concentration.

The relative abundance of mRNAs coding for viral proteins followed the expression profile previously characterized, with mRNAs coding for NS proteins in the range of 1-3% of total viral RNA, and mRNAs coding for capsid VP1 and VP2 proteins in the range of 15-22%, with an exception in presence of CDV 500 µM when range was reduced to 5-8%, an effect possibly linked to a shift in the expression profile of B19V due to the marked inhibition of its replicative activity.

By immunofluorescence assay, a proper evaluation of protein expression could be possible only for the highest moi of 10^4, because at lower moi the small number of positive cells did not allow any reliable quantitative evaluation of inhibitory activity of CDV. 5.0% of cells infected with 10^4 moi were positive for capsid proteins, while a decreasing value were observed in presence on increasing CDV concentrations up to the loss of positive signal in presence of CDV 500 µM.

14.2. Inhibitory effect of cidofovir in EPCs

To test the inhibitory effect of CDV on B19V replication in the natural target cells, EPCs differentiated from PBMC were infected at day 9 ± 1 of culture, the optimum range for viral permissiveness as indicated by previous characterization. Following the same experimental outline as for UT7/EpoS1, EPCs were infected with B19V and cultured in the absence, as a

control, and in the presence of the different concentrations of CDV for a total course of infection of 24 h. This short period of infection was chosen because the highest increase in the amount of viral DNA occurred between 12 hpi and 24 hpi, as shown in Figure, thus considered optimal for assessing the viral activity in a single round of infection. Viral replication was determined by quantification of viral DNA amount present in cells collected at 24 hpi and comparing it with the amount of viral DNA present at 2 hpi in an equivalent aliquot of cells. Calculated amounts of viral DNA at 2 hpi and at 24 hpi are expressed as Log of target copies (geq) normalized to 20000 cells and plotted as a function of the moi, for the different concentrations of CDV studied (Figure 21). As for UT7/EpoS1 cells, also for EPCs the amount of viral DNA within cells is orrelated with the moi used, both at 2 hpi and at 24 hpi, for the different moi used. The slopes for the 2 hpi and 24 hpi sample series are statistically equivalent, indicating a constant relative biological activity of B19V in EPCs, as within UT7/EpoS1 cells. Shift along the Y-axis indicated a lower replicative activity attributable to inhibitory effects of CDV on B19V DNA replication. A statistically significant difference in elevations that could be attributed to the inhibitory effects of CDV on viral DNA replication was evident only for the 500 µM concentration, while no statistically significant differences were seen for CDV 0.1-100 µM.
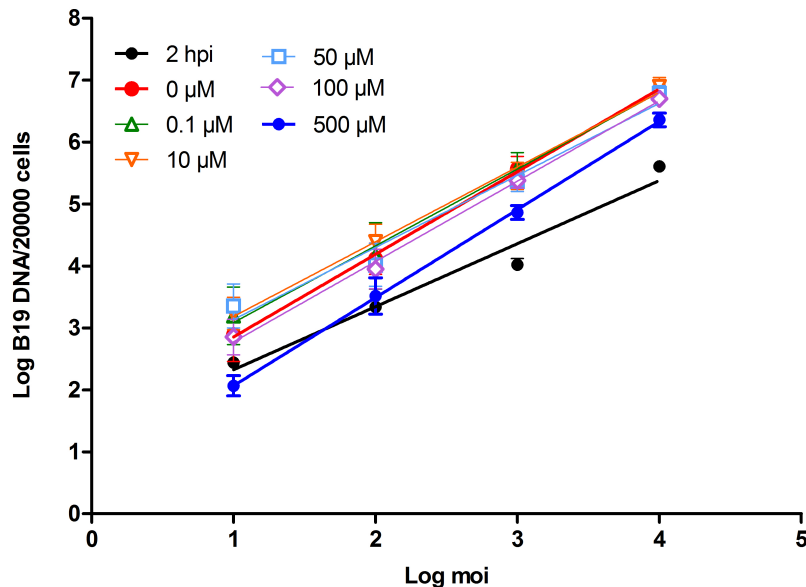

Figure 21: Inhibitory activity of CDV in EPCs cells. Calculated amounts of B19V DNA in infected cells at 2 and 24 hpi were plotted as a function of moi for the different concentrations of CDV tested.

Parallel analysis of total viral RNA synthesised in infected EPCs cells was determined at 24 hpi. Even at the highest concentration of CDV, which showed to reduce viral DNA replication, the amount of total viral RNA at 24 hpi was not significantly different with respect to control sample without drug (Figure 22). Regarding the relative abundance of transcripts, mRNAs coding for NS protein was in the range of 1-3% of total viral RNA, and mRNAs coding for capsid VP1/VP2 proteins was in the range of 35-45%, an expression profile comparable to that previously determined, without any significant correlation with the concentration of CDV.
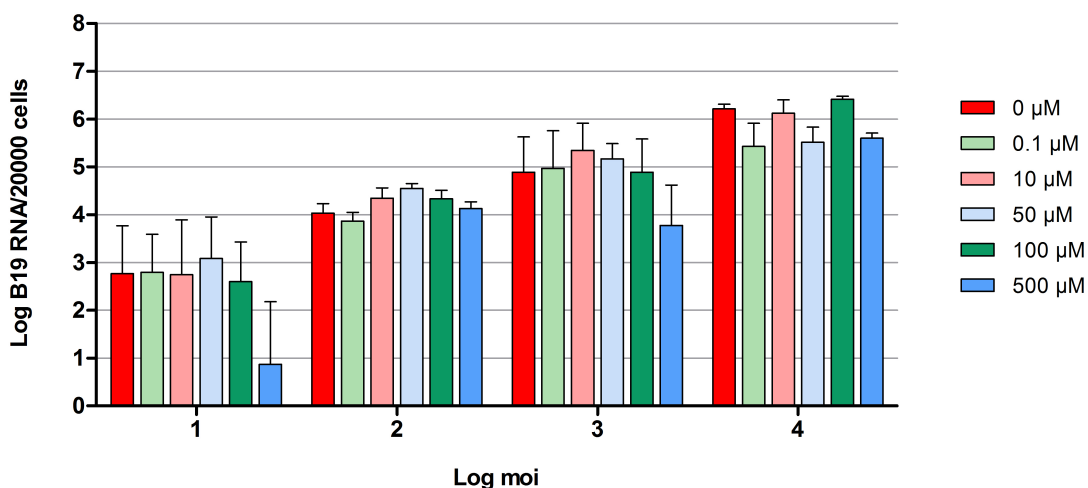
Figure 22: Analysis of variance in the amount of B19V RNA in EPCs cells. Amount of total RNA was measured in infected cells at the different moi and in presence of different CDV concentration.

Expression of viral capsid proteins was also investigated by immunofluorescence assay. The percentage of infected cells treated with CDV 500 µM positive for capsid protein expression was not statistically different from cells incubated in medium alone (10.8 % compared to 14.0% for moi of 10^4, 1.1% compared to 1.8% for moi of 10^3). The effect on CDV on cell viability and proliferation were analysed by alamarBlue and BrdU assay, respectively, in both EPCs and UT7/EpoS1 cells. Data showed the CDV, at any concentrations, possessed neither cytotossic nor cytostatic effects on both cell system studied.

14.3. CDV activity in pre-incubated EPCs

Considering the slight inhibition observed in 24 h-infected EPCs treated with 500 μM CDV, the inhibitory effect of 500 μM CDV was investigated in EPCs throughout a single cycle infection of 48 h, and in EPCs pre-incubated for 24 h in medium supplemented with 500 μM CDV. EPCs on day 9 ± 1 of culture were infected with B19V at 10^4 moi and following the adsorption period, cells were split and grown for 48 h in presence of 500 μM CDV, and in the absence, as control sample. Similarly, EPCs pre-incubated with 500 μM CDV were inoculated, and after 2 h of virus incubation, cultured for 48 h with a fresh medium containing the drug, for a total exposure time to CDV of 72 h. DNA amounts at 48 hpi in the different experimental conditions were compared with those obtained in the control sample, and expressed as percentage of viral replication (Figure 23). B19 viral activity in EPCs was significantly inhibited by 500 μM CDV (72.95 ± 1.81 %), and the drug exposure of EPCs before infection further increased the inhibitory effect up to 92.44 ± 2.44 %.
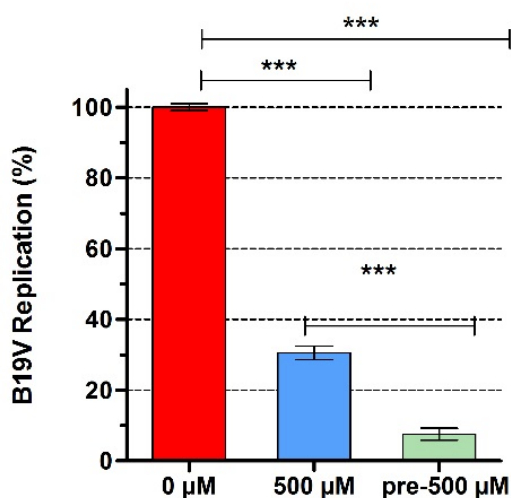
Figure 23: Analysis of CDV-treated EPCs in a time course of infection of 48 h. Percentage of viral replication is reported by calculating viral DNA amounts at 2 hpi and 48 hpi in EPCs treated with 500 μM CDV after infection and in EPCs pre-incubated with 500 μM CDV for 24 f prior to infection.

14.4. CDV activity in serial rounds of EPCs infection

The activity of CDV against B19V replication was assessed in serial rounds of infection in which supernatants of infected EPCs were used as inoculum virus for consecutive infections, under constant drug exposure, and in regular medium as control. In detail, EPCs

at 6 ± 1 day from isolation were inoculated with the viremic serum sample at 10^4 moi, then split and cultured with 500 μM CDV and without. After 72 h, infected cultures were collected and the supernatants were used to inoculate aliquots of the same initial cellular population, at day 9 ± 1 of expansion and differentiation, in a second round of infection. Once more, following 72 h, the cell-culture supernatants were used to infect a new EPCs culture at day 6 ± 1, and following the same experimental design, at day 9 ± 1. A total of four rounds of infection were carried out, each one consisting in an infection cycle of 72 h. Viral replicative activity was evaluated determining viral DNA amount present at 2 hpi and 72 hpi; supernatants were analyzed at 72 hpi to determine the yield of virus released from EPCs, and to measure the viral titers used in the subsequent rounds of infection.
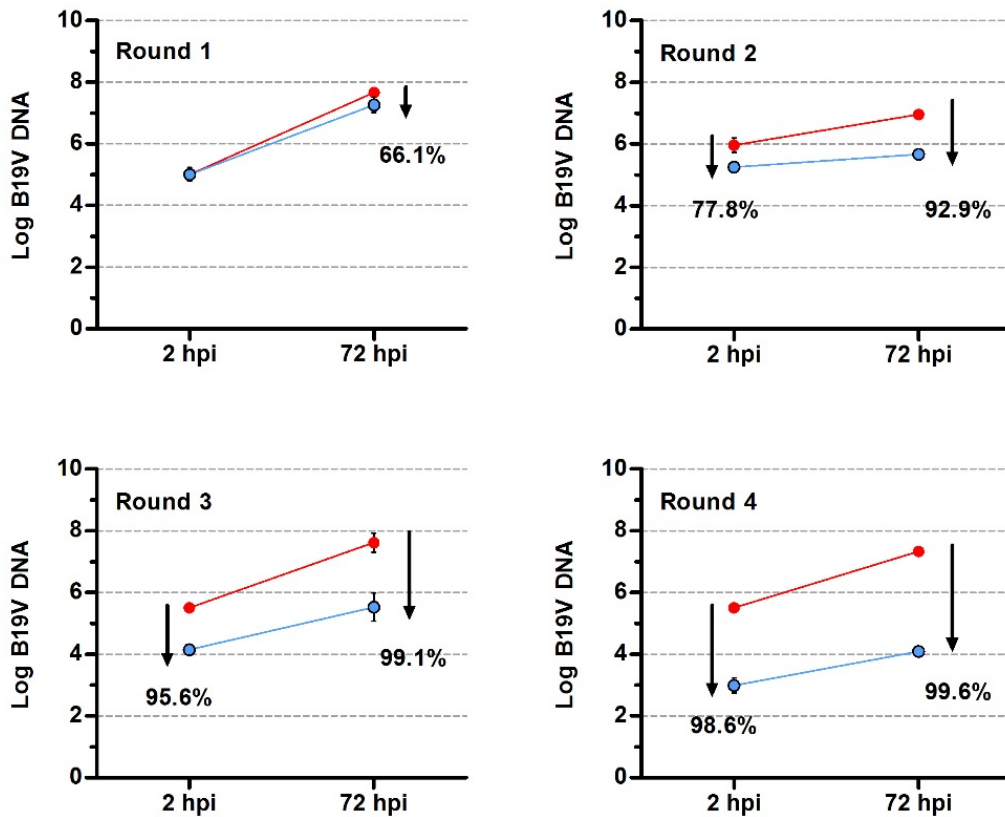
**Figure 24: Effect of CDV in serial rounds of infected EPCs.** Log B19V DNA (geq/20.000 cells) is plotted as function of the time points, for the different rounds of infection, and in the two experimental conditions (0 μM CDV in red; 500 μM CDV in blue). Arrows indicate the reduction in viral amounts and the reported values are the inhibition percentages of treated EPCs relative to untreated cells.

In the treated EPCs and in their supernatants, a progressive reduction of B19V replication was observed. Following 4 consecutive infections, for a total of 12 days of drug exposure, the percentage reduction of B19V DNA within cells was 99.6 ± 1.13 %, and in the supernatants was 98.6 ± 0.62 %.

14.5. CDV activity in long-term EPCs infection

The inhibitory activity of 500 µM CDV was measured in the EPCs throughout a prolonged viral infection. Cells at 6 ± 1 day from isolation were infected, then split and cultured in presence of 500 µM CDV, and in the absence of the drug. Four days after infection, fresh medium with or without CDV was added to the cultures, respectively.

At different time post infection, up to 8 days, EPCs were harvested and B19V DNA was quantified by qPCR, normalized for the number of cells. Similarly to what was obtained in the serial rounds of infection when infection proceed within the differentiating EPCs population and in the presence of CDV, B19V replication was progressively repressed; the inhibitory effect of the drug, determined as percentage of the intracellular B19V DNA in treated EPCs with respect to untreated EPCs reached at the late stage of infection the 81.71 ± 5.02 %. The analysis of B19V DNA in the cell-cultures supernatants at 8 dpi confirmed that CDV led to severe inhibition of B19V yield, reaching the 80.82 ± 8.27 %. The effects of the extended exposure to CDV on EPCs were evaluated in terms of cell viability and proliferation (Table 2).

Time post infection	B19V inhibition	Cell viability	Cell proliferation
48 hpi	67.75± 6.22	95.57± 1.01	88.14± 4.79
96 hpi	71.40± 2.30	93.37± 3.50	75.04± 10.17
8 dpi	81.71± 5.02	96.23± 9.88	68.08± 2.83

Table 2: Effects of CDV in prolonged-exposed EPCs. The effects of CDV (500 µM) on EPCs viability and proliferation were expressed as percentage values, relative to untreated cells (0 µM CDV).

Prolonged incubation with 500 μM of CDV did not reduce EPCs viability, while cell proliferation rate progressively decreased with a cytostatic effect nearly at 30% at 8 days upon exposure.

DISCUSSION

15. DISCUSSION

The human pathogenic parvovirus B19 (B19V) has a marked tropism for human erythroid progenitor cells (85, 86). In vitro, only few myeloblastoid cell lines support viral replication and, even so, in a not complete permissive environment, yelding to a very limited progeny. PBMC isolated from peripheral blood can be cultured and differentiated in vitro toward a population of more mature erythroid cells, providing a culture system of primary target cells highly permissive to B19V replication and expression and suitable to study B19V life cycle and virus-cell interactions (92, 93).

A systemic characterization of B19V replication and expression was assessed in PBMC-derived EPCs cultured in medium containing cellular grow factors able to stimulate a progressive differentiation trough the erythroid lineage.

During the culture period, EPCs show increasing expression of erythroid specific markers, such as CD36, CD71 and CD235a. The presence of markers linked to the susceptibility to B19V was also investigated. Tropism of B19V is mainly determined by the presence on cell surface of the principal receptor, globoside, and a possible role of coreceptors, like α5β1 integrin, in virus uptake was proposed (34, 36). The distribution of globoside within differentiating EPCs followed closely that of other erythroid markers, indicating that this cell population on the whole is potentially susceptible to B19V infection. On the contrary, α5β1 integrins are expressed at constant level, independently of the differentiation stage. B19V productive infection was showed to be restricted to a limited phase during erythroid differentiation, highlighting the close relationship between virus and cellular factors. Thus, viral genome replication and expression was characterized in function of cell differentiation stage.

The extent of viral replication, determined by qPCR, as well as the fraction of productively infected cells, determined by flow-FISH assay, indicate that cells can support B19V more at earlier differentiation stages, between 6-9 days, compared to later stages of erythroid differentiation occurring at 12–15 days, while cells at the first days post isolation (day 3) lead to an abortive infection, even being susceptible to B19V. Furthermore, the extent of

viral replication is correlated to the fraction of productively infected cells that is constantly lower than that showing the presence of erythroid markers and receptor moieties.

The presence and distribution of viral receptors within EPCs will define a susceptible cell population, but is not sufficient to classify a cell population supporting B19V replication. The capacity of cells to support a productive infection will be therefore regulated by intracellular events confined to a particular cell differentiation stage.

A detailed analysis of viral macromolecular synthesis, obtained by qPCR and qRT-PCR, clearly indicates the occurrence of specific patterns related to the specific differentiation stages. The abortive infection in EPCs at a very early stage (3 days) is demonstrated by absence of genome replication and minimal transcriptional activity. This pattern is similar to what detected in other cell types and several cell lines, considered susceptible but not permissive to B19V. Determinants of viral restriction may include inefficient initial steps, such as penetration, uncoating, nuclear import of viral genome, as well as failure to convert the parental ssDNA in dsDNA, thus preventing the generation of a functionally active genomic template. In EPCs at later stages (6-18 days), the productive pattern of infection is constituted by biphasic, coordinated replication and transcription events. Assuming the occurrence of synthesis of the complementary strand, the active dsDNA is transcribed firstly, since total RNA is detected before replication starting. Then, in a second phase, both replication and transcription can occur on the amplifying genome, as by a progressive accumulation of viral nucleic acids trough the course of infection.

Production of the whole set of mRNA is another key factor in the definition of a permissive cellular environment. A series of cis-acting sequences have been mapped on B19V genome and their role in DNA replication and RNA processing experimentally determined. In mRNA processing events, two pattern of expression could be distinguished: an early phase where cleavage at pAp site is prevalent, splicing is relatively low, and mRNA for NS protein is produced in relatively higher abundance, and a late phase where cleavage at pAd site is prevalent, splicing is relatively high, and mRNAs for the VP and the 11 kDa proteins are produced in abundance. This pattern allows early production of NS protein that is necessary for viral replication and late accumulation of capsid proteins necessary for virus packaging and release.
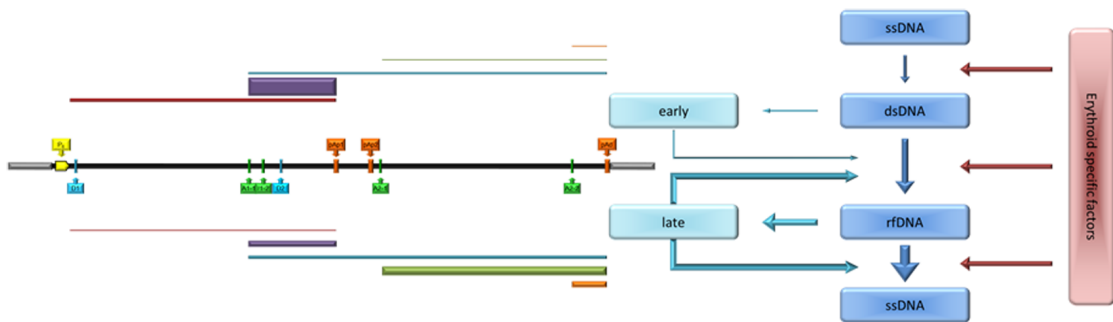
Figure 25: A model for B19V replication and expression. Viral genome can be present in four consecutive states, connected by three state transitions: input ssDNA, initial dsDNA, replicating rfDNA, and product ssDNA. Two functional profiles are identified as "early" (from dsDNA) and "late" (from rfDNA), characterized by a differential abundance and relative composition of transcriptome (compare map in Figure 10). Each profile is involved in regulative loops on genome state transitions. Erythroid specific factors are critical in regulating state transitions and are dependent on the differentiation and physiological state of the cell.

In our experimental conditions, the dynamics of macromolecular synthesis in infected EPCs is in agreement with observations in other experimental systems, such as bone marrow and UT7/EpoS1 cells (63, 64).

However, our results indicate the strong dependence on erythroid differentiation-specific intracellular events, possibly interacting with viral proteins, to regulate a full, productive, macromolecular synthesis. These factors would allow the definition of a complete productive infection cycle, conditioning the switch from the early to the late viral phases.

The importance of such cellular factors is highlighted also by the impaired release of virus from cells infected at the very late stage (18 days), while cells supporting a complete macromolecular synthesis (6-9 days) lead to production and release of new infectious virus. The restriction pattern in virus release, characterizing the very late stage, could be ascribed to an inefficient translation and capsid protein production, as well as defective genome encapsidation and virus packaging.

B19V mediates cell cycle arrest, induces apoptosis, interacts with DNA Damage Response pathway and blocks erythropoiesis (102-109). Productive infection is dependent also by erythropoietin signaling (97) and is enhanced by hypoxic condition (98, 99), through activation of specific signal cascade. Comparative analysis of the erythroid-specific expression profiles during differentiation would allow identifying potential cellular factors and pathways that are the first assumption to achieve a B19V productive infection.

In conclusion, the present work highlights the very strictly adaptation of B19V to a specific cellular target not only identify in the erythroid lineage but also confined to a limited differentiation stage. This strictly adaptation is also the 'strength' of the evolutionary success of B19V whose pathogenic potential affects neither the more undifferentiated cells with staminal properties, nor the terminally differentiated cells with scarce potential and lifespan to support replication. While earlier studies indicated that B19V infection of bone marrow-derived cells increased with cell differentiation identified a permissive population at the BFU-E and CFU-E stage (86), in the PBMC-derived EPCs system here described permissive population corresponds to proerythroblast stage.

A final remark is the possibility to obtain infectious virus suitable for in vitro studies and allowing to overcome the dependence to sera of viremic patients as source of virus. This evidence is in contrast with previous observations that showed a limited virus release even in permissive EPCs (202).

The culture system described, highly permissive to B19V and representing in vitro the natural target cells infected in vivo, provide a reference framework for identify potential antiviral drug active against B19V. To this purpose, the inhibitory effect of Cidofovir (CDV) on B19V replication was investigated in permissively infected EPCs and UT7/EpoS1 cells.

In both cellular systems, a direct relationship was present between multiplicity of infection (moi) and detected amount of viral DNA, as demonstrated by the linear regression curve for 2 hpi (adsorbed/internalised virus) series and 24 hpi (for EPCs) and 72 hpi (for UT7/EpoS1). The effect of the different CDV concentrations on the amount of viral DNA produced in infected cells is evidenced by a Y-axis shift compared to control series without drug. A dose-dependent inhibitory effect of CDV was evident in UT7/EpoS1 cells, with a progressively

reduced replicative activity of B19V in presence of increasing CDV concentrations, up to a complete inhibition with 500 μM CDV. This effect was less evident in peripheral blood derived EPCs, where only the 500 μM concentration showed a significant inhibition of viral replicative activity. Due to the dose-dependent relationship, EC50 and EC90 values can be determined only in UT7/EpoS1 cells, and are comparable to those obtained for dsDNA viruses, having their own DNA polymerases (203). Cellular assays indicated that CDV exhibits any significant cytotoxic or cytostatic effect in both cellular systems, suggesting that inhibitory effects are specific for the virus.

The different activity in the two cellular systems may be ascribed to a different permeability of cells to the compound, or to different mechanisms of interference with the normal metabolism of nucleotides (204). A critical step is the amount of drug that could enter the cells and be converted in the active form. Incorporation of CDV during DNA synthesis may hamper its template activity or causes chain termination. A different degree of incorporation in viral DNA, or a different activity of DNA repair mechanisms, can contribute to the diverse activity of CDV in normal cells like EPCs compared to a myeloblastoid cell line like UT7/EpoS1 (205).

To deeply investigated the CDV action in EPCs, activity in pre-incubated or long-treated EPCs with 500 μM CDV was evaluated.

Firstly, intracellular B19V DNA amounts were measured in EPCs cultured with 500 μM CDV added after virus infection and collected 48 hpi, and in EPCs pre-incubate for 24 h with 500 μM CDV and then infected and cultured in presence of the drug for 48 h, for a total exposure time of 72 h. Comparing the two experimental settings, a remarkable increase in antiviral activity was observed in cells subjected to pre-incubation, in which B19V replication was reduced at minimum levels (<8 %). Considering the slow cellular uptake of CDV, in EPCs treated following the viral adsorption period, B19V synthesis could start before the active diphosphoryl metabolite of CDV reached the effective intracellular levels. As a consequence, CDV activity against B19V replication in this cellular context is lower than which can be obtained with a pre-exposure.

The inhibitory effect of 500 μM CDV against B19V replication was then assessed in prolonged infections of EPCs cultures in which the differentiation process of the

heterogeneous cellular population is reproduced according to two experimental schemes that mimic in vitro what occurs in the bone marrow environment. In the first, cell-culture supernatants of infected EPCs, cultured with and without CDV, were used as inoculum virus for subsequent infections of cells at days 6 and 9 from isolation. Four rounds of infection, each one consisting in a 72 h infectious cycle, were carried for a total exposure time of 12 days. In continuously treated cells, both the intracellular B19V DNA amounts and the viral progeny released from EPCs progressively decreased comparing to untreated cells, indicating that B19V maintains the susceptibility to the drug even upon extended exposure time.

Finally, EPCs were inoculated with B19V at 6 ± 1 day, and cells were grown with 500 μM CDV and without for 8 days, thus, up to the 15 ± 1 day from isolation. B19V DNA amounts in EPCs under constant CDV pressure progressively decreased at levels <20% compared to untreated cells; the observed inhibition of B19V replication, even at the late stage of infection, could be ascribed predominantly to a selective activity of CDV towards the virus since cell proliferation remained close to 70%.

CDV antiviral activity was already demonstrated for dsDNA viruses (206), thus present results not only extend its broad spectrum including a ssDNA virus, but also demonstrated for the first time an inhibitory activity of a drug against B19V.

This is promising for the development of antiviral drugs directed against a human pathogenic virus still lacking of an antiviral treatment.

Considering the limited activity of CDV in EPCs and the nephrotossic side effects in vivo, related compounds would be investigated, such as lipid conjugates characterised by a greater uptake within cells (207). The improved CDV activity in human primary EPCs upon extended exposure confirms that cellular uptake and conversion into active metabolites affect the potency of the drug. The availability of new CDV analogs with increased cell membrane permeability, resulting in greater intracellular levels of active compound, will lead to improved inhibitory activity as well as minor side effects if lower amounts of compound are sufficient to achieve inhibitory activity.

In conclusion, results confirm the restricted tropism of B19V to a limited phase of the erythroid lineage. Further investigation focused on the change in the intracellular events during differentiation would allow the identification of cellular factors regulating viral permissiveness. On the other hand, differentiating EPCs in vitro provide a cell culture system suitable for screening of compounds with potential antiviral activity in a cellular environment close to the primary target cells of B19V infection in vivo. Finally, cidofovir is the first compound with a demonstrated inhibitory activity on B19V replication; thus, overall results are promising for development of a specific antiviral therapy against B19V infection.

REFERENCES

1. YE Cossart, AM Field, B Cant and D Widdows, Parvovirus-like particles in human sera. *The Lancet*, pp. 72-73, 1975.

2. JR Pattison, SE Jones, J Hodgson et al., Parvovirus infections and hypoplastic crisis in sickle-cell anaemia. *The Lancet*, pp. 664-665, 1981.

3. Anderson MJ, Jones SE, SP Fisher Hoch et al., Human parvovirus, the cause of erythema infectiosum (fifth disease)?. *The Lancet*, pp. 1378, 1983.

4. GR Siegl, C Bates, KI Berns, BJ Carter, DC Kelly, E Kurstak and P Tattersall, Characteristics and taxonomy of Parvoviridae. *InterVirology*, vol. 23, pp. 61-73, 1985.

5. International Committee on Taxonomy of Viruses, 2014.

6. SF Cotmore, VC McKie and LJ Anderson, Identification of the major structural and nonstructural proteins encoded by human parvovirus B19 and mapping of their genes by procaryotic expression of isolated genomic fragments. *Journal of Virology*, vol. 60, no. 2, pp. 548–557, 1986.

7. MS Chapman and MG Rossmann, Structure, sequence, and function correlations among parvoviruses. *Virology*, vol. 194, no. 2, pp. 491–508, 1993.

8. M Agbandje, R McKenna, MG Rossmann, S Kajigaya and NS Young, Preliminary X-ray crystallographic investigation of human parvovirus B19. *Virology*, vol. 184, no. 1, pp. 170–174, 1991.

9. M Agbandje, S Kajigaya, R McKenna, NS Young and MG Rossmann, The structure of human parvovirus B19 at 8Å resolution. *Virology*, vol. 203, no. 1, pp. 106–115, 1994.

10. B Kaufmann, AA Simpson, and MG Rossmann, The structure of human parvovirus B19. *Proceedings of the National Academy of Sciences of the United States of America*, vol. 101, no. 32, pp. 11628–11633, 2004.

11. B Kaufmann, PR Chipman, VA Kostyuchenko, S Modrow and MG Rossmann, Visualization of the externalized VP2 N termini of infectious human parvovirus B19. *Journal of Virology*, vol. 82, no. 15, pp. 7306–7312, 2008.

12. SF Cotmore and P Tattersall, Characterization and molecular cloning of a human parvovirus genome. *Science*, vol. 226, no. 4679, pp. 1161–1165, 1984.

13. V Deiss, M Tratschin, M Weitz and G Siegl, Cloning of the human parvovirus B19 genome and structural analysis of its palindromic termini. *Virology*, 175:247-254, 1990.

14. G Gallinella, Parvovirus B19 Achievements and Challenges. ISRN *Virology*, vol. 2013.

15. G Zuccheri, A Bergia, G Gallinella, M Musiani, and B Samorì, Scanning force microscopy study on a single-stranded DNA: the genome of parvovirus B19. *ChemBioChem*, vol. 2, no. 3, pp. 199-204, 2001.

16. A Servant, S Laperche, F Lallemand et al., Genetic diversity within human erythroviruses: identification of three genotypes. *Journal of Virology*, vol. 76, no. 18, pp. 9124–9134, 2002.

17. K Hokynar, M Söderlund-Venermo, M Pesonen et al., A new parvovirus genotype persistent in human skin. *Virology*, vol. 302, no. 2, pp. 224–228, 2002.

18. QT Nguyen, S Wong, ED Heegaard, and KE Brown, Identification and characterization of a second novel human Erythrovirus variant, A6. *Virology*, vol. 301, no. 2, pp. 374–380, 2002.

19. Nguyen QT, Sifer C, Schneider V, Bernaudin F, Auguste V, Garbarg-Chenon A, Detection of an erythrovirus sequence distinct from B19 in a child with acute anemia. *Lancet*, 352:1524, 1998.

20. NL Toan, A Duechting, PG Kremsner et al., Phylogenetic analysis of human parvovirus B19, indicating two subgroups of genotype 1 in Vietnamese patients. *Journal of General Virology*, vol. 87, no. 10, pp. 2941–2949, 2006.

21. A Parsyan, C Szmaragd, JP Allain, and D Candotti, Identification and genetic diversity of two human parvovirus B19 genotype 3 subtypes. *Journal of General Virology*, vol. 88, no. 2, pp. 428–431, 2007.

22. A Ekman, K Hokynar, L Kakkola et al., Biological and immunological relations among human parvovirus B19 genotypes 1 to 3. *Journal of Virology*, vol. 81, no. 13, pp. 6927–6935, 2007.

23. SN Wong, NS Young, and KE Brown, Prevalence of parvovirus B19 in liver tissue: no associations with fulminant hepatitis or hepatitis-associated aplastic anemia. *Journal of Infectious Disease*, 2003, 187:1581-1586.

24. S Sanabani, WK Neto, J Pereira, and EC Sabino, Sequence variability of human erythroviruses present in bone marrow of Brazilian patients with various parvovirus B19-related hematological symptoms. *Journal of Clinical Microbiology*, vol. 44, no. 2, pp. 604–606, 2006.

25. D Candotti, N Etiz, A Parsyan, and JP Allain, Identification and characterization of persistent human erythrovirus infection in blood donor samples. *Journal of Virology*, vol. 78, no. 22, pp. 12169-12178, 2004.

26. JM Hübschen, Z Mihneva, AF Mentis et al., Phylogenetic analysis of human parvovirus B19 sequences from eleven different countries confirms the predominance of genotype 1 and suggests the spread of genotype 3b. *Journal of Clinical Microbiology*, vol. 47, no. 11, pp. 3735–3738, 2009.

27. BJ Cohen, J Gandhi, and JP Clewley, Genetic variants of parvovirus B19 identified in the United Kingdom: implications for diagnostic testing. *Journal of Clinical Virology*, vol. 36, no. 2, pp. 152–155, 2006.

28. P Grabarczyk, A Kalinska, M Kara et al., Identification and characterization of acute infection with parvovirus B19 genotype 2 in immunocompromised patients in Poland. *Journal of Medical Virology*, vol. 83, pp. 142–149, 2011.

29. P Norja, K Hokynar, LM Aaltonen et al., Bioportfolio: lifelong persistence of variant and prototypic erythrovirus DNA genomes in human tissue. *Proceedings of the National Academy of Sciences of the United States of America*, vol. 103, no. 19, pp. 7450–7453, 2006.

30. LA Shackelton and EC Holmes, Phylogenetic evidence for the rapid evolution of human B19 erythrovirus. *Journal of Virology*, vol. 80, no. 7, pp. 3666–3669, 2006.

31. P Norja, AM Eis-Hübinger, M Söderlund-Venermo, K Hedman, and P Simmonds, Rapid sequence change and geographical spread of human parvovirus B19: comparison of B19 virus evolution in acute and persistent infections. *Journal of Virology*, vol. 82, no. 13, pp. 6427-6433, 2008.

32. M Toppinen, MF Perdomo, JU Palo, et al., Bones hold the key to DNA virus history and epidemiology. *Scientific Reports*, 5, 17226, 2015.

33. KE Brown and BJ Cohen, Haemagglutination by parvovirus B19. *Journal of General Virology*, vol. 73, no. 8, pp. 2147–2149, 1992.

34. KE Brown, SM Anderson, and NS Young, Erythrocyte P antigen: cellular receptor for B19 parvovirus. *Science*, vol. 262, no. 5130, pp. 114–117, 1993.

35. KE Brown, JR Hibbs, G Gallinella et al., Resistance to parvovirus B19 infection due to lack of virus receptor (erythrocyte P antigen). *The New England Journal of Medicine*, vol. 330, no. 17, pp. 1192–1196, 1994.

36. KA Weigel-Kelley, MC Yoder, and A Srivastava, $\alpha5\beta1$ integrin as a cellular coreceptor for human parvovirus B19: requirement of functional activation of $\beta1$ integrin for viral entry. *Blood*, vol. 102, no. 12, pp. 3927–3933, 2003.

37. KA Weigel-Van Aken, Pharmacological activation of guanine nucleotide exchange factors for the small GTPase Rap1 recruits high-affinity $\beta1$ integrins as coreceptors for parvovirus B19: improved ex vivo gene transfer to human erythroid progenitor cells. *Human Gene therapy*, vol. 20, no. 12, pp. 1665-1678, 2009.

38. Y Munakata, T Saito-Ito, K Kumura-Ishii et al., Ku80 autoantigen as a cellular coreceptor for human parvovirus B19 infection, *Blood*, vol. 106, no. 10, pp. 3449-3456, 2005.

39. PR Chipman, M Agbandje-Mckenna, S Kajigaya et al., Cryo-electron microscopy studies of empty capsids of human parvovirus B19 complexed with its cellular receptor. *Proceedings of the National Academy of Sciences of the United States of America*, vol. 93, no. 15, pp. 7502-7506, 1996.

40. B Kaufmann, U Baxa, PR Chipman, MG Rossmann, S Modrow, and R Seckler, Parvovirus B19 does not bind to membrane-associated globoside in vitro. *Virology*, vol. 332, no. 1, pp. 189-198, 2005.

41. C. Bönsch, C Kempf, and C Ros, Interaction of parvovirus B19 with human erythrocytes alters virus structure and cell membrane integrity. *Journal of Virology*, vol. 82, no. 23, pp. 11784-11791, 2008.

42. R Leisi, N Ruprecht, C Kempf, C Ros, Parvovirus B19 Uptake Is a Highly Selective Process Controlled by VP1u, a Novel Determinant of Viral Tropism. *Journal of Virology,* vol. 87, no. 24, pp. 13161-13167, 2013.

43. R Leisi, C Di Tommaso, C Kempf, and C Ros, The Receptor-Binding Domain in the VP1u Region of Parvovirus B19. *Viruses*, vol. 8, no. 61, 2016.

44. S Quattrocchi, N Ruprecht, C Bonsch et al., Characterization of the early steps of human parvovirus B19 infection. *Journal of Virology*, vol. 86, pp. 9274-9284, 2012

45. W Guan, S Wong, N Zhi, and J Qiu, The genome of human parvovirus B19 can replicate in non permissive cells with the help of adenovirus genes and produces infectious virus. *Journal of Virology*, vol. 83, no. 18, pp. 9541–9553, 2009.

46. Y Luo and J Qiu, Human parvovirus B19: a mechanistic overview of infection and DNA replication. *Future Virology,* vol. 10, no. 2, pp. 155-167, 2015.

47. K Ozawa, G Kurtzman, and N Young, Replication of the B19 parvovirus in human bone marrow cell cultures. *Science*, vol. 233, no. 4766, pp. 883-886, 1986.

48. K Ozawa, G Kurtzman, and N Young, Productive infection by B19 parvovirus of human erythroid bone marrow cells in vitro. *Blood*, vol. 70, no. 2, pp. 384–391, 1987.

49. SK Tewary, H Zhao, X Deng, J Qiu and L Tang, The human parvovirus B19 non-structural protein 1 N-terminal domain specifically binds to the origin of replication in the viral DNA. *Virology*, vol. 449, pp. 297-303, 2014.

50. MC Blundell, C Beard, and CR Astell, In vitro identification of a B19 parvovirus promoter. *Virology*, vol. 157, no. 2, pp. 534-538, 1987.

51. C Doerig, P Beard, and B Hirt, A transcriptional promoter of the human parvovirus B19 active in vitro and in vivo. *Virology*, vol. 157, no. 2, pp. 539-542, 1987.

52. MC Blundell and CR Astell, A GC-box motif upstream of the B19 parvovirus unique promoter is important for in vitro transcription. *Journal of Virology*, vol. 63, no. 11, pp. 4814-4823, 1989.

53. JM Liu, H Fujii, SW Green, N Komatsu, NS Young, and T Shimada, Indiscriminate activity from the B19 parvovirus P6 promoter in non permissive cells. *Virology*, vol. 182, no. 1, pp. 361-364, 1991.

54. R Gareus, A Gigler, A Hemauer et al., Characterization of cis-acting and NS1 protein-responsive elements in the p6 promoter of parvovirus B19, *Journal of Virology*, vol. 72, no. 1, pp. 609-616, 1998.

55. K Ozawa, J Ayub, and H Yu-Shu, Novel transcription map for the B19 (human) pathogenic parvovirus, *Journal of Virology*, vol. 61, no. 8, pp. 2395-2406, 1987.

56. K Ozawa, J Ayub, and N Young, Functional mapping of the genome of the B19 (human) parvovirus by in vitro translation after negative hybrid selection. *Journal of Virology*, vol. 62, no. 7, pp. 2508-2511, 1988.

57. JS Amand, C Beard, K Humphries, and CR Astell, Analysis of splice junctions and in vitro and in vivo translation potential of the small, abundant B19 parvovirus RNAs. *Virology*, vol. 183, no. 1, pp. 133-142, 1991.

58. W Guan, F Cheng, Q Huang, S Kleiboeker, and J Qiu, Inclusion of the central exon of parvovirus B19 precursor mRNA is determined by multiple splicing enhancers in both the exon and the downstream intron. *Journal of Virology*, vol. 85, no. 5, pp. 2463-2468, 2011.

59. Y Yoto, J Qiu, and DJ Pintel, Identification and characterization of two internal cleavage and polyadenylation sites of parvovirus B19 RNA. *Journal of Virology*, vol. 80, no. 3, pp. 1604-1609, 2006.

60. W Guan, Q Huang, F Cheng, and J Qiu, Internal polyadenylation of the parvovirus B19 precursor mRNA is regulated by alternative splicing. *Journal of Biological Chemistry*, vol. 286, no. 28, pp. 24793-24805, 2011.

61. W Guan, F Cheng, Y Yoto et al., Block to the production of full-length B19 virus transcripts by internal polyadenylation is overcome by replication of the viral genome. *Journal of Virology*, vol. 82, no. 20, pp. 9951-9963, 2008.

62. S Shimomura, S Wong, KE Brown, N Komatsu, S Kajigaya, and NS Young, Early and late gene expression in UT-7 cells infected with B19 parvovirus. *Virology*, vol. 194, no. 1, pp. 149- 156, 1993.

63. F Bonvicini, C Filippone, S Delbarba et al., Parvovirus B19 genome as a single, two-state replicative and transcriptional unit. *Virology*, vol. 347, no. 2, pp. 447-454, 2006.

64. F Bonvicini, C Filippone, E Manaresi, M Zerbini, M Musiani, and G. Gallinella, Functional analysis and quantitative determination of the expression profile of human parvovirus B19. *Virology*, vol. 381, no. 2, pp. 168-177, 2008.

65. SF Cotmore, VC McKie, and LJ Anderson, Identification of the major structural and non structural proteins encoded by human parvovirus B19 and mapping of their genes by

procaryotic expression of isolated genomic fragments. *Journal of Virology*, vol. 60, no. 2, pp. 548-557, 1986.

66. K Ozawa and N Young, Characterization of capsid and non capsid proteins of B19 parvovirus propagated in human erythroid bone marrow cell cultures, *Journal of Virology*, vol. 61, no. 8, pp. 2627-2630, 1987.

67. J St Amand and CR Astell, Identification and characterization of a family of 11-kDa proteins encoded by the human parvovirus B19," *Virology*, vol. 192, no. 1, pp. 121-131, 1993.

68. W Luo and CR Astell, A novel protein encoded by small RNAs of parvovirus B19. *Virology*, vol. 195, no. 2, pp. 448-455, 1993.

69. C Doerig, B Hirt, JP Antonietti, and P Beard, "Non structural protein of parvoviruses B19 and minute virus of mice controls transcription. *Journal of Virology*, vol. 64, no. 1, pp. 387-396, 1990.

70. S Moffatt, N Tanaka, K Tada et al., A cytotoxic non structural protein, NS1, of human parvovirus B19 induces activation of interleukin-6 gene expression. *Journal of Virology*, vol. 70, no. 12, pp. 8485-8491, 1996.

71. Y Fu, KK Ishii, Y Munakata, T Saitoh, M Kaku, and T Sasaki, Regulation of tumor necrosis factor alpha promoter by human parvovirus B19 NS1 through activation of AP-1 and AP-2. *Journal of Virology*, vol. 76, no. 11, pp. 5395-5403, 2002.

72. K Ozawa, J Ayub, S Kajigaya, T Shimada, and N Young, The gene encoding the nonstructural protein of B19 (human) parvovirus may be lethal in transfected cells. *Journal of Virology*, vol. 62, no. 8, pp. 2884-2889, 1988.

73. M Momoeda, S Wong, M Kawase, NS Young, and S Kajigaya, A putative nucleoside triphosphate-binding domain in the nonstructural protein of B19 parvovirus is required for cytotoxicity. *Journal of Virology*, vol. 68, no. 12, pp. 8443-8446, 1994.

74. S Moffatt, N Yaegashi, K Tada, N Tanaka, and K Sugamura, Human parvovirus B19 nonstructural (NS1) protein induces apoptosis in erythroid lineage cells. *Journal of Virology*, vol. 72, no. 4, pp. 3018-3028, 1998.

75. N Sol, J Le Junter, I Vassias et al., Possible interactions between the NS-1 protein and tumor necrosis factor alpha pathways in erythroid cell apoptosis induced by human parvovirus B19. *Journal of Virology*, vol. 73, no. 10, pp. 8762-8770, 1999.

76. Z Zadori, J Szelei, MC Lacoste, et al., A viral phospholipase A2 is required for parvovirus infectivity. *Developmental Cell*, vol. 1, no. 2, pp. 291-302, 2001.

77. S Pillet, Z Annan, S Fichelson, and F Morinet, Identification of a nonconventional motif necessary for the nuclear import of the human parvovirus B19 major capsid protein (VP2). *Virology*, vol. 306, no. 1, pp. 25-32, 2003.

78. S Kajigaya, T Shimada, S Fujita, and NS Young A genetically engineered cell line that produces empty capsids of B19 (human) parvovirus. *Proceedings of the National Academy of Sciences of the United States of America*, vol. 86, no. 19, pp. 7601-7605, 1989.

79. CS Brown, MMM Salimans, MHM Noteborn, and HT Weiland, Antigenic parvovirus B19 coat proteins VP1 and VP2 produced in large quantities in a baculovirus expression system. *Virus Research*, vol. 15, no. 3, pp. 197-211, 1990.

80. CS Brown, JWM Van Lent, JM Vlak, and WJM Spaan, Assembly of empty capsids by using baculovirus recombinants expressing human parvovirus B19 structural proteins. *Journal of Virology*, vol. 65, no. 5, pp. 2702-2706, 1991.

81. S Kajigaya, H Fujii, A Field et al., Self-assembled B19 parvovirus capsids, produced in a baculovirus system, are antigenically and immunogenically similar to native virions. *Proceedings of the National Academy of Sciences of the United States of America*, vol. 88, no. 11, pp. 4646-4650, 1991.

82. C Filippone, N Zhia, S Wong, et al., VP1u phospholipase activity is critical for infectivity of full- length parvovirus B19 genomic clones. *Virology*, vol. 374, no. 2, pp. 444-452, 2008.

83. MMY Fan, L Tamburic, C Shippam-Brett, DB Zagrodney, and CR Astell, The small 11-kDa protein from B19 parvovirus binds growth factor receptor-binding protein 2 in vitro in a Src homology 3 domain/ligand-dependent manner. *Virology*, vol. 291, no. 2, pp. 285-291, 2001.

84. Y Chen, EY Zhang, W Guan et al., The small 11kDa nonstructural protein of human parvovirus B19 plays a key role in inducing apoptosis during B19 virus infection of primary erythroid progenitor cells, *Blood*, vol. 115, no. 5, pp. 1070-1080, 2010.

85. PP Mortimer, RK Humphries, and JG Moore, A human parvovirus-like virus inhibits haematopoietic colony formation in vitro. *Nature*, vol. 302, no. 5907, pp. 426-429, 1983.

86. T Takahashi, K Ozawa, K Takahashi, S Asano, and F Takaku, Susceptibility of human erythropoietic cells to B19 parvovirus in vitro increases with differentiation. *Blood*, vol. 75, no. 3, pp. 603-610, 1990.

87. TF Schwarz, S Serke, B Hottentrager et al., Replication of parvovirus B19 in hematopoietic progenitor cells generated in vitro from normal human peripheral blood. *Journal of Virology*, vol. 66, no. 2, pp. 1273-1276, 1992.

88. KE Brown, J Mori, BJ Cohen, and AM Field, In vitro propagation of parvovirus B19 in primary foetal liver culture, *Journal of General Virology*, vol. 72, no. 3, pp. 741-745, 1991.

89. AL Morey, G Patou, S Myint, and KA Fleming, In vitro culture for the detection of infectious human parvovirus B19 and B19-specific antibodies using foetal haematopoietic precursor cells. *Journal of General Virology*, vol. 73, no. 12, pp. 3313-3317, 1992.

90. S Shimomura, N Komatsu, N Frickhofen, S Anderson, S Kajigaya, and NS Young, First continuous propagation of B19 parvovirus in a cell line. *Blood*, vol. 79, no. 1, pp. 18-24, 1992.

91. E Miyagawa, T Yoshida, H Takahashi et al., Infection of the erythroid cell line, KU812Ep6 with human parvovirus B19 and its application to titration of B19 infectivity. *Journal of Virological Methods*, vol. 83, no. 1-2, pp. 45-54, 1999.

92. S Wong, N Zhi, C Filippone et al., Ex vivo-generated CD36+ erythroid progenitors are highly permissive to human parvovirus B19 replication. *Journal of Virology*, vol. 82, no. 5, pp. 2470-2476, 2008.

93. C Filippone, R Franssila, A Kumar et al., Erythroid progenitor cells expanded from peripheral blood without mobilization or preselection: molecular characteristics and functional competence. *PLoS ONE*, vol. 5, no. 3, Article ID e9496, 2010.

94. KA Weigel-Kelley, MC Yoder, and A Srivastava, Recombinant human parvovirus B19 vectors: erythrocyte P antigen is necessary but not sufficient for successful transduction of human hematopoietic cells. *Journal of Virology*, vol. 75, no. 9, pp. 4110-4116, 2001.

95. Leisi R, M von Nordheim, C Kempf, and C Ros, Specific Targeting of Proerythroblasts and Erythroleukemic Cells by the VP1u Region of Parvovirus B19. Bioconjugate Chemistry, vol. 26, pp. 1923-1930, 2015.

96. K von Kietzell, T Pozzuto, R Heilbronn, T Grössl, H Fechner, and S Weger, Antibody-mediated enhancement of parvovirus B19 uptake into endothelial cells mediated by a receptor for complement factor C1q. *Journal of Virology,* vol. 88, no.14, pp. 8102-8105, 2014.

97. AY Chen, W Guan, S Lou, Z Liu, S Kleiboeker, and J Qiu, Role of erythropoietin receptor signaling in parvovirus B19 replication in human erythroid progenitor cells. *Journal of Virology*, vol. 84, no. 23, pp. 12385-12396, 2010.

98. S Pillet, N Le Guyader, T Hofer et al, Hypoxia enhances human B19 erythrovirus gene expression in primary erythroid cells. *Virology*, vol. 327, no. 1, pp. 1-7, 2004.

99. AY Chen, S Kleiboeker, and J Qiu, Productive parvovirus B19 infection of primary human erythroid progenitor cells at hypoxia is regulated by STAT5A and MEK signaling but not HIFα. *PLoS Pathogens*, vol. 7, no. 6, Article ID e1002088, 2011.

100. F Bonvicini, C Filippone, E Manaresi, M Zerbini, M Musiani, and G Gallinella, HepG2 hepatocellular carcinoma cells are a non-permissive system for B19 virus infection. *Journal of General Virology*, vol. 89, no. 12, pp. 3034-3038, 2008.

101. JM Liu, SW Green, T Shimada, and NS Young, A block in full-length transcript maturation in cells nonpermissive for B19 parvovirus. *Journal of Virology*, vol. 66, no. 8, pp. 4686-4692, 1992.

102. E Morita and K Sugamura, Human parvovirus B19-induced cell cycle arrest and apoptosis. *Seminars in Immunopathology*, vol. 24, no. 2, pp. 187-199, 2002.

103. E Morita, K Tada, H Chisaka et al., Human parvovirus B19 induces cell cycle arrest at G2 phase with accumulation of mitotic cyclins. *Journal of Virology*, vol. 75, no. 16, pp. 7555- 7563, 2001.

104. E Morita, A Nakashima, H Asao, H Sato, and K Sugamura, Human parvovirus B19 nonstructural protein (NS1) induces cell cycle arrest at G1 phase. *Journal of Virology*, vol. 77, no. 5, pp. 2915-2921, 2003.

105. A Nakashima, E Morita, S Saito, and K Sugamura, Human parvovirus B19 nonstructural protein transactivates the p21/WAF1 through Sp1. *Virology*, vol. 329, no. 2, pp. 493-504, 2004.

106. Z Wan, N Zhi, S Wong et al., Human parvovirus B19 causes cell cycle arrest of human erythroid progenitors via deregulation of the E2F family of transcription factors. *Journal of Clinical Investigation*, vol. 120, no. 10, pp. 3530-3544, 2010.

107. Y Luo, S Kleiboeker, X Deng, and J Qiu, Human Parvovirus B19 Infection Causes Cell Cycle Arrest of Human Erythroid Progenitors at Late S Phase That Favors Viral DNA Replication. *Journal of Virology*, vol. 87, pp. 12766-12775, 2013.

108. Y Luo, S Lou, X Deng et al., Parvovirus B19 infection of human primary erythroid progenitor cells triggers ATR-Chk1 signaling, which promotes B19 virus replication. *Journal of Virology*, vol. 85, no. 16, pp. 8046-8055, 2011.

109. S Lou, Y Luo, F Cheng et al., Human parvovirus B19 DNA replication induces a DNA damage response that is dispensable for cell cycle arrest at phase G2/M. *Journal of Virology*, vol. 86, pp. 10748-10758, 2012.

110. MJ Anderson, PG Higgins, LR Davis et al., Experimental parvoviral infection in humans. *The Journal of Infectious Diseases*, vol. 152, pp. 257-265, 1985.

111. M Musiani, M Zerbini, G Gentilomi, M Plazzi, G Gallinella, and S Venturoli, Parvovirus B19 clearance from peripheral blood after acute infection. *Journal of Infectious Diseases*, vol. 172, no. 5, pp. 1360-1363, 1995.

112. A Lindblom, A Isa, O Norbeck et al., Slow clearance of human parvovirus B19 viremia following acute infection, Clinical Infectious Diseases, vol. 41, no. 8, pp. 1201-1203, 2005.

113. T Chorba, P Coccia, and RC Holman, The role of parvovirus B19 in aplastic crisis and erythema infectiosum (fifth disease). *Journal of Infectious Diseases*, vol. 154, no. 3, pp. 383-393, 1986.

114. DM Reid, TMS Reid, and T Brown, Human parvovirus- associated arthritis: a clinical and laboratory description, *The Lancet*, vol. 1, no. 8426, pp. 422-425, 1985.

115. DG White, AD Woolf, and PP Mortimer, Human parvovirus arthropathy. *The Lancet*, vol. 1, no. 8426, pp. 419- 421, 1985.

116.   AD Woolf, GV Campion, A Chishick et al., Clinical manifestations of human parvovirus b19 in adults. Archives of Internal Medicine, vol. 149, pp. 1153-1156, 1989.

117.   SJ Naides, Rheumatic manifestations of parvovirus B19 infection. *Rheumatic Disease Clinics of North America*, vol. 24, pp. 375-401, 1998.

118.   HW Lehmann, P von Landenberg, and S Modrow, Parvovirus B19 infection and autoimmune disease. *Autoimmunity Reviews*, vol. 2, no. 4, pp. 218-223, 2003.

119.   P von Landenberg, HW Lehmann, and S Modrow, Human parvovirus B19 infection and antiphospholipid antibodies. *Autoimmunity Reviews*, vol. 6, no. 5, pp. 278-285, 2007.

120.   JR Kerr, Pathogenesis of human parvovirus B19 in rheumatic disease. *Annals of Rheumatic Diseases*, vol. 59, pp.672-683, 2000.

121.   Y Takahashi, C Murai, S Shibata et al., Human parvovirus B19 as a causative agent for rheumatoid arthritis. *Proceedings of the National Academy of Sciences of the United States of America*, vol. 95, no. 14, pp. 8227-8232, 1998.

122.   M Söderlund, R von Essen, J Haapasaari, et al., Persistence of parvovirus B19 DNA in synovial membranes of young patients with and without chronic arthropathy. *The Lancet*, vol. 349, no. 9058, pp. 1063-1065, 1997.

123.   NPH Miki and JK Chantler, Non-permissiveness of synovial membrane cells to human parvovirus B19 in vitro. Journal of General *Virology*, vol. 73, no. 6, pp. 1559-1562, 1992.

124.   NB Ray, DR Nieva, EA Seftor, Z Khalkhali-Ellis, and SJ Naides, Induction of an invasive phenotype by human parvovirus B19 in normal human synovial fibroblasts. *Arthritis & Rheumatism*, vol. 44, pp. 1582-1586, 2001.

125.   KE Brown, Haematological consequences of parvovirus B19 infection. *Bailliere's Best Practice and Research in Clinical Haematology*, vol. 13, no. 2, pp. 245-259, 2000.

126.   ED Heegaard and KE Brown, Human Parvovirus B19. Clinical Microbiology Reviews, vol. 15, no. 3, pp. 485-505, 2002.

127.   PR Koduri, Parvovirus B19-related anemia in HIV-infected patients. *AIDS Patient Care and STDs*, vol. 14, no. 1, pp. 7-11, 2000.

128.   K Broliden, T Tolfvenstam, S Ohlsson, and JI Henter, Persistent B19 parvovirus infection in pediatric malignancies. *Medical and Pediatric Oncology*, vol. 31, pp. 66-72, 1998.

129. A. Lindblom, M Heyman, I Gustafsson et al., Parvovirus B19 infection in children with acute lymphoblastic leukemia is associated with cytopenia resulting in prolonged interruptions of chemotherapy. *Clinical Infectious Diseases*, vol. 46, no. 4, pp. 528-536, 2008.

130. G Gallinella, E Manaresi, S Venturoli, GL Grazi, M Musiani, and M Zerbini, Occurrence and clinical role of active parvovirus B19 infection in transplant recipients. *European Journal of Clinical Microbiology and Infectious Diseases*, vol. 18, no. 11, pp. 811-813, 1999.

131. K Broliden, Parvovirus B19 infection in pediatric solid-organ and bone marrow transplantation. *Pediatric Transplantation*, vol. 5, no. 5, pp. 320-330, 2001.

132. A Anand, ES Gray, and T Brown, Human parvovirus infection in pregnancy and hydrops fetalis, *The New England Journal of Medicine*, vol. 316, no. 4, pp. 183-186, 1987.

133. JA Jordan and JA Deloia, Globoside expression within the human placenta. *Placenta*, vol. 20, no. 1, pp. 103-108, 1999.

134. CC Wegner and JA Jordan, Human parvovirus B19 VP2 empty capsids bind to human villous trophoblast cells in vitro via the globoside receptor. *Infectious Disease in Obstetrics and Gynecology*, vol. 12, no. 2, pp. 69-78, 2004.

135. G Pasquinelli, F Bonvicini, L Foroni, N Sal, and G Gallinella, Placental endothelial cells can be productively infected by parvovirus B19, *Journal of Clinical Virology*, vol. 44, no. 1, pp. 33-38, 2009.

136. EP de Jong, FJ Walther, ACM. Kroes, and D Oepkes, Parvovirus B19 infection in pregnancy: new insights and management, *Prenatal Diagnosis*, vol. 31, no. 5, pp. 419-425, 2011.

137. HJ Porter, AM Quantrill, and KA Fleming, B19parvovirus infection of myocardial cells. *The Lancet*, vol. 1, no. 8584, pp. 535-536, 1988.

138. A O'Malley, C Barry-Kinsella, C Hughes et al., Parvovirus Infects Cardiac Myocytes in Hydrops Fetalis. *Pediatric and Developmental Pathology*, vol. 6, no. 5, pp. 414-420, 2003.

139. M Enders, A Weidner, I Zoellner, K Searle, and G Enders, Fetal morbidity and mortality after acute human parvovirus B19 infection in pregnancy: prospective evaluation of 1018 cases. *Prenatal Diagnosis*, vol. 24, no. 7, pp. 513-518, 2004.

140. EP DeJong, IT Lindenburg, JM van Klinketal, Intrauterine transfusion for parvovirus B19 infection: long-term neurodevelopmental outcome. *American Journal of Obstetrics & Gynecology*, vol. 206, pp. e1-e5, 2012.

141. L. Andréoletti, N Léveque, C Boulagnon, C Brasselet, and P Fornes, Viral causes of human myocarditis. *Archives of Cardiovascular Diseases*, vol. 102, no. 6-7, pp. 559-568, 2009.

142. R. Dettmeyer, R Kandolf, A Baasner, S Banaschak, AM Eis-Hübinger, and B Madea, Fatal parvovirus B19 myocarditis in an 8-year-old boy. *Journal of Forensic Sciences*, vol. 48, no. 1, pp. 183-186, 2003.

143. K Munro, MC Croxson, S Thomas, and NJ Wilson, Three cases of myocarditis in childhood associated with human parvovirus (B19 virus). *Pediatric Cardiology*, vol. 24, no. 5, pp. 473-475, 2003.

144. U Kühl, M Pauschinger, T Bock et al., Parvovirus B19 infection mimicking acute myocardial infarction. *Circulation*, vol. 108, no. 8, pp. 945-950, 2003.

145. T Bock, K Klingel, and R Kandolf, Human parvovirus B19-associated myocarditis. *The New England Journal of Medicine*, vol. 362, no. 13, pp. 1248-1249, 2010.

146. Bültmann, K Klingel, K Sotlar et al., Fatal parvovirus B19-associated myocarditis clinically mimicking ischemic heart disease: an endothelial cell-mediated disease. *Human Pathology*, vol. 34, no. 1, pp. 92-95, 2003.

147. J Lassen, AK Jensen, P Bager et al., Parvovirus B19 infection in the first trimester of pregnancy and risk of fetal loss: a population-based case-control study. *American Journal of Epidemiology*, vol. 176, no. 9, pp. 803–807, 2012.

148. JR Kerr, HJ O'Neill, PV Coyle, W Thompson, An outbreak of parvovirus B19 infection; a study of clinical manifestations and the incidence of fetal loss. *International Journal of Medical* Science, vol. 163, pp. 65-67. 1994.

149. G Schreiber, SH Kleinman, SA Glynn et al., Prevalence and quantitation of parvovirus B19 DNA levels in blood donors with a sensitive polymerase chain reaction screening assay. *Transfusion*, vol. 47, no. 10, pp. 1756-1764, 2007.

150. K Kooistra, HJ Mesman, M de Waal, MH Koppelman, and HL Zaaijer, Epidemiology of high-level parvovirus B19 viraemia among Dutch blood donors, 2003-2009. *Vox Sang*, vol. 100, pp. 261-266, 2011.

151. 151 GJ Hsu, BS Tzang, CC Tsai, CC Chiu, CY Huang, and TC Hsu, Effects of human parvovirus B19 on expression of defensins and Toll-like receptors. *The Chinese Journal of Physiology*, vol. 54, pp. 367-376, 2011.

152. YM Guo, K Ishii, M Hirokawa et al., CpG-ODN 2006 and human parvovirus B19 genome consensus sequences selectively inhibit growth and development of erythroid progenitor cells," Blood, vol. 115, no. 22, pp. 4569-4579, 2010.

153. H Sato, J Hirata, M Furukawa et al., "Identi cation of the region including the epitope for a monoclonal antibody which can neutralize human parvovirus B19," *Journal of Virology*, vol. 65, no. 4, pp. 1667-1672, 1991.

154. 154 H. Sato, J. Hirata, N Kuroda, H Shiraki, Y Maeda, and K Okochi, Identification and mapping of neutralizing epitopes of human parvovirus B19 by using human antibodies. *Journal of Virology*, vol. 65, no. 10, pp. 5485-5490, 1991.

155. K Yoshimoto, S Rosenfeld, N Frickhofen et al., A second neutralizing epitope of B19 parvovirus implicates the spike region in the immune response. *Journal of Virology*, vol. 65, no. 12, pp. 7056-7060, 1991.

156. T Saikawa, S Anderson, M Momoeda, S Kajigaya, and NS Young, Neutralizing linear epitopes of B19 parvovirus cluster in the VP1 unique and VP1-VP2 junction regions. *Journal of Virology*, vol. 67, no. 6, pp. 3004-3009, 1993.

157. SAnderson, M Momoeda, M Kawase, S Kajigaya, and NS Young, Peptides derived from the unique region of B19 parvovirus minor capsid protein elicit neutralizing antibodies in rabbits. *Virology*, vol. 206, no. 1, pp. 626-632, 1995.

158. SJ Rosenfeld, K Yoshimoto, S Kajigaya et al., Unique region of the minor capsid protein of human parvovirus B19 is exposed on the virion surface. *Journal of Clinical Investigation*, vol. 89, no. 6, pp. 2023-2029, 1992.

159. SJ Rosenfeld, NS Young, D Alling, J Ayub, and C Saxinger, Subunit interaction in B19 parvovirus empty capsids. *Archives of Virology*, vol. 136, no. 1-2, pp. 9-18, 1994.

160.   A Concoran, S Doyle, D Waldron et al., Impaired Gamma Interferon Responses against Parvovirus B19 by Recently Infected Children. *Journal of Virology*, vol. 74, no. 21, pp. 9903-9910, 2000.

161.   T Tolfvenstam, A Lundqvist, M Levi, B Wahren, and K Broliden, Mapping of B-cell epitopes on human Parvovirus B19 non-structural and structural proteins. *Vaccine*, vol. 19, no. 7-8, pp. 758-763, 2000.

162.   A von Poblotzki, A Gigler, B Lang, H Wolf, and S Modrow, Antibodies to parvovirus B19 NS-1 protein in infected individuals. *Journal of General Virology*, vol. 76, no. 3, pp. 519–527, 1995.

163.   A von Poblotzki, C Gerdes, U Reischl, H Wolf, and S Modrow, Lymphoproliferative responses after infection with human parvovirus B19. *Journal of Virology*, vol. 70, no. 10, pp. 7327–7330, 1996.

164.   R Franssila, K Hokynar, and K Hedman, T helper cell- mediated in vitro responses of recently and remotely infected subjects to a candidate recombinant vaccine for human parvovirus B19. *Journal of Infectious Diseases*, vol. 183, no. 5, pp. 805-809, 2001.

165.   T Tolfvenstam, A Oxenius, DA Price et al., Direct ex vivo measurement of CD8+ T-lymphocyte responses to human parvovirus B19. *Journal of Virology*, vol. 75, no. 1, pp. 540-543, 2001.

166.   A Isa, O Norbeck, T Hirbod et al., Aberrant cellular immune responses in humans infected persistently with parvovirus B19. Journal of Medical *Virology*, vol. 78, no. 1, pp. 129-133, 2006.

167.   A Isa, V Kasprowicz, O Norbeck et al., Prolonged activation of virus-specific CD8+ T cells after acute B19 infection. *PLoS Medicine*, vol. 2, no. 12, article e343, pp. 1280-1291, 2005.

168.   R Franssila and K Hedman, T-helper cell-mediated interferon-γ, interleukin-10 and proliferation responses to a candidate recombinant vaccine for human parvovirus B19, *Vaccine*, vol. 22, no. 27-28, pp. 3809-3815, 2004.

169.   R Franssila, J Auramo, S Modrow et al., T helper cell- mediated interferon-gamma expression after human parvovirus B19 infection: persisting VP2-speci c and transient

VP1u-speci c activity. *Clinical and Experimental Immunology*, vol. 142, no. 1, pp. 53-61, 2005.

170. V Kasprowicz, A Isa, T Tolfvenstam, K Jeffery, P Bowness, and P Klenerman, Tracking of peptide-specific CD4+ T-cell responses after an acute resolving viral infection: a study of parvovirus B19," *Journal of Virology*, vol. 80, no. 22, pp. 11209- 11217, 2006.

171. A Isa, A Lundqvist, A Lindblom, T Tolfvenstam, and K Broliden, Cytokine responses in acute and persistent human parvovirus B19 infection. *Clinical and Experimental Immunology,* vol. 147, no. 3, pp. 419-425, 2007.

172. C Lunardi, M Tiso, L Borgato et al., Chronic parvovirus B19 infection induces the production of anti-virus antibodies with autoantigen binding properties. *European Journal of Immunology*, vol. 28, pp. 936-948, 1998.

173. C Lunardi, E Tinazzi, C Bason, M Dolcino, R Corrocher, and A Puccetti, Human parvovirus B19 infection and autoimmunity, *Autoimmunity Reviews*, vol. 8, no. 2, pp. 116-120, 2008.

174. K Thammasri, S Rauhamäki, L Wang et al., Human Parvovirus B19 Induced Apoptotic Bodies Contain Altered Self-Antigens that are Phagocytosed by Antigen Presenting Cells. *PLoS ONE*, vol. 8(6): e67179, 2013.

175. A Kumar, MF Perdomo, A Kantele, L Hedman, K Hedman, and R Franssila, Granzyme B mediated function of Parvovirus B19-specific CD4+ T cells. Clinical & Translational Immunology, vol. 4, e39, 2015.

176. F. Bonvicini, E Manaresi, G Gallinella, GA Gentilomi, M Musiani, and M Zerbini, Diagnosis of fetal parvovirus B19 infection: value of virological assays in fetal specimens. *BJOG*, vol. 116, no. 6, pp. 813-817, 2009.

177. G Gallinella, E Zu , G Gentilomi et al., Relevance of B19 markers in serum samples for a diagnosis of parvovirus B19- correlated diseases. *Journal of Medical Virology*, vol. 71, no. 1, pp. 135-139, 2003.

178. G Gentilomi, M Zerbini, M Musiani et al., In situ detection of B19 DNA in bone marrow of immunodeficient patients using a digoxigenin-labelled probe. *Molecular and Cellular Probes*, vol. 7, no. 1, pp. 19-24, 1993.

179. G Gallinella, NS Young, and KE Brown, In situ hybridisation and in situ polymerase chain reaction detection of parvovirus B19 DNA within cells. *Journal of Virological Methods*, vol. 50, no. 1-3, pp. 67-74, 1994.

180. F Bonvicini, C Filippone, E Manaresi et al., Peptide nucleic acid-based in situ hybridization assay for detection of parvovirus B19 nucleic acids. *Clinical Chemistry*, vol. 52, no. 6, pp. 973-978, 2006.

181. SA Baylis, L Ma, DJ Padley, AB Heath, and MW Yu, Collaborative study to establish a World Health Organization International genotype panel for parvovirus B19 DNA nucleic acid amplification technology (NAT)-based assays. *Vox Sanguinis*, vol. 102, no. 3, pp. 204-211, 2012.

182. E Manaresi, G Gallinella, E Zu, F Bonvicini, M Zerbini, and M Musiani, Diagnosis and quantitative evaluation of parvovirus B19 infections by real-time PCR in the clinical laboratory. *Journal of Medical Virology*, vol. 67, no. 2, pp. 275- 281, 2002.

183. G Gallinella, F Bonvicini, C Filippone et al., Calibrated real-time PCR for evaluation of parvovirus B19 viral load. *Clinical Chemistry*, vol. 50, no. 4, pp. 759-762, 2004.

184. F Bonvicini, E Manaresi, G Bua, S Venturoli, and G Gallinella, Keeping pace with parvovirus B19 genetic variability: a multiplex genotype-specific quantitative PCR assay. *Journal of Clinical Microbiology,* vol. 51, pp. 3753-3759, 2013.

185. LJ Anderson, C Tsou, and RA Parker, Detection of antibodies and antigens of human parvovirus B19 by enzyme- inked immunosorbent assay. *Journal of Clinical Microbiology*, vol. 24, no. 4, pp. 522-526, 1986.

186. E Manaresi, G Gallinella, S Venturoli, M Zerbini, and M Musiani, Detection of parvovirus B19 IgG: choice of antigens and serological tests. *Journal of Clinical Virology*, vol. 29, no. 1, pp. 51-53, 2004.

187. JW Harris, Parvovirus B19 for the hematologist. American Journal of Hematology, vol. 39, pp. 119-130, 1992.

188. RF Lamont, JD Sobel, E Vaisbuch et al., Parvovirus B19 infection in human pregnancy. *BJOG*, vol. 118, no. 2, pp. 175- 186, 2011.

189. F Bonvicini, C Puccetti, NC Salfi et al., Gestational and fetal outcomes in B19 maternal infection: a problem of diagnosis. *Journal of Clinical Microbiology*, vol. 49, pp. 3514–3518, 2011.

190. Y Crabol, T Benjamin, F Rozenberg et al., Intravenous Immunoglobulin Therapy for Pure Red Cell Aplasia Related to Human Parvovirus B19 Infection: A Retrospective Study of 10 Patients and Review of the Literature. *Clinical Infectious Diseases*, vol. 56, pp. 968-977, 2013.

191. JR Kerr, VS Cunniffe, P Kelleher, RM Bernstein, and IN Bruce, Successful Intravenous Immunoglobulin Therapy in 3 Cases of Parvovirus B19-Associated Chronic Fatigue Syndrome. *Clinical Infectious Diseases*, vol. 36, pp. 100-106, 2003.

192. HW Lehmann, A Plentz, P von Landenberg, E Müller-Godeffroy and S Modrow, Intravenous immunoglobulin treatment of four patients with juvenile polyarticular arthritis associated with persistent parvovirus B19 infection and antiphospholipid antibodies. *Arthritis Research and Therapy*, vol. 6, 2004.

193. L Mouthon and O Lortholary, Intravenous immunoglobulins in infectious diseases: where do we stand?. *Clinical Microbiology and Infection*, vol. 9, pp. 333-338, 2003.

194. R Ballou, JL Reed, W Noble, NS Young, and S Koenig, Safety and Immunogenicity of a Recombinant Parvovirus B19 Vaccine Formulated with MF59C.1. *The Journal of Infectious Disease,* vol. 187, pp. 675-678, 2003.

195. D Bernstein, HM. El. Sahlyb, WA. Keitel et al., Safety and immunogenicity of a candidate parvovirus B19 vaccine. *Vaccine*, vol. 29, pp.7353-7367, 2011.

196. S Chandramoulia, A Medina-Selbyb, D Coit et al., Generation of a parvovirus B19 vaccine candidate. *Vaccine*, vol. 31, pp. 3872-3878, 2013.

197. KE Brown, NS Young, BM Alving, and LH Barbosa, Parvovirus B19: implications for transfusion medicine. Summary of a workshop. *Transfusion*, vol. 41, no. 1, pp. 130-135, 2001.

198. D Juhl, M Ozdemir, J Dreier, S Gorg, and H Hennig, Look-back study on recipients of Parvovirus B19 (B19V) DNA-positive blood components. *Vox Sanguinis*, vol. 109, pp. 305-311, 2015.

199. G Marano, S Vaglio, S Pupella et al., Human Parvovirus B19 and blood product safety: a tale of twenty years of improvements. *Blood Transfusion*, vol. 13, pp. 184-196, 2015.

200. C Wakamatsu, F Takakura, E Kojima et al., Screening of Blood Donors for Human Parvovirus B19 and Characterization of the Results. *Vox Sanguinis*, vol. 76, pp. 14-21, 1999.

201. B Cohen, S Beard, WA Knowles et al., Chronic anemia due to parvovirus B19 infection in a bone marrow transplant patient after platelet transfusion. *Transfusion*, vol. 37, pp. 947-952, 1997

202. R Wolfisberg, N Ruprecht, C Kempf, and C Ros, Impaired genome encapsidation restricts the in vitro propagation of human parvovirus B19. *Journal of Virological Methods,* vol. 193, pp. 215-225, 2013.

203. SL Williams-Aziz, CB Hartline, EA Harden, et al., Comparative activities of lipid esters of cidofovir and cyclic cidofovir against replication of herpesviruses in vitro. *Antimicrobial Agents and Chemotherapy*, vol. 49, pp. 3724-3733, 2005.

204. WC Magee and DH Evan, The antiviral activity and mechanism of action of (S)-[3-hydroxy-2-(phosphonomethoxy)propyl] (HPMP) nucleosides. A*ntiviral Research*, vol. 96, pp. 169-180, 2012.

205. T De Schutter, G Andrei, D Topalis, L Naesens, and R Snoeck, Cidofovir selectivity is based on the different response of normal and cancer cells to DNA damage. *BMC Medical Genomics,* vol. 6, 2013.

206. E De Clercq and A Holy, Acyclic nucleoside phosphonates: a key class of antiviral drugs. *Nature Reviews Drug Discovery*, vol. 44, pp. 928-940, 2005.

207. CH Rinaldo, R Gosert, E Bernhoff, S Finstad, and HH Hirsch, 1-O- hexadecyloxypropyl cidofovir (CMX001) effectively inhibits polyomavirus BK replication in primary human renal tubular epithelial cells. *Antimicrobial Agents and Chemotherapy*, vol. 54, pp. 4714-4722, 2010.

PUBLICATION LIST

Results obtained during the PhD course are presented in the following publications.

1) Parvovirus B19 replication and expression in differentiating erythroid progenitors cells.

Bua G, Bonvicini F, Manaresi E, Gallinella G. PLoS ONE: 11(2): e0148547, 2016.

2) Flow-FISH Assay for the quantitative analysis of parvovirus B19 infected cells.

Manaresi E, Bua G, Bonvicini F, Gallinella G. J Virol Methods, 223:50-54, 2015.

3) Antiviral effect of cidofovir on parvovirus B19 replication.

Bonvicini F, Bua G, Manaresi E, Gallinella G. *Antiviral Res.* Jan;113:11-8, 2015.

4) Single-cell chemiluminescence imaging of parvovirus B19 life cycle.

Bonvicini F, Mirasoli M, Manaresi E, Bua G, Calabria D, Roda A, Gallinella G. *Virus Res.* 26;178(2):517-521, 2013

5) Keeping pace with parvovirus b19 genetic variability: a multiplex genotype-specific quantitative PCR assay.

Bonvicini F, Manaresi E, Bua G, Venturoli S, Gallinella G. *J Clin Microbiol.* 2013 Nov;51(11):3753-3759, 2013.

- Inhibitory Effect of Cidofovir on Parvovirus B19 Replication. Bua G, Bonvicini F, Manaresi E, Gallinella G. 28th International Conference on Antiviral Research (ICAR) - Rome, 11-15 May 2015.

- Cidofovir exerts an inhibitory effect on parvovirus B19 replication. Bonvicini F, Bua G, Manaresi E, Gallinella G. 3rd Antivirals Congress - Amsterdam, 12- 14 October 2014.

- In vitro derived erythroid progenitor cells as a model system to assess inhibitory effects of potential antiviral drugs on B19V replication. BonviciniF, Bua G, Manaresi E, Gallinella G. 3rd Antivirals Congress - Amsterdam, 12-14 October 2014.

- In vitro derived erythroid progenitor cells as a model system for studying B19V-cell interactions. Bua G, Manaresi E, Bonvicini F, Gallinella G. 17TH Annual Meeting of ESCV - Prague, 28 September-01 October 2014

- Inhibitory activity of the antiviral drug cidofovir against Parvovirus B19. Bonvicini F, <u>Bua G</u>, Manaresi E, Gallinella G. 17TH Annual Meeting of ESCV - Prague, 28 September-01 October 2014.

- Antiviral effect of Cidofovir on B19V replication. Bonvicini F, <u>Bua G</u>, Manaresi E, Gallinella G. 15TH Biennial International Parvovirus Workshop - Bordeaux, 22-26 June 2014.

- Flow-FISH assay for detection of Parvovirus B19 nucleic acids at single-cell level. Manaresi E, <u>Bua G</u>, Bonvicini F, Gallinella G. 15TH Biennial International Parvovirus Workshop - Bordeaux, 22-26 June 2014.

- Cellule progenitrici eritroidi ottenute da sangue perififerico come sistema per lo studio della replicazione ed espressione di B19V. <u>Bua G</u>, Manaresi E, Bonvicini F, Gallinella G. X Congresso Nazionale della Società Italiana di Microbiologia Farmaceutica - Chieti, 6-7 June 2014.

- Effetti inibitori di farmaci antivirali a largo spettro nei confronti di Parvovirus B19. Bonvicini F, <u>Bua G</u>, Manaresi E, Gallinella G. X Congresso Nazionale della Società Italiana di Microbiologia Farmaceutica - Chieti, 6-7 June 2014.

- Analysis on Parvovirus B19 life cycle at single cell level by chemiluminescent imaging assays. Gallinella G, Bonvicini F, <u>Bua G</u>, Manaresi E, Mirasoli M, Zangheri M, Roda A. 5th European Congress of Virology - Lyon, 11-14 September 2013.

- Towards the integration of Real Time PCR in lab on chip devices. Calabria D, Mirasoli M, Zangheri M, Bonvicini F, <u>Bua G</u>, Gallinella G, Roda A. XXIV Congresso Nazionale della Divisione di Chimica Analitica della SCI - Setri Levante, 15-19 Settembre 2013.